Geophysical Monitoring for Climatic Change

No. 13

Summary Report 1984

U.S. DEPARTMENT OF COMMERCE

NATIONAL OCEANIC AND ATMOSPHERIC ADMINISTRATION

ENVIRONMENTAL RESEARCH LABORATORIES

Geophysical Monitoring for Climatic Change No. 13

Summary Report 1984

Everett C. Nickerson, Editor
Air Resources Laboratory
Geophysical Monitoring for Climatic Change

Boulder, Colorado

February 1986

U.S. DEPARTMENT OF COMMERCE
Malcolm Baldrige, Secretary

National Oceanic and Atmospheric Administration

Environmental Research Laboratories
Vernon E. Derr, Director

NOTICE

Mention of a commercial company or product does not constitute an endorsement by NOAA Environmental Research Laboratories. Use for publicity or advertising purposes of information from this publication concerning proprietary products or the tests of such products is not authorized.

CONTENTS

GMCC ORGANIZATIONAL CHART

GMCC Staff, 1984

Director's Office

James Peterson, Director
Bernard Mendonca, Deputy Director
Jeanne Kelsey, Secretary
Roland Christofferson, CIRES
Dale Gillette, Physical scientist
Paul David Herrera, CO-OP
Lori Neff, Scientific Data Clerk
Everett C. Nickerson, Meteorologist
Rita Rosson, Clerk-Typist
Russell Schnell, CIRES
Chandra Shastri, CIRES
L. Paul Steele, Guest Scientist
David Wuertz, CO-OP

Acquisition and Data Management Group

Gary Herbert, Chief
Karen Ciocchetti, Secretary
Bonnie, Hill, Secretary
Richard Clark, Computer Programmer
Teresa Davenport, Physical Science Aid
Joseph Drewno, Physical Science Aid
Edward Green, CIRES
Joyce Harris, Computer Specialist
Troy Higgins, Jr. Fellow
Gloria Koenig, Computer Programmer
Steve Roughton, Physical Science Aid
Kenneth Thaut, Electronic Technician

Aerosols and Radiation Monitoring Group

John DeLuisi, Chief
Karen Ciocchetti, Secretary
Bonnie Hill, Secretary
James Baumhover, Electronic Technician
Barry Bodhaine, Meteorologist
Ellsworth Dutton, Meteorologist
Linda Mitchell, CIRES
Stuart Naegele, CIRES
Martz Oryshchyn, Physical Science Aid
Jeffrey Pratt, Physical Science Aid
Timothy Quakenbush, Physical Science Aid
Traci Simms, Physical Science Aid
Kenneth Thorne, CIRES
Wolfgang Raatz, NRC Postdoctoral Research Associate

Carbon Dioxide Group

Richard Gammon, Chief
Rita Brown, Secretary
Susan Dozier, Secretary
Brian Anderson, Physical Science Aid
Thomas Conway, Research Chemist
Bryan Dickerson, CO-OP

Christopher Fortescue, Physical Science Aid
Tom Gorczyca, CIRES
Bradley Halter, Meteorologist
Gary Horton, CIRES
Kenneth Masarie, CIRES
Ted Myers, Physical Science Aid
John Parker, CO-OP
Kirk Thoning, CIRES
Alberta Vieira, CO-OP
Lee Waterman, Chemist

Monitoring Trace Gases Group

Walter Komhyr, Chief
Rita Brown, Secretary
Bradley Chaffee, Physical Science Aid
Susan Dozier, Secretary
Robert Evans, CIRES
Marc Fish, Physical Science Aid
Paul Franchois, CIRES
Robert Grass, Physicist
Thomas Jones, Physical Science Aid
Kent Leonard, CIRES
Samuel Oltmans, Physicist
Frank Polacek, III, Meteorological Technician
Thayne Thompson, Physicist
Ronald Thorne, Physical Science Aid

Barrow Observatory

Daniel Beard, Station Chief
Daniel Endres, Electronic Technician
Steve Fahnenstiel, Station Chief
Timothy Wolfe, Electronic Technician

Mauna Loa Observatory

Elmer Robinson, Director
Judith Pereira, Secretary
Arnold Austring, Physical Scientist
John Chin, Physicist
Thomas DeFoor, Electrical Engineer
Thomas Garcia, Physical Science Aid
GuoAn Ding, Guest Scientist
Dorothy Johnson, Physical Science Aid
Darryl Kuniyuki, Jr. Fellow
Stephen Lent, Physical Science Aid
Cynthia McFee, NOAA Corps
Lisa McPherson, Physical Science Aid
Mamoru Shibata, Electronic Technician
Alan Yoshinaga, Chemist

Samoa Observatory

Donald Nelson, Station Chief
Roger Williams, Electronic Technician
Efaraima Peau, W. G. Laborer

South Pole Observatory

Frank Migaiolo, NOAA Corps, Station Chief
Robert Platzer, Electronic Technician
James Waddell, NOAA Corps, Station Chief
Mark Mihalic, Electronic Technician

GEOPHYSICAL MONITORING FOR CLIMATIC CHANGE

NO. 13

SUMMARY REPORT 1984

1. SUMMARY

At MLO, the main event of the year was the eruption of Mauna Loa on March 25 and 3 weeks of lava flow down the northeast slope of the mountain. One effect was severance of the electrical power line to the observatory. A temporary generator was installed in late April and full, regular service was restored on July 24. New scientific activities during the year included upgrade of the lidar system, installation of a gas chromatograph for in situ CO_2 and CH_4 measurements, initiation of weekly ozonesondes, and start-up of high precision UV radiation measurements.

At BRW, the year was highlighted by smooth, uneventful operations. Both interior and exterior of the observatory were renovated, including new carpeting, painting, and sound insulation. The GMCC and cooperative measurement programs had few problems.

At SMO, we significantly improved facilities by adding a new remote sampling building on the ridge. This prefabricated structure will house both GMCC and OGC operations, but in separate rooms. The photovoltaic system received final testing and certification. The system is working well and generating solar-powered electricity at the observatory. The land lease for use of Samoan communal land was renogotiated for another 5-year term. Negotiations were rather delicate since a successor had not yet been chosen for Chief Iuli, Togi, who died in September 1983.

At SPO, snow buildup around the CAF continued to be a major problem of growing concern. This is causing immediate logistical problems and the potential for severe drifting if CAF is not raised soon. A new meteorological tower was installed. Equipment performance for GMCC and cooperative programs was exceptional.

The ongoing GMCC core measurement programs continued at the four observatories. These programs include CO_2, total column ozone, ozone vertical distribution, surface ozone, stratospheric water vapor, CFC-11 and -12, N_2O, stratospheric aerosols, volumetric aerosol scattering coefficient, CN concentration, solar radiation, meteorological variables, and precipitation chemistry. In addition, a wide variety of cooperative programs were conducted for university, other agency, and foreign investigators.

In the Aerosols and Radiation Group, a computationally efficient model for direct and global solar flux in the atmosphere was adapted to the four observatories for comparison to our measurements. The model will be used to study anomalies in the data and to develop cloud climatologies. The special program for measurements of albedo at SPO continued. A thorough analysis was completed of the MLO lidar record from 1974-1983. The range of optical

thickness exceeded two orders of magnitude from a quiescent period in 1976-1977 to the striking El Chichon event of 1982. The altitude of maximum aerosol backscatter from El Chichon reached the remarkable value of 27 km!

The Carbon Dioxide Group continued the long-term in situ CO_2 measurements at the observatories and flask analyses of CO_2 and CH_4 at 24 sites. The mean CO_2 global growth rate for 1984 was about 1.5 ppm/year. The effects of the 1982-83 El Niño/Southern Oscillation waned as the global CO_2 distribution returned to more normal patterns. The flask methane measurement program continued to mature, showing a long-term concentration increase of about 1% per year, distinct seasonal variations, and significant large-scale latitudinal gradients. Special projects included installation of a gas chromatograph at MLO to compare its results to the NDIR method of CO_2 measurements, collection of flask samples aboard occasional oceanographic cruises (Long Lines Expedition to the equatorial and south Atlantic and NOAA DISCOVERER to the equatorial and north Pacific), and application of a two-dimensional carbon cycle model for comparison to the GMCC measurements.

The Trace Gases Group continued responsibility for total ozone observations at 16 sites; the longest records date back to the early 1960's. A highlight of the year was the initiation of an agreement with NOAA/NESDIS for GMCC to provide data validation information for the SBUV/2 satellite-based ozone profiling instrument. GMCC measurements for NESDIS will include total ozone at 16 select Dobson sites, weekly vertical ozone profiles by ozonesondes at three sites, and vertical profiles by the Umkehr technique at seven automated Dobson sites. The program became operational in 1985. The observatory surface ozone records from 1973-1984 were analyzed for long-term trends. Secular increases at BRW and MLO contrast with decreases of SMO; the cause is postulated to be general circulation changes. Monthly balloon soundings of stratospheric water vapor at Boulder continued. Ongoing flask measurements of CCl_3F and CCl_2F_2 at the observatories showed long-term increases of about 10 ppt/yr and 17 ppt/yr, respectively.

The Acquisition and Data Management Group oversaw development and installation of a new data acquisition system at the observatories. Station climatologies showed, for example, an all-time record minimum temperature at Barrow of -50.0°C and near normal wind rose distributions at SMO and SPO. Many isobaric atmospheric trajectories were computed with emphasis on Arctic locations in support of AGASP, precipitation chemistry research, and Southern Hemisphere sites. Further development of the isentropic model included extension of the lowest surface to 1000 mb and capability to produce forward trajectories.

Many scientists from universities and other government agencies continued to use the observatories as a base for cooperative research. Summary reports from several of these projects are included here. They cover such topics as precipitation quantification at Barrow, CO_2 isotope measurements, high resolution solar UV observations at MLO, analyses of background chemistry of precipitation, CFC-13 trends at BRW, description of the Antarctic Tracer Experiment, analyses of data from the AGASP experiment, and measurements of submicron particles from meteorites at SPO.

2. OBSERVATORY REPORTS

2.1 Mauna Loa

FACILITIES

The major event for MLO during 1984 was undoubtedly the March-April eruption of Mauna Loa. There had been a 9-yr quiet period since the small summit eruption in 1975.

The 1984 Mauna Loa eruption began at about 1:30 a.m., March 25 with lava fountaining in the southwest corner of the summit crater. Within 2 to 3 hours, 80% of the crater was covered by lava and there was concern that lava might flow from the crater toward MLO. Fortunately this did not happen because the eruptive activity soon shifted to the northeast rift zone. By about 5 p.m. on the 25th, the major activity had moved to the 9,200-ft level on the northeast rift, 2,000 ft below MLO, and concern over the safety of the facility lessoned greatly.

The Mauna Loa eruption continued for 3 weeks until April 15. An early major impact on MLO operations was the inundation by flowing lava of the power line serving the Observatory on March 26. After the eruption activity ceased, it was possible to set up a large motor generator on the power line about 10 miles from MLO and beginning on April 28, this generator powered the Observatory until regular power-line service was restored on July 24. Throughout the eruption, considerable extra effort was required of the MLO staff and the staff of the NCAR High Altitude Observatory which shares the MLO site. In addition, vital cooperation was provided by the local electrical utility and our local governmental agencies.

The MLO observational routine was generally back to normal on the generator power on April 28, and the switch back to the power line in July was uneventful. USGS scientists estimated that the 1984 Mauna Loa eruption produced 220×10^6 m^3 of lava and covered an area of about 48 km^2. The MLO staff was awarded a NOAA Special Act award for its service during the eruption.

Elmer Robinson was appointed Director of MLO and assumed his position on July 1, 1984.

A program to upgrade the MLO lidar system was begun in August with the support of a grant from EPA.

A specially designed automatic gas chromatograph was put into service for CO_2 and CH_4 monitoring in March, taken out of service during the eruption, and put back into service in September.

An ozonesonde program was begun in December. The balloon releases are scheduled weekly from the Hilo NWS station and are in support of the NOAA-F satellite SBUV observations to determine ozone profiles based on backscattered UV. Support for ozonesonde operations and other SBUV satellite support activities at MLO is provided by NESDIS.

The CAMS units were substituted for ICDAS in November and after the usual post-installation problems, operations were generally satisfactory in early December. It should be assumed that there were breaks in the records of most instruments during the ICDAS to CAMS changeover period of November 26-30.

Mr. GuoAn Ding, PRC, arrived at MLO February 22, 1984 to spend approximately 1 year as a visiting scientist. The purpose of his visit was to become thoroughly familiar with baseline monitoring so that he could guide PRC activities in this scientific area. His visit ended in January 1985.

The safety of the MLO electrical system was augmented by operating each pump through a separately fused connector designed to blow if the pump load increases through an overload. This should guard against pumps overheating and posing fire hazards.

PROGRAMS

The principal programs carried out at MLO during 1984 are listed in table 1. Brief comments on some of the programs are given below. It should be assumed, however, that all electrical instruments were down between March 25 and April 28 because of the loss of the power line due to the advancing lava flow.

Table 1.--Summary of sampling programs at MLO in 1984

Program	Instrument	Sampling Frequency	Remarks
Gases			
CO_2	URAS-2T infrared analyzer	Continuous	
	3-L glass flasks	1 pair wk^{-1}	MLO and Kumukahi seacoast
	0.5-L glass flasks, P[3]	1 pair wk^{-1}	MLO and Kumukahi
	0.5-L glass flasks, through analyzer	1 pair wk^{-1}	MLO only
	5-L evacuated glass flasks	1 pair wk^{-1}	MLO and Kumukahi
Surface ozone	Dasibi ozone meter	Continuous	
Total ozone	Dobson spectrophotometers nos. 63, 65, and 76	3 day^{-1}	No. 65, Jan-Jul Auto-Dobson No. 76, Mar-Dec
Ozone profile	Dobson spectrophotometers nos. 63, 65, 76	3 day^{-1}	Umkehr, Auto-Dobson No. 76, Mar-Dec
	Balloonborne ECC	1 wk^{-1}	From Hilo Airport beginning Dec
CFC-11, CFC-12, and N_2O	300-mL stainless steel flasks	1 pair wk^{-1}	
Aerosols			
Condensation Nuclei	Pollak CNC	Discrete	Weekdays
	G.E. CNC	Continuous	
Optical properties	Four-wavelength nephelometer	Continuous	450, 550, 700, 850 nm
Stratospheric aerosols	Lidar	Discrete	694.3 nm; average 1 profile wk^{-1}
Skylight polarization*	Polarizing radiometer	Discrete	320,365, 400, 500, 600, 700, 800, 900 nm; narrowband
Solar Radiation			
Global irradiance	Eppley pyranometers with Q, GG22, OG1, and RG8 filters	Continuous	
Direct irradiance	Eppley pyrheliometers (2) with Q, filters	Continuous	
	Eppley pyrheliometer with Q, OG1, RG2, and RG8 filters	Discrete	

Table 1.--Summary of sampling programs at MLO in 1984--Continued

Programs	Instrument	Sampling frequency	Remarks
Solar Radiation--Cont.			
Direct irradiance	Eppley pyrheliometer with 13 filters*	Continuous	
	Eppley/Kendall active cavity radiometer	Discrete	
Diffuse irradiance	Eppley pyranometer with shading disk and Q filter	Continuous	
Turbidity	J-series 1982 sunphotometers	Discrete	380,500, 778, 862 nm; narrowband
	WPL seven-wavelength sunphotometer*	Continuous	380, 422, 500, 596, 680, 778, 862 nm; narrowband
	PMOD three-wavelength sunphotometer	Continuous	380, 500, 778 nm; narrowband
Meteorology			
Air Temperature	Thermistor (aspirated)	Continuous	2 m height
	Max.-min. thermometers	1 day^{-1}	Standard shelter
	Hygrothermograph	Continuous	MLO and Kulani Mauka
Dewpoint temperature	Dewpoint hygrometer	Continuous	
Relative humidity	Hygrothermograph	Continuous	MLO and Kulani Mauka
Pressure	Capacitance transducer	Continuous	
	Microbarograph	Continuous	
	Mercurial barometer	Discrete	
Wind (speed and direction)	Bendix Aerovane	Continuous	6 m height
Precipitation	Rain gauge, 8-in	1 day^{-1}	
	Rain gauge, 8-in	1 wk^{-1}	Kulani Mauka
	Rain gauge, weighing	Continuous	
Total precipitable water	HAO infrared hygrometer	Continuous	
Precipitation Chemistry			
pH	pH meter	Discrete	Rainwater collections, 5 sites
Conductivity	Conductivity bridge	Discrete	Rainwater collections, 5 sites
Chemical components	Ion chromatograph	Discrete	Rainwater collections, 5 sites
Cooperative Programs			
CO_2 (SIO)	Infrared analyzer (Applied Physics)	Continuous	
CO_2, ^{13}C, N_2O (SIO)	5-L evacuated glass flasks	1 pair wk^{-1}	MLO and Kumukahi
Surface SO_2 (EPA)	Chemical bubbler system	Every 12 days	24-hr (00-24 hr) sample
CO_2, CO, CH_4, $^{13}C/^{12}C$† (CSIRO)	Pressurized glass flask sample	1 mo^{-1}	MLO, started Feb
CO_2, CH_4 and other trace gases† (NCAR)	Evacuated stainless steel flasks	1 pair wk^{-1}	MLO and Kumukahi
HNO_3 and HCL vapor† (Colorado College)	Special sampling system	4 periods yr^{-1}	First sample in Oct at MLO
Total surface particles (DOE)	High-volume sampler	Continuous	Dependent on wind direction; 1 filter wk^{-1}
Total suspended particles (EPA)	High-volume sampler	Every 12 days	24-hr (00-24 hr) sample
Atmospheric electricity* (NOAA)	Field mill, air conductivity meter	Continuous	
Ultraviolet radiation (Temple Univ.)	Ultraviolet radiometer (erythema)	Continuous	Radiation responsible for sunburning of of skin
Ultraviolet radiation† (Smithsonian)	7-wavelength UV radiometer	Continuous	Measurements began Aug
Precipitation collection (DOE)	Exposed collection pails	Continuous	
Precipitation collection† (ISWS)	Aerochemetric automatic collector	Continuous	Analysis for ^{7}BE and ^{10}BE started Feb
Precipitation collection (Univ. of Virginia)	Aerochemetric automatic collector	Continuous	Organic acid analysis
Wet-dry deposition (ISWS)	Aerochemetric automatic collector	Continuous	NADP
Aerosol chemistry (Univ. of Maryland	Nuclepore filters	Continuous	Upslope-downslope discrimination
Aerosol chemistry (Univ. of Arizona	Quartz filters	Continuous	Upslope-downslope discrimination
^{13}C (USGS, Denver)	10-L stainless steel flasks	Biweekly	
Radiocarbons* (USGS, Menlo Park)	NaOH collector	Discrete	
Carbon Monoxide (Max Planck Inst.)	Chemical reaction with HgO	Continuous	
Ozone and SO_2 (AES, Canada)	Brewer MK I spectrophotometer	Discrete	
Various trace gases (Oregon Grad. Center)	Stainless steel flasks	1 set wk^{-1}	MLO and Kumukahi

*Indicates program discontinued during 1984.
†Indicates new program initiated during 1984.

Carbon Dioxide

The concentration of atmospheric CO_2 was monitored continuously by the URAS-2 infrared analyzer during 1984. The instrument performed satisfactorily without major problems. Preliminary results indicate that the rate of increase of CO_2 concentration was approximately 1.35 ppm yr^{-1} for 1984.

The weekly CO_2 flask sampling programs at MLO and Cape Kumukahi were continued during the year. No flasks were lost or broken during shipment during the year. Some special flask samples were taken during the Mauna Loa eruption, but because of the extensive plume over much of the island they were of questionable value.

Outgassing from the volcanic caldera at the summit of Mauna Loa and from vents along the northeast rift caused disruptions of some of the CO_2 records in every month of the year. As in past years, it occurred mainly between 0000 and 0800 LST during the downslope wind regime. The frequency of the monthly occurrences are listed in table 2. The frequency of outgassing increased very markedly after the March eruption of Mauna Loa. Fume emissions and steam from one or more vents along the upper portion of the northeast rift zone were frequently visible. During the actual eruption, MLO as well as the whole Island of Hawaii, was frequently enveloped in volcanic plume.

Table 2.--Monthly occurrences of outgassing from the volcanic caldera on Mauna Loa during 1984

	Jan	Feb	Mar	Apr	May	Jun	Jul	Aug	Sep	Oct	Nov	Dec
No. of days	4	4	10*	*	14	19	16	25	18	22	21	14
Percent of days	13	14	42*	*	45	63	52	81	60	71	70	45

*Mauna Loa eruption on March 25 interrupted the CO_2 record from March 25 to April 28, 1984.

Ozone

Total ozone in the atmospheric column was measured routinely during 1984. In addition, the Dobson spectrophotometer was used for measuring the ozone profile by the Umkehr technique on 5 days per week until the automated Dobson went into regular service in June.

On March 12, automated Dobson No. 76 was put into service at MLO. The Mauna Loa eruption and other start-up problems delayed the collection of satisfactory data until June. Dobson observations were made during the power interruption using the manual instrument and a battery power source. Manual Dobson No. 65 was operated in parallel with the auto-Dobson in June and July for a system intercomparison. In July an intercomparison was run between Dobson Nos. 76, 65, and 83.

Surface ozone concentrations were obtained using the Dasibi UV photometeric instrument. Calibrations were carried out weekly.

Surface Aerosol Measurements

The G.E. CNC operated continuously with few maintenance or other problems except for the 5-day period, February 5 to 10, when a valve shaft froze. The Pollak counter was operated in the normal manner during the year. Both the G.E. CNC and Pollak instruments were down during the eruption power outage, although a few observations were taken with the Pollak using auxiliary power. Because of the extensive volcanic plumes, those data are of questionable value.

The nephelometer operated satisfactorily from January until June, except for the eruption period. In June, the signal output became increasingly intermittent. Various repairs were made between June and September, but when totally satisfactory performance was not attained, the unit was returned to GMCC Boulder in October for complete rebuilding.

Stratospheric Aerosols - Lidar

Lidar observations were carried out, weather permitting, on approximately a weekly schedule. The total number of observations during the year totaled 37. The stratospheric aerosol loading from the spring 1982 El Chichon eruption continued the decreasing trend established in 1983 with about a 50% decrease between the beginning and end of the year. There were apparently no new injections of volcanic aerosols into the stratosphere in 1984.

The eruptions of the local island volcanoes, Mauna Loa and Kilauea, had no impact on the stratospheric aerosol burden because neither resulted in explosive eruption activity. The power outage resulting from the Mauna Loa eruption interrupted the lidar observations for about 2 months, and during this time period the components were moved to Hilo for checking and maintenance.

During the summer of 1984, work supported by an EPA grant was begun to upgrade the MLO lidar system. This upgrade will include new optical components, mounting configuration, and a data acquisition system.

Meteorology

Meteorological measurements were continued without major problems or significant change in instruments during 1984.

Solar Radiation

The solar radiation program consists of several components: continuous solar measurements using both stationary and tracking instruments; discrete observations on a routine, weather-permitting basis; discrete manual, high-precision observations; and calibrations and intercomparisons of instruments using MLO facilities and instruments as working standards. All of these activities were carried out in 1984. The Mauna Loa eruption impacted on these measurements to some extent through the heavy fume production both during the actual eruption and for some period afterwards. Periods likely to be affected

by volcanic fumes were identified and data obtained during such periods were flagged for special consideration.

A normal incidence pyrheliometer, four global pyranometers with Q, GG22, OG1, and RG8 cutoff filters, and a diffuse Q pyranometer with shading disk were operated throughout the year to obtain continuous radiation measurements. The GG22 pyranometer developed a problem with condensation on the inside of the dome in September. When local maintenance could not bring about a long-term correction, the sensor was returned to GMCC, Boulder, for mothballing in January 1985 (at which time it was decided to discontinue measurements with the GG22). A filter-wheel pyrheliometer with Q, OG1, RG2, and RG8 cutoff filters was operated to obtain discrete broadband radiation measurements. Transmission generally increased slightly as the year progressed.

The active solar tracker and the 32-channel DAS operated the whole year with only minor problems in the automated solar dome. The dome and shutter controllers operated reasonably well, although there were some problems with the dome positioning motor and controller in June and again in August. Instruments mounted in the solar dome included a normal incidence pyrheliometer, an infrared water vapor meter, a seven-wavelength sunphotometer (retired from operation in January 1985), a three-wavelength PMOD sunphotometer, and an active cavity radiometer. Overall operation was fairly good during the year.

Turbidity measurements were obtained with hand-held sunphotometers J321 (380 and 500 nm) during the early part of the year before being replaced in April by instruments J202 (380 and 500 nm) and J314 (778 and 862 nm) for the rest of the year. These two sunphotometers were used at MLO during previous years and were returned to MLO after maintenance and calibration.

Skylight polarization measurements were terminated in July when an equipment failure could not be remedied. Measurements to that date indicated a return to near background stratospheric aerosol conditions following the significant loading caused by El Chichon in March-April 1982.

Precipitation Chemistry

The GMCC precipitation chemistry program continued without difficulties at about the same level of activity as in prior years. The MLO program consists of the collection and analysis of precipitation collected at five local sites. MLO also carries out the analysis of precipitation samples collected on the Island of Kauai and at GMCC observatories BRW, SMO, and SPO. The analysis of snow samples from SPO and rain water samples from SMO were 1984 additions to the existing MLO laboratory schedule. Weekly samples are collected at both those GMCC sites. Several cooperative programs in precipitation and deposition augment the GMCC program.

Cooperative Programs

The large number of cooperative programs at MLO continued in normal operation through 1984. A brief summary of some of these activities follows with an emphasis on the more recent additions.

A program of high precision UV radiation measurements at 7 wavelengths (295-325 nm) was begun in August at MLO by the SRBL. These data are important in assessing the potential impact of changes in the ozone layer and add considerable detail to the erythema (sunburn) radiation data gathered at MLO for a number of years by Temple University.

Precipitation collection for chemical analysis continued to be an important area of study. One new precipitation analysis program was the collection of samples for beryllium 7 and 10 analysis for the ISWS. Collections of precipitation for organic acid analysis at the University of Virginia continued as did sample collections for DOE and NADP.

Aerosol particle samples were collected on a weekly schedule using Nuclepore filters for the University of Maryland and quartz filters for the University of Arizona. Both programs used a sampler-controller which was activated on the basis of time of day, wind speed and direction, and condensation nuclei concentration. Total particle filters were also collected for DOE using a wind direction discriminating sampler controller. The purpose of these sampler-controllers is to separate sample collections according to upslope and downslope air masses. Downslope air should be representative of mid-tropospheric conditions while upslope air masses may contain various amounts of material with a recent origin at the earth's surface. High-volume sample data were also taken for EPA using standard EPA methods with one 24-hr filter sample taken every 12 days. This EPA observational data series began in 1971 although there have been some significant breaks in the record.

Total ozone and SO_2 in the atmosphere were measured for AES during the year with a Brewer MK I spectrophotometer. The CO analyzer of the Max Planck Institute, Mainz, Germany, was operated throughout the year, although there were a number of periods of downtime due to mechanical problems.

The SIO Applied Physics infrared CO_2 analyzer operated without major problems during 1984 in parallel with the GMCC CO_2 analyzer. Flask samples of air from MLO and Cape Kumukahi continued to be supplied to SIO on a weekday basis.

Flask sample collections were made both at MLO and at the seacoast at Cape Kumukahi. Flask collections at MLO were begun in 1984 for the Australian CSIRO. This group is analyzing the MLO samples for the $^{13}C/^{12}C$ ratio as well as for CO, CO_2, and CH_4. Other continuing flask sample programs include those of the OGC, NCAR, SIO. A new sampling program was begun at MLO in October 1984 when Dr. B. Huebert, Colorado College, set up a sampler for nitric acid and hydrochloric acid vapors. Collections are made for 2-wk periods every 3 months by Colorado College investigators.

REFERENCES

Lockwood, J. P., N. G. Banks, T. T. English, L. P. Greenland, D. B. Jackson, D. J. Johnson, R. Y. koyanagi, K. A. McGee, A. T. Okamura, and J. M. Rhodes, 1985. The 1984 eruption of Mauna Loa Volcano, Hawaii, EOS, 66:169-171.

2.2 Barrow

FACILITIES

Operation of the NARL facility was transferred from the USGS to UIC, a native corporation, on October 1, putting our long-term supply of electrical service in question. By the end of 1984, negotiations were under way with the Air Force to have the DEW line station supply our power.

The Barrow GMCC Observatory was featured in a local newspaper article and on the front page of the Los Angeles Times in connection with Arctic Haze. A reporter from National Geographic Magazine visited in November.

Starting in August, personnel were on duty at the station 7 days per week. An IBM PC was used to demonstrate the feasibility of transferring data with Boulder over the FTS phone lines. The station photocopier was purchased, and the lease agreement terminated, with the purchase price equal to 11 months rent.

The observatory was extensively renovated in August. All rooms were carpeted and painted, and instruments were rearranged in conjunction with the CAMS installation. The roof-top blowers were removed and outlets rewired in June. By October the sampling room ceiling and east wall were covered with sound-deadening acoustic tile and an outdoor walkway was built around the station and between the station and garage. The garage was insulated and a high BTU heater installed in February.

The GMCC housing unit received a coating of exterior foam insulation in August which should prevent future ceiling water damage caused by freeze-out of interior water vapor. A problem with the tank water liner was solved and the pump repaired in December.

In August, delivery was taken on a 1983 Dodge Crewcab truck from the GSA fleet in Anchorage. GSA also took over the GMCC Suburban and is now billed for the fuel and maintenance costs of these two vehicles. The blue GMC pickup had a new engine installed in May. The trucks performed well in 1984 with the usual number of minor repairs and flat tires. The Sidewinder ATV continued to be troublesome and is to be excessed in 1985. A new freight sled was built and the Bombi tracked vehicle was renovated in December.

PROGRAMS

CAMS

On August 7-16 the Barrow Observatory became the first in the GMCC chain to be changed over to CAMS operation. For the remainder of the year, except for two power outages, a 100% data acquisition uptime was experienced. Problems during this initial period have been few and minor in nature. Several software bugs have turned up. The boxes will infrequently auto-restart, and the primary tape drive will occasionally develop a write error and switch to the backup drive. The performance of CAMS is far superior to the previous ICDAS system in terms of reliability and ease of operation and repair.

Carbon Dioxide

The continuous analyzer system was completely replumbed in August. The ground air line was removed at this time. In November, a new chart recorder with felt-tipped pens replaced the aging, troublesome inked chart recorder.

A new greaseless stopcock 3L flask was introduced to the program in 1984 and will someday replace the 5L flasks.

Surface Ozone

Surface ozone data were collected without interruption except for a 2-week period in May when the Dasibi ozone detector and ozone generator were in Boulder for calibration and service.

Surface Aerosols

The G.E. CNC operated intermittently, with several long periods of good operation. The unit flooded six times in 1984 and twice had a problem which caused the breaker to trip after several hours of operation. The nephelometer and Pollak counter continued to perform well.

Solar Radiation

Early problems with poor noise rejection at the millivolt level by CAMS were overcome with the addition of a pre-amplifier board in early 1985. In October, an HP71 based data acquisition system was installed to replace an aging chart recorder. This system has performed well, yielding good measurements at millivolt signal levels with resolution down to microvolts.

In December, infrared radiation measurements began with the installation of two pyrgeometers.

Meteorology

During the first half of the year problems were experienced with the wind direction portion of the Aerovane. With the installation of CAMS, a new Aerovane, a pressure transducer, two aspirated thermocouples, and a dew point hygrometer were put online. An intermittent frosting problem occurred in the dew point hygrometer as winter temperatures approached and the unit quit operation in December. All other meteorological instruments performed well.

COOPERATIVE PROGRAMS

The SRBL radiation monitoring program was discontinued on November 19.

A new pump system was installed in January for DOE.

For several months during the summer, a navigational antenna was operated 100 yards north of the station by Offshore Navigation, Inc. Our support included use of our road for access and a small amount of 110V electricity. The purpose of their operation was to fix the position of oil exploration ships in the Arctic Ocean.

Table 3. Summary of Sampling Programs at BRW in 1984

Program	Instrument	Sampling Frequency
Gases		
CO_2	URAS-2T infrared analyzer	Continuous
	0.5-L glass flasks P[3]	1 pair wk^{-1}
	0.5-L glass flasks, through analyzer	1 pair wk^{-1}
	5-L evacuated glass flasks	1 pair wk^{-1}
	3-L evacuated glass flasks	1 pair wk^{-1}
Surface ozone	Dasibi ozone meter	Continuous
Methane	0.5-L glass flasks	1 pair wk^{-1}
CFC-11, CFC-12, and N_2O	300-mL stainless steel flasks	1 pair wk^{-1}
Aerosols		
Condensation Nuclei	Pollak CNC	Discrete
	G.E. CNC	Continuous
Optical properties	Four-wavelength nephelometer	Continuous
Solar Radiation		
Global irradiance	Eppley pyranometers with Q and RG8 filters	Continuous
Direct irradiance	Tracking NIP	Continuous
Direct irradiance	Eppley pyrheliometer with Q, OG1, RG2, and RG8 filters	Discrete
Terrestrial (IR) radiation	Eppley pyrgeometer	Continuous
Turbidity	Sunphotometers with 380-, 500-, 778-, and 862-nm narrowband filters	Discrete
Sky documentation	All-sky camera (Fisheye)	Discrete
Meteorology		
Air Temperature	Thermistor	Continuous
	Max.-min. thermometers	1 day^{-1}
Dewpoint temperature	Dewpoint hygrometer	Continuous
Pressure	Capacitance transducer	Continuous
	Microbarograph	Continuous
	Mercurial barometer	Discrete
Wind (speed and direction)	Bendix Aerovane	Continuous
Precipitation Chemistry		
pH	pH meter (samples analyzed at MLO)	Discrete
Conductivity	Conductivity bridge (samples analyzed at MLO)	2 mo^{-1}
Cooperative Programs		
Total surface particulates (DOE)	High-volume sampler	Continuous (1 filter wk^{-1})
Aerosol chemistry (URI)	High-volume sampler	Continuous (2 filters wk^{-1})
Global radiation (SRL)	6 Eppley pyranometers	Continuous
Ultraviolet radiation (Temple Univ.)	Ultraviolet radiometer	Continuous
CO_2, ^{13}C, N_2O (SIO)	5-L evacuated glass flasks	1 pair wk^{-1}
Precipitation gauge (ASCS)	Wyoming shielded precipitation gauge	2 mo^{-1}
Carbonaceous particles (LBL)	Dichotomous sampler (Quartz and Millipore filters)	Continuous (1 set of filters wk^{-1})
	High-volume filter	Continuous (1 filter wk^{-1})
	Daily Millipore sampler	Continuous (1 filter day^{-1})
Various trace gases (OGC)	Stainless steel flasks	1 set wk^{-1} (3 flasks set^{-1})
Magnetic fields (USGS)	Magnetometer	1 station check wk^{-1})
^{13}C (USGS)	10-L stainless steel flasks	1 pair mo^{-1}
Various trace gases (NCAR)	3-L stainless steel flasks	1 pair wk^{-1}
$^{13}C/^{12}C$ (CSIRO)	5-L glass flasks	1 pair mo^{-1}

2.3 Samoa

FACILITIES

The Samoa GMCC facility gained a significant addition in late 1984 when a new remote sampling building was erected adjacent to the ridge sampling tower. The original OGC building, in place since July 1978, and the old prefab building left over from the 1981 SEAREX project, were removed to make room the new building.

The new building is a prefabricated structure built by the EKTO Company. It arrived in late October and was assembled on site. Steve Crawford from the OGC, assisted in removal of the old OGC building and erection of the EKTO.

One feature of the EKTO is that it is large enough (16' × 20') to combine both GMCC and OGC operations under one roof. A partition separates the internal space into two rooms, with separate entrances, air conditioners, and electrical supplies. A separate entrance for the gas chromatograph compartment also ensures minimum disruption from pedestrian traffic associated with other GMCC programs.

A primary reason for purchasing the EKTO structure was its non-contaminating structural materials. Flask samples obtained from the interior of another EKTO structure in Samoa and analyzed by the OGC for evidence of room contamination, exhibited very low concentration of potential contaminants. Additionally the SEAREX EKTO building had weathered well in the Samoa climate.

Data Acquisition

During October 1984, the Samoa ICDAS system, in place since Observatory operations began in January 1976, was taken offline for the last time and new CAMS boxes were installed to acquire data and control GMCC equipment. Ed Green was at Samoa to implement the changeover. The new system went online easily and operated trouble free through the end of the year.

Samoa PV System

The Samoa photovoltaic system "officially" went online 15 February 1984 after final testing and certification by Gary Herbert. After instrumenting the arrays with temperature and three-component wind sensors, a final set of IV curves was obtained as part of the final acceptance procedure for the project. The system remained online for the rest of the year.

Although the system installation had been completed in 1983, problems with the inverter and array disconnect switch delayed startup until early 1984. In October, when installation of the SMO/GMCC CAMS units occurred, a specially modified CAMS unit was installed for controlling the PV system. The PV CAMS unit was designed to control the PV system battery charging operations. Evidence suggested adequate insulation levels were present to recharge the PV system storage batteries, but getting the energy into the

batteries from the arrays was not as efficient as necessary, and net daily losses of battery state of charge (SOC) became evident after initial system startup. The CAMS controller unit improved the efficiency of the daily recharging cycle.

The battery storage system was sized to operate the PV load for approximately 2 days if cloudiness prevented an adequate daily charging cycle. A battery charger was designed into the system to automatically come online and charge the batteries using commercial power if the battery SOC/voltage decreased to a specified level. During 1984, the charger automatically switched on only four or five times. Although the charger was too small to actually increase SOC of the batteries, it could maintain system operation and prevent very deep discharge of the batteries until the solar energy source returned and a normal charging cycle could be restored.

SAMOA LEASE RENEGOTIATION

Samoa GMCC Observatory property is Samoan communal land leased from the Iuli family in Tula village. The original lease, signed in 1974, stipulates a renegotiation of the lease every 5 years.

The first renegotiation was conducted in 1979 by N. W. Stiewig. A second renegotiation occurred in 1984 and was conducted by Jim Watkins, who was with GMCC for a few years in the early 1970's and was extensively involved in the original Samoa GMCC lease arrangement and subsequent design and construction of the Observatory. He arrived in Samoa 29 February and departed 4 March. While on the island, meetings were held with the American Samoan Government officials and the negotiator for the Iuli family, Salanoa S. P. Aumoaualogo, a High Chief from Tula Village. A negotiator for the Iuli family was necessary because a successor had not been chosen for Chief Iuli, Togi, who passed away suddenly in September 1983. High Chief Salanoa was suggested as the Iuli family negotiator and through his efforts and Jim Watkins, a new 5-year agreement was reached, through the 15th year of the current 20-year lease. An option to renew for 20 additional years exists.

PROGRAMS

GMCC Programs

The complement of GMCC programs at the Samoa Observatory remained unchanged during 1984 and are listed in table 1.

Cooperative Programs

A CO_2 flask sampling program for Dr. Graeme Pearman, CSIRO, was initiated in March. A once-per-month sampling schedule will be maintained for at least 2 years. Its purpose is to gather data concerning the CO_2 cycle.

Table 4.--Summary of sampling programs at SMO in 1984

Program	Instrument	Sampling Frequency
Gases		
CO_2	URAS-2T infrared analyzer	Continuous
	0.5-L glass flasks P[3]	1 pair wk^{-1}
	0.5-L glass flasks, through analyzer	1 pair wk^{-1}
	5-L evacuated glass flasks	1 pair wk^{-1}
Surface ozone	Dasibi ozone meter	Continuous
Total ozone	Dobson spectrophotometer no. 42	3 day^{-1}
Methane	0.5-L glass flasks	1 pair wk^{-1}
CFC-11, CFC-12, and N_2O	300-mL stainless steel flasks	1 pair wk^{-1}
Aerosols		
Condensation Nuclei	Pollak CNC	Discrete
	G.E. CNC	Continuous
Optical properties	Four-wavelength nephelometer	Continuous
Solar Radiation		
Global irradiance	Eppley pyranometers with Q and RG8 filters	Continuous
	Eppley pyranometers with Q filters on tilted mounts	Continuous
Direct irradiance	Eppley pyrheliometer with Q filter	Continuous
Direct irradiance	Eppley pyrheliometer with Q, OG1, RG2, and RG8 filters	Discrete
Turbidity	Sunphotometers with 380-, 500-, 778-, and 862-nm narrowband filters	Discrete
Meteorology		
Air Temperature	Thermistor	Continuous
	Max.-min. thermometers	1 day^{-1}
	Hygrothermograph	Continuous
	Thermistor	1 day^{-1}
Dewpoint temperature	Dewpoint hygrometer	Continuous
Relative humidity	Hygrothermograph	Continuous
	Sling psychrometer	Discrete
Pressure	Capacitance transducer	Continuous
	Microbarograph	Continuous
	Mercurial barometer	Discrete
Wind (speed and direction)	Bendix Aerovane	Continuous
Precipitation	Polyethylene funnel, bottle	1 day^{-1}
Precipitation Chemistry		
pH	Corning model 125 meter with semimicro combination electrode	1 day^{-1} (GMCC); 1 wk^{-1} (NADP)
Conductivity	Beckman model RC-16C meter	1 day^{-1} (GMCC); 1 wk^{-1} (NADP)
Cooperative Programs		
CO_2, ^{13}C, N_2O (SIO)	5-L evacuated glass flasks	1 pair wk^{-1}
ALE project: CFC-11, CFC-12, N_2O, CH_3CCl_3, CCl_4 (OGC)	HP5840A gas chromatograph	1 h^{-1}
ALE project: CH_4, CO, CO_2 (OGC)	Carle gas chromatograph	3 h^{-1}
Various trace gases (OGC)	Stainless steel flasks	1 set wk^{-1} (3 flasks set^{-1})
^{13}C, ^{18}O, CO_2 (CSIRO)	5-L glass flasks	1 set mo^{-1}
^{13}C (USGS)	10-L stainless steel flasks	2 pair mo^{-1}
Wet-dry deposition (NADP)	HASL wet-dry collector (new Chemetrics, Dec 81)	1 wk^{-1}, wet; 2 mo^{-1}, dry
Bulk deposition (EML)	Plastic bucket	1 mo^{-1}
Hi-Vol sampler (EML)	Hi-Vol pump and filter	1 wk^{-1}
Hi-Vol sampler (SEASPAN Project)	Hi-Vol pump and filter with clean	1 wk^{-1}

2.4 South Pole

FACILITIES

Amundsen-Scott South Pole Station is the most remote of the four GMCC Observatories. The South Pole station is situated at the south geographic pole on the polar plateau at an elevation of over 2,835 meters. The average yearly temperature is -49°C. Due to its unique environment and remoteness, South Pole station is only accessible during the Austral summer by aircraft from about 01 November until about 10 February. All resupply and replacement of personnel must be made during this period, with the possible exception of an air-drop in mid-winter (June). The station is isolated from the outside world from February through October.

Considering the number of projects carried out by the GMCC program, equipment performance was exceptional. Other than minor equipment failures, the problems were few, and remedied quickly. At year's end, all programs were online and operating properly with two exceptions. The NOAA GC was offline until new standard gas arrived and albedo pyrgeometer was offline until a replacement dome arrived. Both programs were reinstated shortly after Pole opening.

All GMCC and cooperative projects are located in the Clean Air Facility (CAF). Snow buildup around the CAF continues to be a major problem and a growing concern for GMCC programs. Stack icing, air intakes plugged with blowing snow, and direct line of sight for total ozone and solar observations are immediate problems, and many more will arise if the CAF is not raised in the near future.

During March 1984 major improvements in distribution of station power reduced overall noise levels and virtually eliminated power brownouts. In early May all GMCC electronic instrumentation was integrated into the CAF isolation transformer.

PROGRAMS

Table 5 lists the sampling programs carried out during the 1983-84 season.

Gas Sampling

The CO_2 program required a minimum number of repairs and/or modifications during the course of the year. The Dobson worked well all year and remained in calibration with no noticeable drift. Continuous surface ozone readings were taken with the Dasibi ozone monitor, and no major problems were encountered. The gas chromatograph and HP integrator worked flawlessly the entire year.

Table 5.--Summary of sampling programs at SPO in 1984

Program	Instrument	Sampling Frequency	Length of Record
Gases			
CO_2	URAS-2T infrared analyzer	Continuous	Jan 74-present excl. Nov 78-Nov 79)
	0.5-L glass flasks P[3]	1 pair (2 wk)$^{-1}$	Jun 81-present
	0.5-L glass flasks, through analyzer	1 pair (2 wk)$^{-1}$	Nov 79-present
Surface ozone	Dasibi ozone meter	Continuous	Jan 76-present
Total ozone	Dobson spectrophotometer no. 80	3 day^{-1}	Dec 63-present
Methane	0.5-L glass flasks	1 pair wk^{-1}	1984
CFC-11, CFC-12, and N_2O	300-mL stainless steel flasks	1 pair wk^{-1}	Jan 77-Dec 79
		1 pair wk^{-1}, summer; 1 pair mo^{-1}, winter	Jan 80-present
	Gas chromatograph	2 analyses/wk^{-1}	Dec 83-present
Aerosols			
Condensation Nuclei	Pollak CNC	Discrete	Jan 74-present
	G.E. CNC	Continuous	Jan 74-present
Optical properties	Four-wavelength nephelometer	Continuous	Jan 79-Dec 79; Jan 81-present
Solar Radiation			
Global spectral irradiance	Eppley pyranometers with Q, OG1, and RG9 filters	Continuous	Feb 74-present
	Eppley pyrheliometer with Q, OG1, RG2, and RG8 filters	Discrete	Jan 77-present
Turbidity	Sunphotometers with 380-, 500-, 778-, and 862-nm narrowband filters	Discrete	Jan 74-present
Albedo	Eppley pyranometers with Q and RG8 filters, downward-facing	Continuous	Jan 82-present
Terrestrial (IR) radiation	Eppley pyrgeometers, upward- and downward-facing	Continuous	Mar 83-present
Total water vapor	Infrared solar hygrometer	Discrete	Summer
Meteorology			
Air Temperature	Platinum resistor	Continuous	Mar 77-present
Snow temperature	Platinum resistor .5 cm	Continuous	Apr 83-present
Pressure	Capacitance transducer	Continuous	Dec 75-present
	Microbarograph	Continuous	Feb 80-present
	Mercurial barometer	2 times/day	Jan 80-present
Wind speed/direction	Bendix Aerovane recorder	Continuous	
Cooperative Programs			
CO_2, ^{13}C, N_2O (SIO)	5-L evacuated glass flasks	2 mo^{-1} (3 flasks sample^{-1})	1957-present
Total surface particulates (DOE)	High-volume sampler	Continuous (1 filter wk^{-1})	May 70-present
Aerosol physical properites (SUNYA)	Pollak CNC with diffusion battery	Discrete	Jan 74-present
	Nuclepore filters	Discrete	Nov 83-present
Carbon aerosol (LBL)	High-volume sampler	Continuous	Jan 82-present
Various trace gases (OGC)	Stainless steel flasks	Twice mo^{-1} (3 flasks set^{-1})	1980-present
$^{13}C/^{12}C$, CH_4 (USGS)	10-L stainless steel cylinder	1 mo^{-1} (2 cylinders sample^{-1})	Jan 81-present
^{14}C (NOAA/ARL	3,000 psi spheres	500 psi day^{-1}	1972-present
Snow acidity (NOAA/ARL)	125-mL Nalgene flasks	Weekly	1982-present
CH_4, CO (NCAR)	Baseline gas chromatograph	Daily	Apr 83-present
	Aluminum flasks	Weekly	Apr 83-present
$^{14}C/^{12}C$ NaOH samples (USGS)	Gas bubbler	20 days/month	Summer 83 to present
Atmospheric Tracer Exp. (Los Alamos Nat. Lab.)	CH_4 detector	3-60 day periods	Summer 83 present
Cosmic Dust Collection (Univ. of Pittsburgh)	Cosmic dust collector	Continuous	Summer 83 present
Interhemispheric $^{13}C/^{14}C$ (CSIRO)	Flasks	2 Flasks/month	Summer 83 present

Surface Aerosols

The Pollak performed extremely well this year and comparisons with the G.E. CNC were generally very good. The G.E. CNC also performed well for the entire year with the exception of two short problem periods. With small changes in concentrations it followed the Pollak closely; however, large variations in concentration caused the G.E. CNC to require recalibration.

Solar Radiation

Installation and data acquisition began in March for the new IR upward- and downward-viewing pyrgeometers. The replacement of the battery supply with DC power supply for both pyrgeometers reduced voltage variations to less than 0.001 V.

With the exception of data gathered by the solar infrared hygrometer in November and early December, the remainder of the solar radiation equipment performed very well.

During the summer several major problems occurred to the nephelometer. In the last week of December one channel went to zero and all recovery techniques would not bring it back again. This was determined to be a short to ground caused by the multiplexer/digitizer signal input board. Repairs were completed at the end of January.

From February through May there were numerous memory losses for one of more channels for the nephelometer. The problem was eventually diagnosed and the random memory crashes were eliminated.

Meteorology

In December a new meteorological tower was constructed 300 feet from the CAF at grid 110 degrees, the southeast boundary to the clean air sector. On 18 January the Bendix-Friez Aerovane was mounted on the new tower at 34 feet, height of the trace gas stack intake. The addition of this and other meteorological instruments was a joint project with A. Hogan of SUNYA to determine low level wind shear, vertical wind speed, and low level temperature gradient.

Between January 18 and 23, Tom DeFoor examined the temperature measurement system at the SPO. The SPO air temperature measured approximately 3°C cooler than the temperature measured at the SPO Weather Station. The sensor installation of the two sensors was similar and could not account for the temperature differences. All electronic and sensor problems with the GMCC equipment were repaired and adjustments were performed using a new 0°C temperature source and the -62.67°C sensor test plug. As a result, good agreement between the two temperature channels was achieved; however, both channels now read approximately 2°C warmer than the official temperature at the station meteorological office.

ICDAS

No problems were encountered with the minicomputer, voltage regulator, tape drive, or clock. At the beginning of the year an input board on the MUX shorted and caused the loss of one channel of data input from the nephelometer, and several problems existed with the teletype.

During the course of the year, frequency variations due to large electrical power requirements during welding caused over 30 ICDAS crashes. After transfer of the ICDAS system to an isolated power transformer, the ICDAS system was less susceptible to crashes; however, this was not always the case. Any time welding operations occurred, ICDAS and electronic instrumentation had to be checked.

COOPERATIVE PROGRAMS

The majority of the cooperative sampling programs listed in table 5 experienced no major difficulties during the course of the year.

In December, two Gill Aerovanes were installed on the new met tower at 13 and 84 feet. Unfortunately, however, numerous problems were experienced throughout the year with the 84-foot Aerovane.

The NCAR gas chromatograph and its supporting systems experienced several problems during the year. When the station opened, the 5 volt regulator was faulty and was replaced. Carbon monoxide could not be analyzed because the instrument was not sensitive enough. In February, the flame ionization detector failed because the collector connection was corroded. The repair lasted one month and failed again. A second attempt to repair the same problem failed. A new flame ionization detector was received on the mid-winter airdrop, and after installation, the gas chromatograph was back on line.

3. AEROSOLS AND RADIATION GROUP

3.1 Continuing Programs

SURFACE AEROSOLS

The GMCC aerosol monitoring program continued during 1984 as in previous years. Condensation nucleus (CN) concentration and aerosol scattering extinction coefficient (σ_{sp}) were measured continuously at BRW, MLO, SMO, and SPO. A G.E. automatic CNC operates continuously and a Pollak CNC provides daily calibration points at each station. A four-wavelength nephelometer at each station continuously measures σ_{sp} at 450-, 550-, 700-, and 850-nm wavelengths.

Figure 1 shows daily geometric means of σ_{sp} and CN concentration at the GMCC stations for 1984. Angstrom exponents calculated from the four-wavelength light scattering data are shown in the upper portions of the graphs. Only CN concentrations are shown for MLO because of major problems with the MLO four-wavelength nephelometer during 1984. Monthly geometric means of the entire data record for each station are shown in fig. 2. Monthly geometric means for 1984 for BRW, MLO, SMO, and SPO are tabulated in table 1. Monthly geometric means for 1983 for MLO are also included in table 1 because they were omitted from the GMCC annual report for 1983.

The BRW data in fig. 1 show elevated σ_{sp} values in excess of 10^{-5} m^{-1} in the springtime, typical of the well-known Arctic Haze. This regular annual cycle is apparent in the BRW long-term record shown in fig. 2 with monthly means exceeding 10^{-5} m^{-1} in the spring and below 10^{-6} m^{-1} in the summer. The BRW CN record shows a more variable semiannual cycle with maxima usually occurring in March and August, and minima usually occurring in June and November.

The MLO CN data shown in fig. 1 are typical for Mauna Loa and are most likely representative of the background troposphere for this region of the atmosphere. The long-term record of σ_{sp} in fig. 2 shows an annual cycle with a maximum in April-May which is caused by the long-range transport of Asian desert dust in the upper troposphere to the vicinity of Hawaii.

The SMO σ_{sp} and CN data continue as in previous years with no significant annual cycle or long-term trend. Bodhaine and DeLuisi (1985) presented a detailed analysis of the Samoa data set.

The SPO CN data show a strong annual cycle with a maximum greater than 100 cm^{-3} in the austral summer and a minimum of about 10 cm^{-3} in the winter. The σ_{sp} data show a cycle dominated by events in the austral winter. These events are caused by the transport of seasalt in the upper troposphere from stormy regions near the coast to the interior of the continent. An analysis of the SPO data set and case studies of the winter seasalt events were presented by Bodhaine et al. (1986).

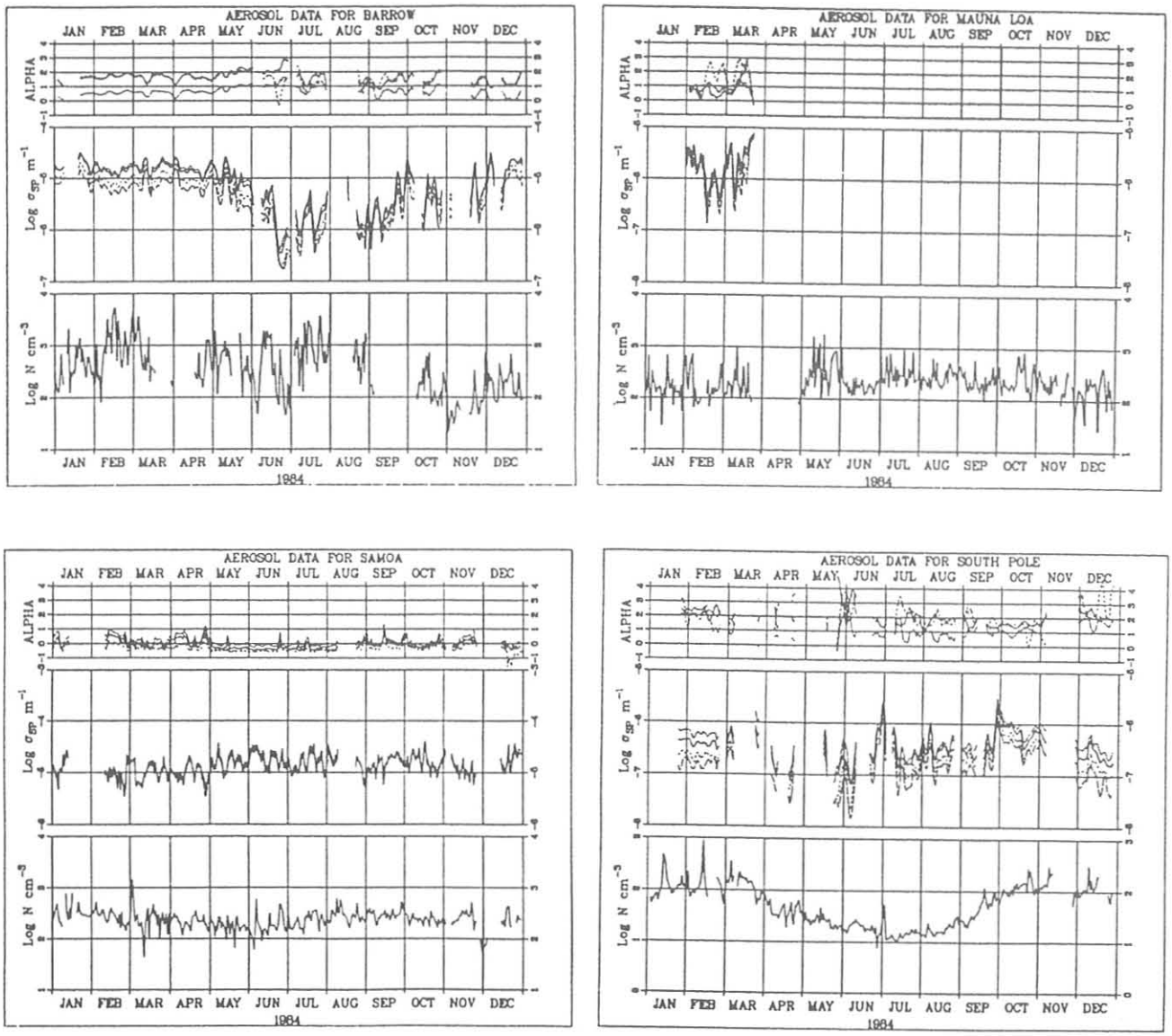

Figure 1.--Daily geometric means of σ_{sp} and CN data at BRW, SMO, and SPO, and CN data at MLO for 1984. For each station, CN concentration lower is shown as a solid line. σ_{sp} data (middle) are shown for 450 (dotted), 550 (solid), 700 (dashed), and 850 nm (long-dashed). Angstrom exponents (upper) were calculated from 450- and 550-nm (dotted), 550- and 700-nm (solid), and 700- and 850-nm (dashed) σ_{sp} data.

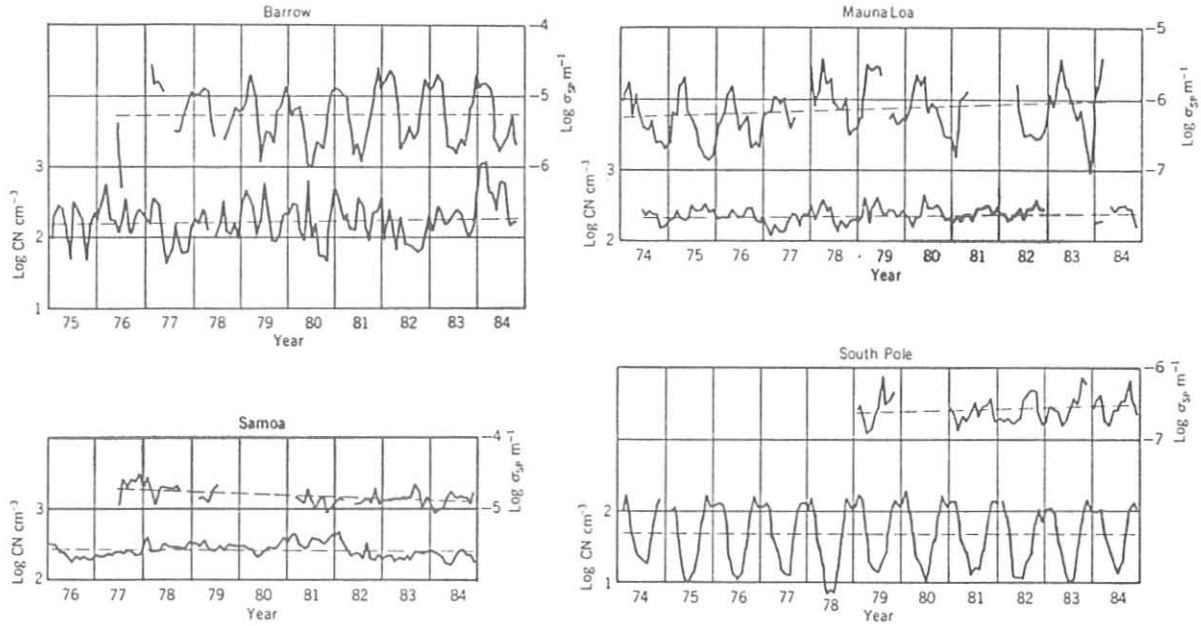

Figure 2.--Monthly geometric means of σ_{sp} and CN data for the entire data record, as in fig. 1. The straight dashed lines are least-squares linear trend lines.

SOLAR AND THERMAL RADIATION

Direct and global broadband solar radiation monitoring at the four baseline observatories continued throughout 1984. The measurement programs which make up the basic solar radiation program at all four sites are given in table 2.

Certain additional radiation monitoring projects are carried out at the GMCC observatories. Table 3 lists the additional radiation measurements at each observatory.

All data acquired from projects listed in tables 2 and 3 are either routinely edited and archived or made available on request if feasible. The GMCC ARM staff processes, interprets, and publishes the data as applicable to present research interests, some of which are discussed later.

As in previous years, the GMCC traveling standard pyranometer and pyrheliometer were operated for a period of several to many days, side-by-side, with station instruments at each station. The traveling standards are calibrated on a yearly basis at the NOAA Solar Radiation Calibration Facility in Boulder. Data quality assurance checks are performed daily by observatory personnel. Starting in 1985, daily comparisons of measured broadband solar data and clear sky model calculations will be made at each observatory. A comparison of the clear-sky model performance versus the historical GMCC solar data base is given later in this report.

Table 1.--Monthly geometric means of CN concentration (cm^{-3}) and σ_{sp} (m^{-1}) at 450, 550, 700, and 850 nm for MLO during 1983 and for BRW, MLO, SMO, and SPO during 1984.

	Jan	Feb	Mar	Apr	May	Jun	Jul	Aug	Sep	Oct	Nov	Dec
BRW 1984												
CN	398	952	673	401	456	273	776	761	139	156	70	173
σ_{sp}(450)	1.89-5	1.57-5	1.86-5	1.61-5	1.23-5	2.76-6	2.21-6	2.43-6	3.59-6	6.52-6	5.43-6	1.60-5
σ_{sp}(550)	1.76-5	1.40-5	1.65-5	1.44-5	1.03-5	2.14-6	1.84-6	2.12-6	3.14-6	5.73-6	4.71-6	1.50-5
σ_{sp}(700)	1.24-5	9.20-6	1.10-5	9.87-6	6.39-6	1.26-6	1.26-6	1.61-6	2.29-6	3.97-6	3.25-6	1.09-5
σ_{sp}(850)	9.22-6	6.51-6	8.01-6	7.30-6	4.44-6	9.45-7	9.25-7	1.25-6	1.75-6	2.99-6	2.39-6	8.36-6
MLO 1983												
CN	251	338	283	342	334	308	343	375	451	318	194	179
σ_{sp}(450)	1.56-6	1.06-6	2.12-6	4.34-6	1.64-6	1.54-6	9.43-7	6.40-7	8.73-7	4.87-7	1.19-7	2.47-7
σ_{sp}(550)	1.18-6	7.97-7	1.75-6	3.52-6	1.37-6	1.34-6	8.82-7	5.07-7	6.55-7	3.17-7	9.15-8	1.86-7
σ_{sp}(700)	9.99-7	6.58-7	1.35-6	2.92-6	1.16-6	1.27-6	8.87-7	4.57-7	5.35-7	2.28-7	7.03-8	1.40-7
σ_{sp}(850)	5.95-7	3.71-7	9.53-7	2.19-6	9.13-7	1.10-6	5.54-7	3.03-7	3.65-7	1.54-7	5.02-8	1.06-7
MLO 1984												
CN	152	201	187	82	320	193	317	276	235	249	212	150
σ_{sp}(450)	8.92-7	1.59-6	3.13-6	-	-	-	-	-	-	-	-	-
σ_{sp}(550)	7.93-7	1.35-6	2.70-6	-	-	-	-	-	-	-	-	-
σ_{sp}(700)	6.96-7	1.17-6	2.11-6	-	-	-	-	-	-	-	-	-
σ_{sp}(850)	4.14-7	8.66-7	1.54-6	-	-	-	-	-	-	-	-	-
SMO 1984												
CN	292	272	248	211	175	177	224	282	294	238	235	192
σ_{sp}(450)	1.37-5	9.61-6	1.04-5	1.04-5	1.41-5	1.72-5	1.41-5	1.57-5	1.53-5	1.59-5	1.25-5	1.75-5
σ_{sp}(550)	1.27-5	8.53-6	1.01-5	9.45-6	1.41-5	1.76-5	1.42-5	1.54-5	1.47-5	1.55-5	1.20-5	1.79-5
σ_{sp}(700)	1.25-5	7.82-6	1.02-5	9.00-6	1.50-5	1.91-5	1.52-5	1.60-5	1.45-5	1.57-5	1.20-5	1.85-5
σ_{sp}(850)	1.28-5	7.87-6	1.09-5	9.33-6	1.65-5	2.11-5	1.67-5	1.71-5	1.47-5	1.64-5	1.24-5	2.13-5
SPO 1984												
CN	117	111	126	43	25	18	14	18	43	116	138	111
σ_{sp}(450)	6.34-7	6.00-7	6.69-7	2.40-7	1.89-7	3.36-7	3.38-7	4.27-7	4.75-7	9.00-7	4.82-7	3.39-7
σ_{sp}(550)	4.09-7	3.89-7	4.55-7	1.84-7	1.62-7	2.77-7	2.81-7	3.65-7	3.69-7	7.27-7	3.49-7	2.37-7
σ_{sp}(700)	2.30-7	2.24-7	2.73-7	1.12-7	9.76-8	1.75-7	1.80-7	2.38-7	2.59-7	4.99-7	2.02-7	1.39-7
σ_{sp}(850)	1.39-7	1.63-7	2.18-7	7.60-8	6.76-8	1.14-7	1.14-7	1.70-7	1.74-7	3.73-7	1.43-7	7.52-8

A compact exponential format is used for such that 1.89-5 = 1.89×10^{-5}.

All observatory programs remained basically unchanged during 1984 with the following exceptions.

In September a new albedo instrument support rack was installed at the South Pole. This greatly improved leveling capability of the mounted instruments. Leveling of the albedo instruments is critical during times that they are faced up for comparison with the fixed upward-facing pyranometer and pyrgeometer. It is believed that the new albedo rack is too low to obtain a representative reflectance from the snow surface. Plans are to raise the reflectance measurement height to about 10 feet in 1985.

An experimental pyranometer designed to prevent the deterioration of the RG8 filter dome in tropical environments was taken offline at Samoa after it was determined that it produced erroneous results. A protective clear dome intended to protect the RG8 glass led to overheating of the instrument.

In late 1984 the GMCC field data acquisition system, ICDAS, was replaced by the new CAMS. Conversion to CAMS and the preamplifiers was completed by early 1985.

Table 2.--GMCC basic radiation monitoring measurements

Instrument	Quantity Measured	Wavelength
Tracking pyrheliometer	Direct solar	0.28-3.0 μm
Pyranometer (Quartz)	Global sky	0.28-3.0 μm
Pyranometer (RG8)	Global sky	0.695-3.0 μm
Filter wheel pyrheliometer	Direct solar	0.28-3.0 μm
OG1	Direct solar	0.530-3.0 μm
RG2	Direct solar	0.63-3.0 μm
RG8	Direct solar	0.695-3.0 μm
Spectral sunphotometer	aerosol optical depth	380, 500, 778 862 nm

Table 3.--GMCC radiation measurements specific to individual observatories

Location	Instrument	Quantity Measured	Wavelength
South Pole	RG8 tracking pyrheliometer	Direct sun	0.695-3.0 μm
	Pyrgeometer	Sky infrared	4.0-5.0 μm
	Inverted pyrgeometer	Surface infrared	4.0-50. μm
	Inverted pyranometer	Surface reflected	0.28-3.0 μm
Mauna Loa	Shaded pyranometer	Diffuse sky	0.28-3.0 μm
	Solar IR hygrometer	Precipitable H_2O	1.06, 1.13 μm
	Solar IR hygrometer	Precipitable H_2O	0.88, 0.94 μm
	Absolute cavity	Direct solar	All
	PMOD/GMCC sunphotometer	Continuous aerosol Optical depth	380, 500, 778 nm
	OG1 Pyranometer	Global sky	0.530-3.0 μm
Barrow	Pyrgeometer	Sky infrared	4.0-50. μm
	Inverted pyrgeometer	Surface infrared	4.0-50. μm
	Inverted pyranometer	Surface reflected	0.28-3.0 μm

RADIATION CLIMATOLOGY AND MODEL COMPARISON

A computationally efficient physical mathematical model for direct and global solar flux in the atmosphere developed by Bird (1982) was adapted to model solar flux at the four GMCC observatories. The model calculates direct and global solar flux as a function of location, elevation, time, precipitable

water vapor, total ozone, aerosol scattering and absorption, surface albedo, and extraterrestrial flux. Computed daily flux totals for an entire year were compared to 8 years of observed daily total global flux for each GMCC site. The 8 years of data used are for 1977 through 1983, edited for unacceptable data, and archived at NCDC as hourly integrals as described by Dutton et al. (1985) (fig. 3). Only days where the edited record is complete between sunrise and sunset are used. The observations are from continuous measurements (1 per second) during all sky conditions. The atmospheric constituent climatology used in the model for each observatory, was compiled as a monthly average of observations of precipitable water, total ozone and spectral aerosol optical depth. Aerosol absorption was held fixed at .02, and surface albedo was determined appropriate for each station. The extraterrestrial flux was set at 1368 W/M^2, but adjusted for the earth's orbit. Figure 3 shows daily totals of extraterrestrial, modeled, and observed global solar flux for each GMCC observatory.

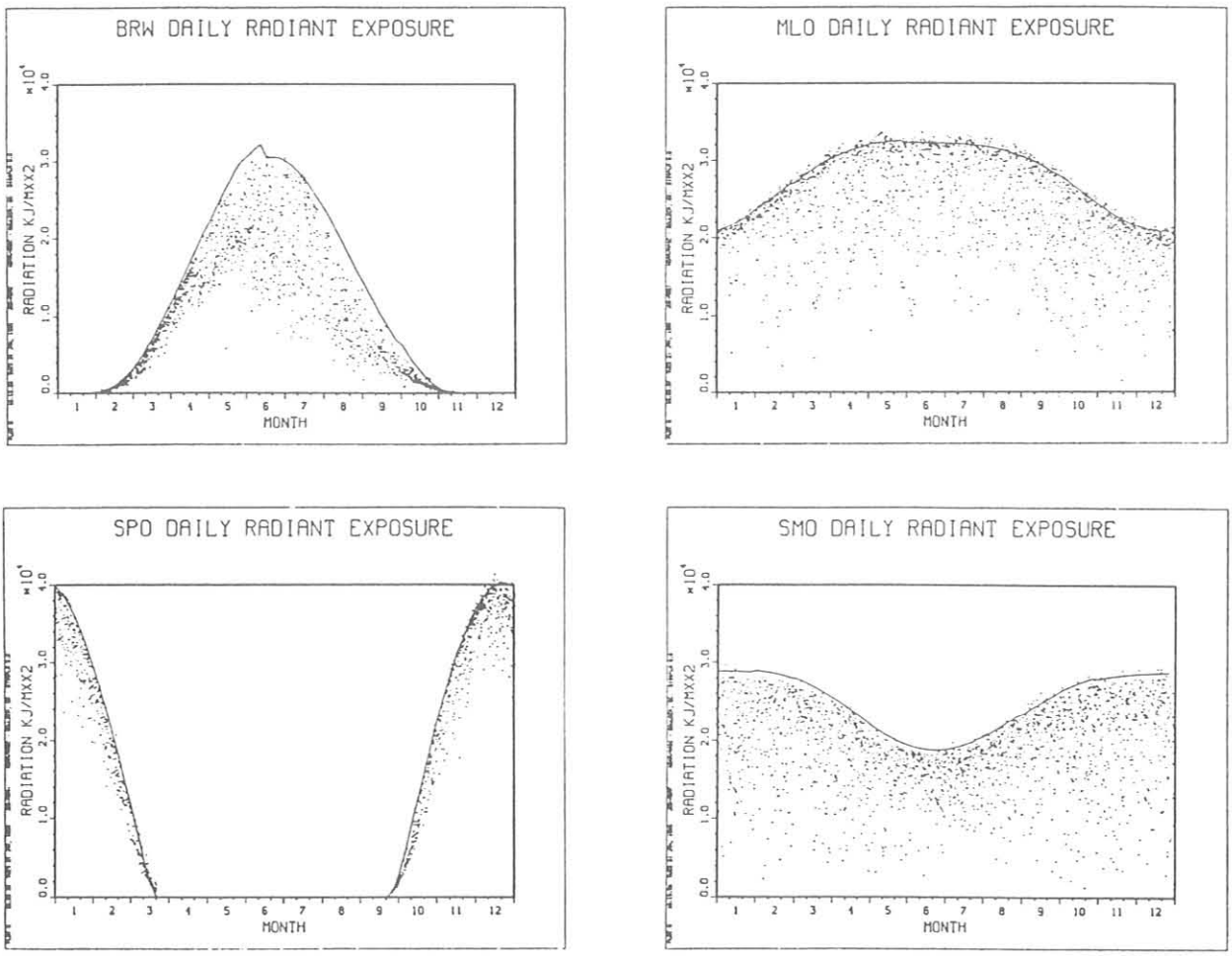

Figure 3.--Plot of daily totals of solar radiant exposure on a horizontal surface for each observatory. Uppermost smooth curve is the extraterrestrial value, the scattered points are observed values for 1976-1983, and solid line near the upper limit of the observation is the modeled clear-sky value using the Bird model described in the text.

Since the observed values in fig. 3 contain the influence of clouds, but the modeled values do not, the model represents only completely clear days or the upper limit of the observed data. Considering the good agreement between the modeled and the observed data, it is important to point out that there was no tuning or other connection between the two except for the absolute calibration reference of the observed data and the calibration of the extraterrestrial value used in the model.

Present and future work comparing the solar model to GMCC data will include refinement of radiatively active constituent climatologies, examination of annual and anomalous variability in the data, examination of direct and diffuse components, and developing cloud climatologies.

SOUTH POLE ALBEDO

Starting in late January 1982, continuous measurement of the surface albedo has been made by GMCC at the South Pole. During this period, several adjustments have been made to the measurement apparatus, but the general measurement strategy remains the same. One Eppley global pyranometer faces up and the other with the same filter faces down with occasional periods when both are faced up when the calibration of one is normalized to the other. Measurements were originally made with three spectral filters, OG1, RG8, and Quartz, but since 1983 with only two, RG8 and Quartz. Initial results show a daily average quartz albedo of 0.93 for overcast conditions to 0.82 for clear-sky conditions.

LIDAR

The historical lidar data record that began in the fall of 1974 at MLO has been analyzed for certain climatological features. With the exception of fig. 4, all figures shown in this section have been smoothed. Figure 4 shows

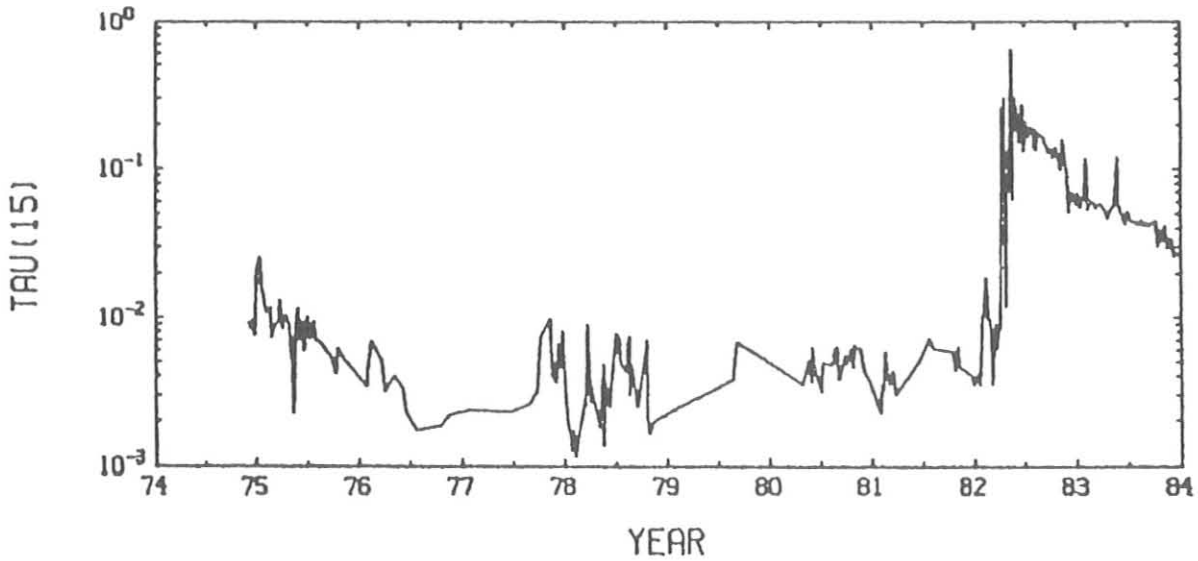

Figure 4.--Optical thickness (λ = 694 nm) vs time of stratospheric aerosols at Mauna Loa observed by lidar.

a plot of lidar optical thickness vs time. The beginning of the plot shows the decaying stratospheric aerosol from De Fuego that erupted 14 October 1974. Following De Fuego, a rather quiescent period ensued until the Mystery Cloud was observed in January 1982, followed by the immense signal from El Chichon which erupted in March and April 1982. Observations during the quiescent period implied a lower threshold value of 0.002 optical thickness for stratospheric aerosol. Interestingly, during the years 1977-1980, annual stratospheric aerosol loading profiles (optical thickness km^{-1}) showed no maximum near 20 km.

Figure 5 shows the altitude of the peak scattering ratio, i.e. one plus the backscattering mixing ratio of aerosols to gas, for the entire lidar record. Of note here are the low maximum-backscattering altitudes of De Fuego, some other volcanic activity not widely separated in time viz., St. Helens (18 May 1980), Ulawun (7 October 1980), Alaid (27 April 1981), Pagan (15 May 1981), and Mystery Cloud (early January 1982). El Chichon stands out strikingly, reaching a peak altitude of 27 km.

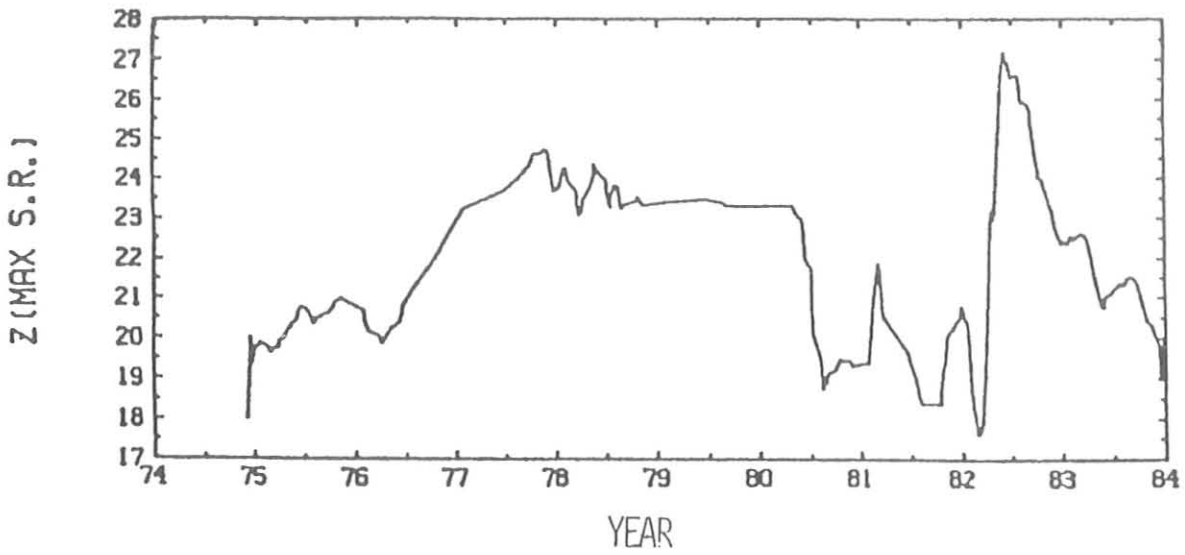

Figure 5.--Altitude of the peak scattering ratio (Rayleigh + Aerosol)/Rayleigh vs time, observed by lidar at Mauna Loa.

Figure 6 shows the altitude of the median optical mass. Interestingly, the mystery cloud median optical mass was the lowest and the El Chichon cloud was very high.

Figure 7 shows the 2/3 width of optical mass centered at 1/6 above and 1/6 below the entire lidar optical mass profile. Note the thin layering of the two most significant stratospheric clouds De Fuego and El Chichon during the earliest stages of these events. Note also, the broad layering during the quiescent period.

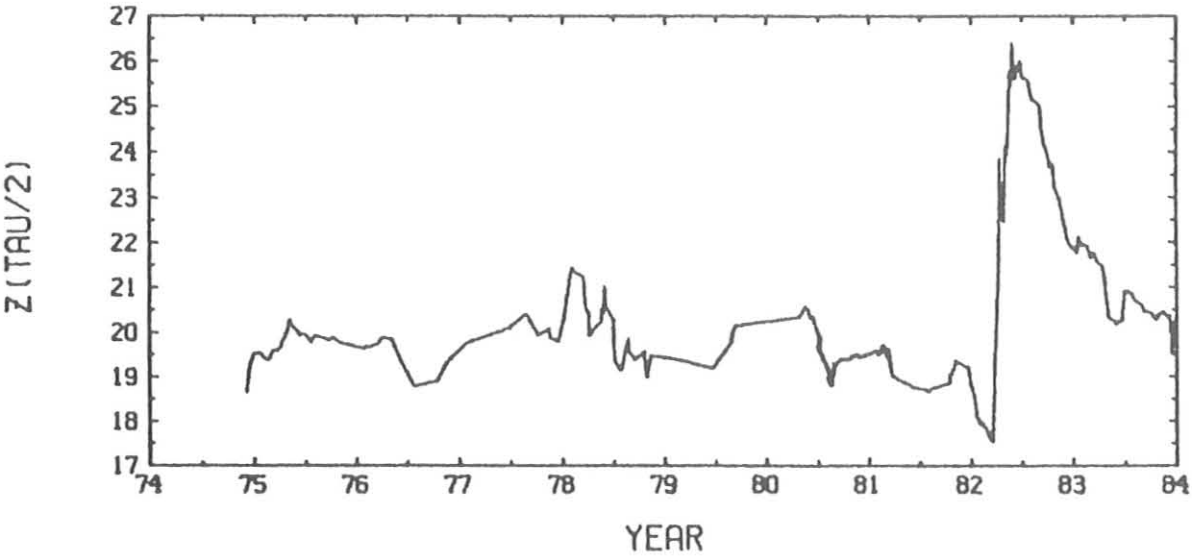

Figure 6.--Altitude of the median optical mass of stratospheric aerosol profile (km^{-1}) observed by lidar at Mauna Loa.

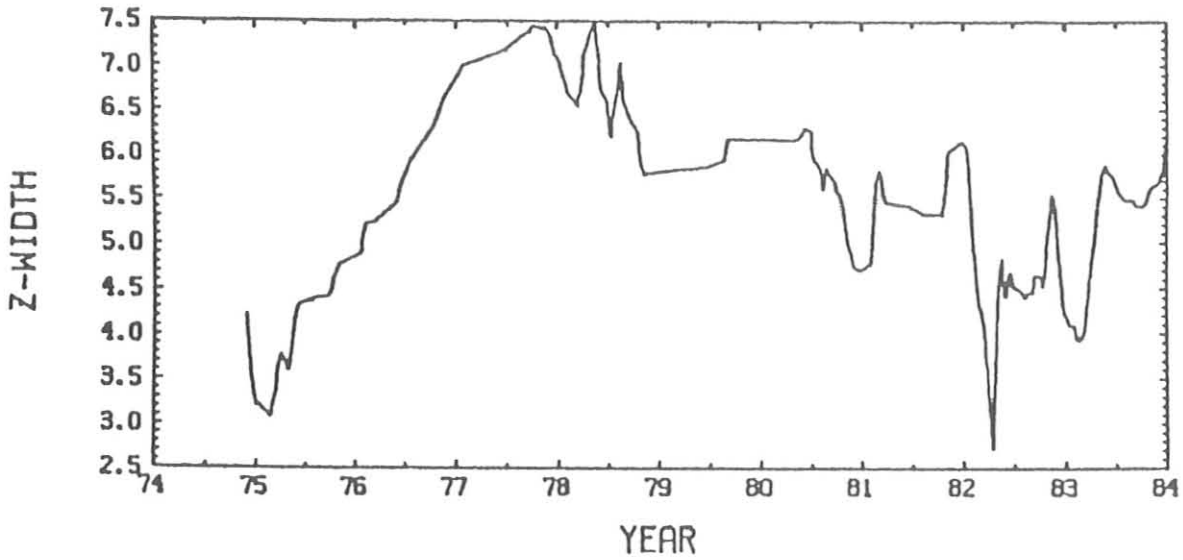

Figure 7.--The 2/3 central width of optical mass of stratospheric aerosol profile (km^{-1}) observed by lidar at Mauna Loa.

Table 4 shows exponential diminution rate constants for volcanic clouds over Mauna Loa. The reciprocal of the constant T* represents the time for a volcanic cloud to diminish to 1/e of its optical thickness. Data sources are either the Mauna Loa transmission observations or lidar observations. Note, that as a cloud ages, its diminution rate gets smaller.

Table 4.--Diminution rate (exponential) constant for volcanic clouds over Mauna Loa

Years	Volcano	$T^*(yr^1)$	Source
1965-1966	Agung	1.0	Trans
1965-1969	Agung	0.5	Trans
1975-1976.5	DeFuego	0.91	Lidar
1982 (Apr-Dec)	El Chichon	1.70	Lidar
1983	El Chichon	0.78	Lidar
1984	El Chichon	0.55	Lidar
1982-1984	El Chichon	1.04	Lidar

3.2 References

Bodhaine, B. A., and J. J. DeLuisi, 1985. An aerosol climatology of Samoa. J. Atmos. Chem., in press.

Bodhaine, B. A., J. J. DeLuisi, J. M. Harris, P. Houmere, and S. Bauman, 1986. Transport of chemical species to the South Pole. Tellus, in press.

DeLuisi, J., T. DeFoor, K. Coulson, F. Fernald, and K. Thorn, 1984: Lidar observations of stratospheric aerosol over Mauna Loa Observatory: 1974-1981. NOAA Data Report, ERL ARL-4, NOAA Environmental Research Laboratories, Boulder, CO, 107 pp.

DeLuisi, J., T. DeFoor, K. Coulson, F. Fernald, and K. Thorne, 1985: Lidar observations of stratospheric aerosol over Mauna Loa Observatory: 1982-1983. NOAA Data Report, ERL ARL-5, NOAA Environmental Research Laboratories, Boulder, CO, 78 pp.

Harris, J. M. and E. C. Nickerson (ed), 1984: Geophysical Monitoring for Climatic Change No. 12, Summary Report 1983, Environmental Res. Labs, Boulder, CO , 184 pp.

Wagner, A. J., 1985: The climate of spring 1984 - An unusually cold and stormy season over much of the United States, Monthly Weather Review, 113, No. 1, Jan. 1985, 149-169.

4. CARBON DIOXIDE GROUP

4.1 Continuing Programs

CONTINUOUS ANALYZERS

Continuous CO_2 measurements by in situ NDIR analyzers at the four GMCC stations (BRW, MLO, SMO, SPO) continued in 1984. May 1984 marked the 10th anniversary of measurements by GMCC at MLO. The complete record of provisional monthly mean data for the continuous analyzers is presented in fig. 1 and in table 1. The eruption of the Mauna Loa volcano in late March resulted in over a month's loss of data. There has also been a significant increase in CO_2 variability at MLO since the eruption due to outgassing by the volcano. The mean year-to-year difference from 1983 to 1984 for the four stations was 1.55 ppm (using an interpolated value of 346.3 ppm for April at MLO), which is slightly higher than the mean CO_2 global growth rate of 1.5 ppm/yr since 1976, and is due to an anomalously high difference of 1.9 ppm for BRW between 1983 and 1984.

Data acquisition procedures remained the same for most of 1984, until the new CAMS data acquisition units were installed. The changeover from ICDAS to CAMS occurred in August at BRW, in October at SMO, and in November at MLO and SPO. Some changes in data processing with CAMS occurred, which include computing hourly means by compensating for any changes in drift and sensitivity of the NDIR analyzer, and by calibrating the working standard gases at weekly intervals using a non-linear method discussed by Komhyr et al. (1985). A description of the CAMS design and of the CO_2 CAMS operation can be found in GMCC Summary Report No. 12 (Harris, 1984, pp. 69-72).

The in-house calibration of CO_2-in-air reference gases for GMCC continued in 1984. Two-hundred fourteen tanks were calibrated during the year. All calibrations are traceable to the GMCC secondary standards which have been calibrated manometrically and by NDIR measurements by C. D. Keeling at SIO.

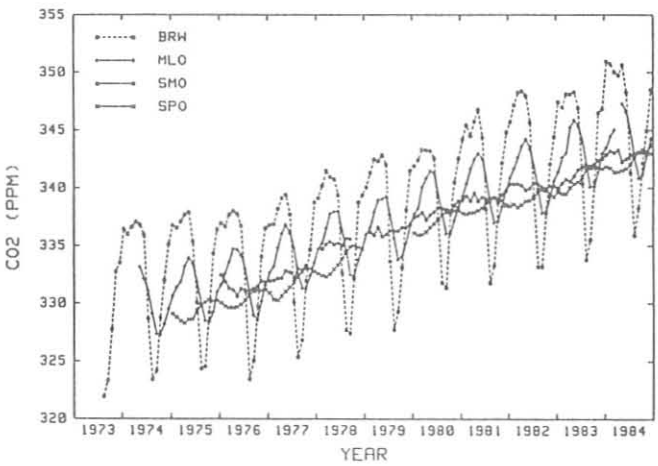

Figure 1--Provisional selected monthly mean CO_2 concentrations from continuous measurements at BRW, MLO, SMO and SPO. Values are in ppm with respect to dry air (X81 mole fraction scale).

Table 1.--Provisional selected monthly and annual mean CO_2 concentrations (ppm relative to dry air-X81 mole fraction scale) for continuous measurements at BRW, MLO, SMO and SPO.

Year	Jan	Feb	Mar	Apr	May	Jun	Jul	Aug	Sep	Oct	Nov	Dec	Annual mean
BRW													
1973	--	--	-	--	--	--	--	322.0	323.4	327.8	332.7	333.5	--
1974	336.5	336.0	336.7	337.1	336.9	335.9	328.7	323.5	324.2	328.8	332.0	335.2	332.6
1975	336.8	336.6	337.1	337.7	337.9	335.4	330.1	324.4	324.6	329.2	334.3	336.5	333.4
1976	337.0	336.7	337.7	338.0	337.8	336.8	331.0	323.5	325.1	329.8	334.1	336.6	333.7
1977	336.8	336.9	338.2	339.2	339.4	337.7	330.1	325.4	326.8	332.0	334.7	338.8	334.7
1978	339.1	340.2	341.5	341.0	340.8	339.4	332.6	327.7	327.4	332.1	338.8	339.4	336.7
1979	340.1	341.3	342.5	342.4	342.9	342.0	333.6	327.7	329.3	333.1	338.1	341.5	337.9
1980	341.9	342.4	343.4	343.3	343.3	342.6	337.3	331.8	331.4	337.9	340.5	342.6	339.9
1981	344.3	345.5	344.6	345.8	346.8	344.4	338.2	331.8	333.3	338.8	342.2	344.9	341.7
1982	345.8	347.2	348.3	348.4	348.0	345.7	339.2	333.2	333.2	337.9	342.1	344.5	342.8
1983	347.5	347.0	348.1	348.1	348.3	347.0	340.4	333.8	335.5	340.6	346.5	346.8	344.1
1984	351.0	350.7	350.0	349.8	350.7	348.3	341.3	335.9	338.3	342.2	345.0	348.5	346.0
MLO													
1973	--	--	--	--	--	--	--	--	--	--	--	--	--
1974	--	--	--	--	333.1	332.1	331.1	329.1	327.4	327.3	328.2	329.6	--
1975	330.6	331.4	331.9	333.2	333.9	333.4	331.9	330.0	328.5	328.4	329.2	331.0	331.1
1976	331.6	332.6	333.6	334.7	334.7	334.2	333.0	330.8	329.0	328.6	330.2	331.6	332.0
1977	332.7	333.2	334.9	336.1	336.8	336.1	334.8	332.6	331.3	331.2	332.4	333.5	333.8
1978	334.7	335.2	336.5	337.8	338.0	338.0	336.4	334.5	332.5	332.3	333.8	334.8	335.4
1979	336.0	336.6	337.9	339.0	339.1	339.3	337.6	335.7	333.8	334.1	335.3	336.8	336.8
1980	337.8	338.3	340.1	340.9	341.5	341.3	339.4	337.7	336.1	336.1	337.2	338.4	338.7
1981	339.3	340.4	341.7	342.5	343.0	342.5	340.9	338.7	337.1	337.1	338.5	339.9	340.1
1982	340.9	341.7	342.7	343.7	344.3	343.4	342.0	340.0	337.8	338.0	339.2	340.6	341.2
1983	341.4	342.7	343.0	345.3	345.9	345.4	344.2	342.1	340.1	340.2	341.4	343.0	342.9
1984	343.6	344.5	345.1	--	347.3	346.6	345.0	342.7	340.9	341.1	342.8	344.3	344.2
SMO													
1973	--	--	--	--	--	--	--	--	--	--	--	--	--
1974	--	--	--	--	--	--	--	--	--	--	--	--	--
1975	--	--	--	--	--	--	--	--	--	--	--	--	--
1976	332.4	331.9	331.3	331.2	330.6	331.3	331.1	331.1	331.3	331.5	331.9	331.9	331.5
1977	331.9	332.0	332.1	332.2	332.8	332.7	332.2	333.1	332.9	333.3	--	--	--
1978	--	334.7	335.2	335.4	335.1	335.3	335.0	335.7	335.6	--	--	--	--
1979	--	336.2	336.0	336.6	335.9	336.0	336.4	336.3	336.3	336.6	336.6	336.9	--
1980	337.5	337.6	337.9	337.3	337.7	338.0	338.3	338.3	338.2	338.1	338.5	338.9	338.0
1981	339.0	339.3	338.9	339.6	338.9	339.2	339.0	339.2	339.2	338.9	339.5	339.8	339.2
1982	340.4	340.4	340.4	340.3	339.9	340.0	340.5	340.4	340.1	340.0	340.2	340.2	340.2
1983	340.0	340.5	340.8	340.6	341.1	341.6	341.9	341.9	341.9	342.1	342.4	342.6	341.4
1984	342.9	343.2	343.1	343.3	342.3	342.6	342.9	343.0	343.2	343.1	343.1	343.7	343.0
SPO													
1973	--	--	--	--	--	--	--	--	--	--	--	--	--
1974	--	--	--	--	--	--	--	--	--	--	--	--	--
1975	329.1	328.8	328.5	328.3	328.6	328.6	329.4	329.8	330.1	330.3	330.2	330.2	329.3
1976	330.1	329.8	329.6	329.6	329.7	329.9	330.3	330.7	331.0	331.1	331.1	331.1	330.3
1977	330.9	330.3	330.3	330.6	331.0	331.4	331.8	332.2	332.7	333.0	333.0	332.7	331.7
1978	332.6	332.4	332.3	332.5	333.0	333.3	333.8	334.4	334.9	335.0	334.9	334.7	333.7
1979	--	--	--	--	--	--	--	--	--	--	--	--	--
1980	336.1	336.0	336.0	336.2	336.6	336.9	337.4	337.7	337.9	338.1	338.0	338.0	337.1
1981	337.8	337.8	337.9	337.9	338.1	338.3	338.7	339.0	339.2	339.1	338.9	338.5	338.4
1982	338.5	338.6	338.4	338.6	338.9	338.9	339.2	339.6	339.9	339.8	339.5	339.2	339.1
1983	339.7	339.5	339.5	340.0	340.4	340.5	341.0	341.6	341.7	341.8	341.8	341.7	340.8
1984	341.8	341.7	341.4	341.4	341.5	341.7	342.0	342.7	343.1	343.4	343.2	343.0	342.2

FLASK SAMPLE CO_2 MEASUREMENTS

The purpose of the GMCC Flask Sampling program is to measure the global distribution of atmospheric CO_2 concentration with a greater spatial resolution than is practical by in situ monitoring. Collecting whole air samples in glass flasks for subsequent analysis in the GMCC laboratory in Boulder is a cost-effective way to obtain CO_2 concentration data from a global network of remote sites. The information obtained in this way is used to locate regional scale sources and sinks of CO_2 and to study the global carbon cycle, both directly and through carbon cycle models.

In 1984, samples were collected once or twice per week at the 24 sites shown in fig. 2. The sampling and analytical procedures have been described by Komhyr et al. (1983) and Komhyr et al. (1985). In 1984, flask sampling was begun at Christmas Island in the equatorial Pacific Ocean and at Cape Grim, Tasmania. The Christmas Island site fills a major gap in our network coverage between Guam and Samoa in the Pacific Ocean. This site was added to the network through the cooperation of C. D. Keeling at SIO. The sampling at Cape Grim is a cooperative effort with G. Pearman and P. Fraser of the Australian CSIRO. Initial indications are that Cape Grim is a much better location for CO_2 sampling at this latitude than the site at Kaitorete Spit, New Zealand. After a sufficient period of overlap, sampling at the New Zealand site may be terminated due to interference by local vegetation, agricultural activity, and proximity to anthropogenic sources in Christchurch. An additional benefit of sampling at Cape Grim is the opportunity for intercomparing data with another prominent CO_2 measurement program. Intercomparisons of this sort are useful in monitoring and improving the sampling methodology and comparability of measurements made by different groups.

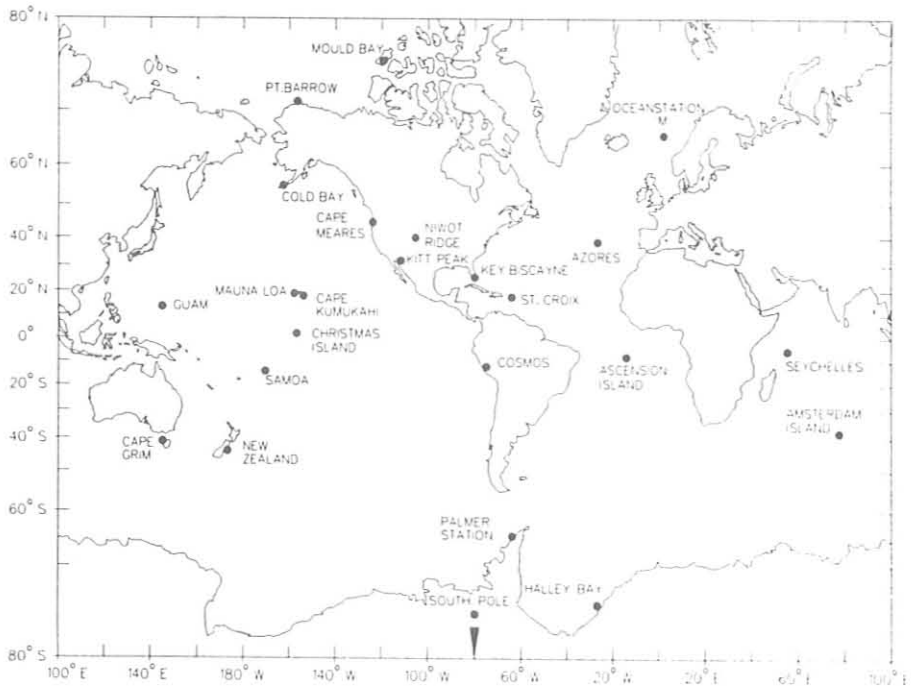

Figure 2.--Locations of GMCC flask sampling network sites in 1984

The first year (1983) of samples from Halley Bay, Antarctica was received in Boulder in 1984. The data appear to be of high quality and provide valuable information concerning CO_2 gradients in the Southern Hemisphere. The sites at which samples were collected in 1984 are listed in table 2.

Table 2.--GMCC CO_2 flask network sampling sites during 1984

Code	Station	Latitude (deg)	Longitude (deg)	Elevation (m)
AMS	Amsterdam I.	37.95S	77.53E	150
ACS	Ascension I.	7.92S	14.42W	54
AVI	St. Croix, VI	17.75N	64.75W	3
AZR	Terceira I., Azores	38.75N	27.08W	30
BRW	Barrow, AK	71.32N	156.60W	11
CBA	Cold Bay, AK	55.20N	162.72W	25
CGO	Cape Grim, Tasmania	40.68S	144.73E	94
CHR	Christmas I.	2.00N	157.30W	3
CMO	Cape Meares, OR	45.00N	124.00W	30
COS	Cosmos, Peru	12.12S	75.33W	4600
GMI	Guam, Mariana I.	13.43N	144.78E1	2
HBA	Halley Bay, Ant.	75.67S	25.50W	0
KEY	Key Biscayne, FL	25.67N	80.17W	3
KPA	Kitt Peak, AZ	32.00N	112.00W	2095
KUM	Cape Kumukahi, HI	19.52N	154.82W	3
MBC	Mould Bay, Canada	76.23N	119.33W	15
MLO	Mauna Loa, HI	19.53N	155.58W	3397
NWR	Niwot Ridge, CO	40.05N	105.63W	3749
NZL	New Zealand	43.83S	172.63E	3
PSA	Palmer Station, Ant.	64.92S	64.00W	10
SEY	Mahé I., Seychelles	4.67S	55.17E	3
SMO	Cape Matatula, Am. Samoa	14.25S	170.57W	30
SPO	South Pole, Ant.	89.98S	24.80W	2810
STM	Station M	66.00N	2.00E	0

In 1984 ~6000 flasks were analyzed for CO_2 concentration. Of these ~4000 were from the flask network and the remainder were from cruises or were test flasks used to monitor the operation of the analytical apparatus. As described in Harris and Nickerson (1984), many of the network flasks are also analyzed for CH_4 concentration by gas chromatography. This project is described in the next section of this report.

The 1983 flask data have been reprocessed to take into account drifts in the concentrations of the flask analysis reference gases and analyzer non-linearity. These data are essentially final pending recalibration in 1985 of the GMCC secondary standards at the WMO CO_2 Central Laboratory at SIO. The 1984 flask data have not yet been reprocessed and should be considered provisional. The annual mean CO_2 concentrations for the network are summarized in table 3.

Table 3.--Annual mean atmospheric CO_2 concentrations (ppm relative to dry air--X81 mole fraction scale) for the flask network sites

Station	1968	1969	1970	1971	1972	1973	1974	1975	1976	1977	1978	1979	1980	1981	1982	1983	1984
AHS	0	0	0	0	0	0	0	0	0	0	0	(335.9)	337.8	339.3	339.4	341.1	(342.2)
ASC	0	0	0	0	0	0	0	0	0	0	0	[337.3]	338.8	339.7	340.7	342.6	343.7
AVI	0	0	0	0	0	0	0	0	0	0	0	337.1	339.6	340.4	340.9	342.0	343.2
AZR	0	0	0	0	0	0	0	0	0	0	0	0	338.4	339.6	341.2	343.0	344.4
BRW	0	0	0	327.4	330.2	332.0	333.4	333.0	333.9	335.0	336.6	337.7	340.2	341.5	342.7	344.0	345.4
CBA	0	0	0	0	0	0	0	0	0	0	0	337.8	339.9	341.3	341.9	343.4	345.3
CGO	0	0	0	0	0	0	0	0	0	0	0	0	0	0	0	0	342.0
CHR	0	0	0	0	0	0	0	0	0	0	0	0	0	0	0	0	344.8
CMO	0	0	0	0	0	0	0	0	0	0	0	0	0	0	341.2	342.9	344.8
FLK	0	0	0	0	0	0	0	0	0	0	0	0	0	339.7	0	0	0
GMI	0	0	0	0	0	0	0	0	0	0	0	337.7	340.0	341.2	341.0	342.7	344.2
HBA	0	0	0	0	0	0	0	0	0	0	0	0	0	0	0	341.4	342.5
KEY	0	0	0	0	0	330.7	[333.4]	0	332.7	335.2	336.7	338.8	(340.2)	342.0	341.6	343.4	345.1
KUM	0	0	0	0	0	0	0	0	332.3	334.4	335.7	337.4	339.3	340.4	341.2	342.5	344.1
MBC	0	0	0	0	0	0	0	0	0	0	0	0	340.3	341.9	342.5	343.7	345.6
MKO	0	0	0	0	0	0	0	0	0	0	0	337.3	0	0	0	0	0
MLO	0	[322.8]	325.2	0	0	0	0	0	332.1	333.6	335.2	336.7	338.9	340.4	341.0	342.5	343.9
NWR	323.1	324.1	325.6	325.2	326.3	330.2	[334.0]	0	332.1	334.8	335.7	337.0	338.1	339.9	340.9	342.4	344.6
NZL	0	0	0	0	0	0	0	0	0	0	0	0	0	0	0	340.7	342.4
PSA	0	0	0	0	0	0	0	0	0	0	333.9	335.2	(337.5)	340.0	339.8	341.0	342.7
SEY	0	0	0	0	0	0	0	0	0	0	0	0	339.3	340.1	340.5	340.8	344.0
SMO	0	0	0	0	0	[330.2]	330.8	330.7	331.5	332.8	334.3	336.0	338.1	339.3	340.4	341.4	343.0
SPO	0	0	0	0	0	0	0	329.4	330.2	331.5	333.7	335.5	336.7	338.5	339.3	340.8	342.1
STC	0	324.0	326.4	326.9	327.6	0	0	0	0	0	0	0	0	0	0	0	0
STM	0	0	0	0	0	0	0	0	0	0	0	0	0	341.9	341.7	342.6	344.8

Note: () = number of interpolated points $\geq$ one-half of total number of points; [] = incomplete year.

Several events occurred in 1984 which affected the data records for some sites. Problems in shipping procedures resulted in flask shortages and, therefore, gaps in sampling at Seychelles. This was solved by air freighting a large supply of flasks to the site so that delays in mail service could be tolerated. At Halley Bay it was discovered that during the austral winter, the sample taker changed the location of sampling which resulted in sampling grossly contaminated air. Fortunately, the samples collected before and after winter, and two samples collected during the winter, were collected properly, and have enabled the calculation of an annual mean concentration. At Amsterdam Island, also during winter-over, the sample taker experienced some personal problems which resulted in several large gaps in the record and some doubts about the techniques used in collecting the samples that were taken. This was followed by a summer season during which a new station was constructed accompanied by more gaps in sampling. Thus, the annual mean calculated for 1984 at Amsterdam Island is somewhat uncertain pending further examination of all the data. At Palmer Station, also during winter-over, the samples were collected through a manifold connected to an outside sampling stack. It appears that in August 1984, the manifold may have developed a leak allowing room air to contaminate the samples; however, most of the Palmer Station record is good and it was not difficult to eliminate the obviously contaminated samples.

The annual mean CO_2 concentrations for 1981-1984 are plotted vs. latitude in fig. 3. It is clear that the network is improving in its ability to define the latitude gradient. Christmas Island is especially crucial in determining location and magnitude of the local maximum in CO_2 concentration near 5° N. Also the addition of Halley Bay and Cape Grim are confirming the suggestion of a local maximum between 40° S and the South Pole. The quality and resolution of this data provides a very good set of constraints for assessing the ability of various models to simulate the global carbon cycle and transport of CO_2 in the atmosphere. Also note in fig. 3 the suppression of the equatorial maximum during 1982. Gammon et al. (1984) have suggested that this effect was due to reduced upwelling of CO_2-rich deep water in the equatorial Pacific during the ENSO event of 1982-83. Figure 3 shows a partial recovery of this feature in 1983 and a complete recovery in 1984, again more clearly defined by the data from Christmas Island.

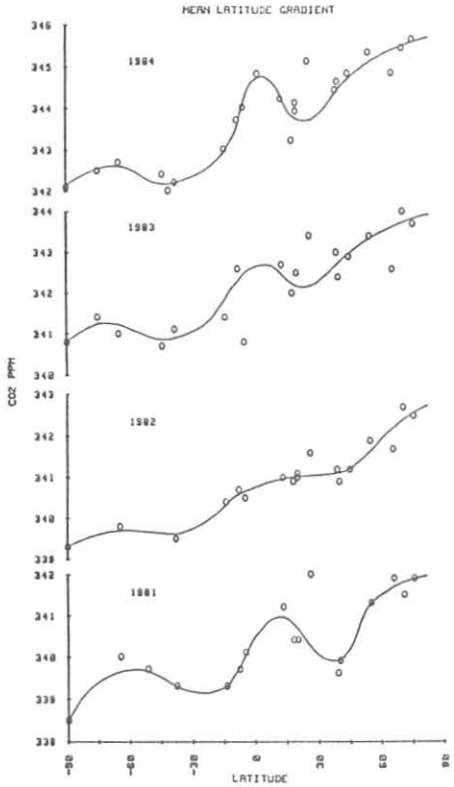

Figure 3.--Annual mean CO_2 concentrations vs. latitude for the GMCC Flask Sampling Network. Key Biscayne (26°N) has not been used in drawing the curves.

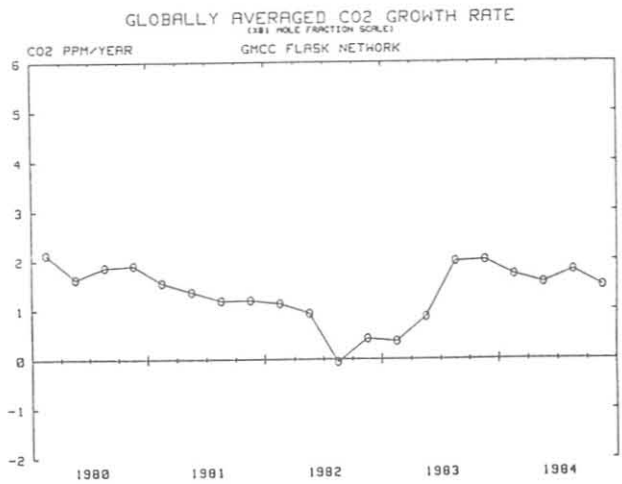

Figure 4.--Globally averaged CO_2 growth rate calculated from the GMCC Flask Network data.

The global mean annual growth rate calculated quarterly from the flask network data is plotted in fig. 4. It was suggested by Gammon et al. (1984) that the decrease in the growth rate observed during 1982 was also a result of the unusually intense ENSO event. The rebound of the growth rate in 1983 to unusually high values of ~2.0 ppm/yr is consistent with the results of Bacastow (1976). In 1984 the growth rate has returned to a value of ~1.5 ppm/yr, more typical of the mean value over the past decade.

Plans for the flask network in 1985 include possible termination of sampling at New Zealand; initiation of sampling at Shemya Island, Alaska; Alert, N.W.T., Canada; Midway Island; and South Georgia Island; and continued studies on the use of greaseless stopcock flasks. The 1983 and 1984 flask data will be finalized and archived with WMO and with DOE/CDIC.

FLASK SAMPLE METHANE MEASUREMENTS

The measurement of atmospheric methane in air samples collected from the NOAA/GMCC CO_2 flask network continued through 1984. These measurements were begun in 1983 as a cooperative program between CSIRO, NOAA/GMCC and OGC (see GMCC Summary Report No. 12, 1983, pp. 163-165). During 1984 there were 22 active sites in this globally distributed flask sampling network, and these are indicated both in fig. 2 and table 2.

Results obtained at two of these sites (South Pole and Mould Bay) from the beginning of the program through to the end of 1984 are shown in fig. 5. Data from the South Pole illustrates clearly the features found at all sites south of Samoa, with a smooth seasonal cycle and an average long-term increase of approximately 1% per year. These measurements represent the first reported observation of a complete seasonal cycle of atmospheric methane at the South Pole. The long-term growth rate, as well as the phase and amplitude of the seasonal cycle are highly consistent with results from several years of measurements reported by Fraser et al. (1984) for the site at Cape grim in northwest Tasmania.

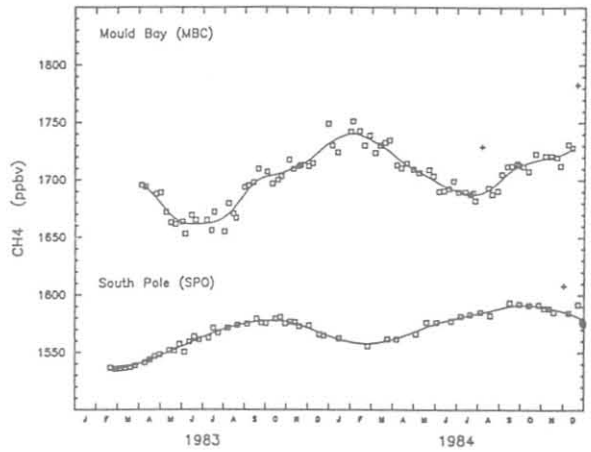

Figure 5.--Atmospheric methane at SPO and Mould Bay, Canada. Square symbols represent individual flask measurements and are normally the mean of two replicate determinations. The cross symbols indicate values which are not believed to represent background conditions. The fitted lines are cubic splines (Reinsch, 1967), and are fitted to only those data considered to be background values.

The results from Mould Bay illustrate that at sites in the Northern Hemisphere there is a more complex seasonal variation, a larger amplitude, and a difference in phase of the seasonal changes to those seen in the Southern Hemisphere. Nevertheless, the long-term growth rate found at the northern sites is similar to those measured at sites in the south. Another feature apparent from the data shown here is the significant latitudinal gradient, averaging an 8% difference in concentration between these two sites during this period.

A complete description of this program and 2 years of data from all sites is reported by Steele et al. (1985).

4.2 Special Projects

INTRODUCTION

In addition to in situ CO_2 monitoring at the four baseline observatories and the flask sampling network, the CO_2 Group undertakes special projects which are deemed appropriate to meeting overall program objectives. These projects involve field measurements intended to supplement or expand on the data from our existing sites and the development and evaluation of CO_2 measurement technology. Also, studies are undertaken to analyze and interpret the CO_2 data sets and to investigate various aspects of the global carbon cycle and atmospheric transport of CO_2. Several activities of this type which occurred in 1984 are described in this section.

MEASUREMENTS OF CO_2 AND CH_4 BY GAS CHROMATOGRAPHY AT MAUNA LOA OBSERVATORY

In 1983 the GMCC CO_2 Group received two gas chromatographs constructed by R. Weiss of SIO. These instruments are designed to measure CO_2 concentration with a precision comparable to that of non-dispersive infrared analyzers, and are also capable of measuring CH_4 (Weiss, 1981). After laboratory tests of the precision, linearity and accuracy were performed, a chromatograph was installed at MLO in March 1984. The chromatograph operated successfully and data were collected until the eruption of Mauna Loa on 25 March 1984. Because components of the chromatograph system are susceptible to damage during power failures, it was decided not to restart the chromatograph until regular line power (as opposed to generator power) was restored to the observatory. The chromatograph was restarted in September 1984, and ran successfully through the end of the year.

The objective of this project is to compare the gas chromatographic to the NDIR method of CO_2 monitoring at a baseline observatory. The frequency of volcanic outgassing of CO_2 during 1984 has made this comparison somewhat difficult. Since the GC makes six discrete measurements each hour, whereas the NDIR analyzer makes essentially continuous measurements, it is unsatisfactory to compare the two results during periods of highly variable CO_2 concentration. Figure 6 shows a comparison of hourly means during 4 days in October chosen for a lack of volcanic activity and a CO_2 concentration showing little short-term variability. This comparison suggests an offset of ~0.1 ppm between the two measurements with a scatter (1σ) of ~0.14 ppm. The 0.1 ppm offset may be due to inaccuracies in the concentration values assigned to the reference gas tanks used by each system. This will be investigated further after the GMCC secondary standards are recalibrated at SIO, and any drift corrections are applied to the assigned tank values. In general, the agreement between the two methods looks quite good.

An added advantage of the GC method is the simultaneous measurement of CH_4, an infrared absorbing gas of considerable interest with respect to climate change (see, for example, Ramanathan, et al., 1985). As discussed in Harris and Nickerson (1984), and elsewhere in this report, GMCC in cooperation with OGC and CSIRO has been measuring atmospheric CH_4 concentration in samples from the CO_2 flask network since 1983. The MLO GC CH_4 data are useful in looking at the nature of the variability observed in the flask sample data. Figure 7 shows daily means calculated from the high frequency discrete samples of the MLO GC superimposed on the one-sample-per-week-flask record.

First, it is interesting to note the excellent agreement between the in situ and flask sample measurements, especially considering that the flask sample measurements are made with a different type of chromatograph. Secondly, it is clear from the in situ measurements that the day-to-day and week-to-week variability in atmospheric CH_4 exhibits structure which is likely related to atmospheric transport and the action of sources and sinks. In the flask record, variations of this frequency are manifested as scatter since samples are only collected once each week.

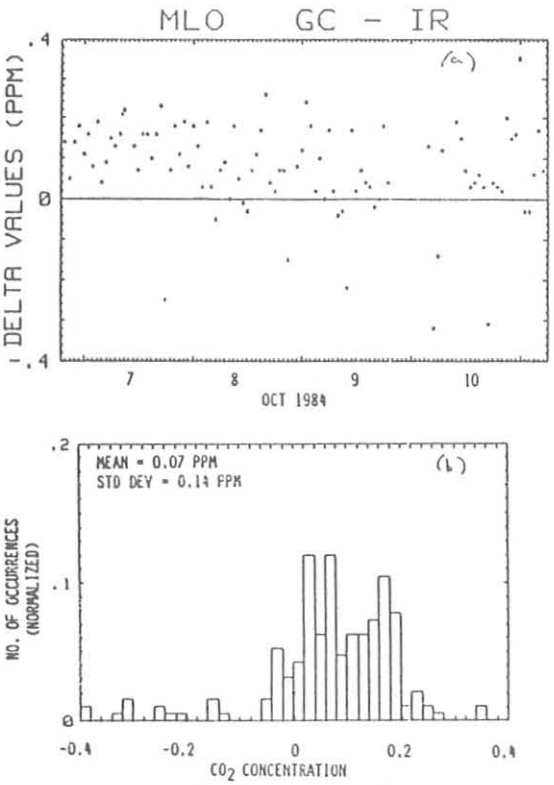

Figure 6.--Comparison of CO_2 measurements by the NDIR and GC methods at MLO. a) Differences between GC and NDIR hourly means for 7-10 October. b) Histogram of the differences.

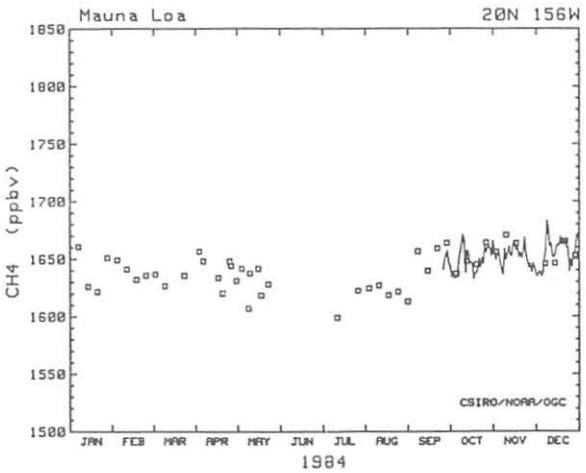

Figure 7.--Comparison of in situ (solid line) and flask measurements (squares) of atmospheric CH_4 at MLO.

The continued operation of the MLO GC during 1985 will enable a more thorough evaluation of the method for measuring CO_2 and will provide a record of CH_4 concentration which will nicely complement the flask sample record.

SHIPBOARD MEASUREMENTS OF ATMOSPHERIC CO_2

In 1984 the CO_2 Group continued to collect flask samples aboard occasional oceanographic cruises. The purpose of this project is to make detailed measurements of atmospheric CO_2 (and CH_4) concentrations over large regions of the earth's surface to assess the ability of the limited number of stations in the CO_2 flask network to determine the global distribution of atmospheric CO_2. The results from cruises in 1982 and 1983 have generally supported the representativeness of the flask network, while demonstrating that the network is not able to locate steep latitudinal gradients or resolve the variation of CO_2 with longitude (Bodhaine and Harris, 1983; Harris and Nickerson, 1984).

The cruise tracks for two sampling programs completed in 1984 are shown in fig. 8. The Long Lines expedition aboard the R/V KNORR took place in October 1983 and January 1984 in the equatorial and South Atlantic Ocean. The cruise of the NOAA R/V DISCOVERER covered the equatorial and South Pacific Ocean during February through May 1984.

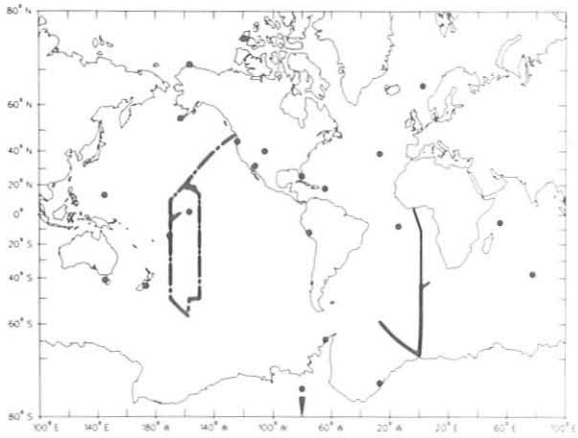

Figure 8.--Long Lines Expedition October 1983 and January 1984 (——) and the 1984 DISCOVERER cruise (-•-). The solid circles show the locations of the GMCC Flask Network sites.

The CO_2 concentrations determined from the flask samples collected during the Long Lines expedition are plotted vs. latitude in fig. 9. The plotted points represent averages of pairs of simultaneously collected flasks or, when the two members of a pair differ by more than 0.5 ppm, the lower value is plotted. For this cruise 15 of the 40 pairs failed to meet the 0.5 ppm criterion, with most of the bad pairs occurring during the first leg (October 1983 . Also plotted in fig. 9 is a curve showing the CO_2 concentration interpolated from a zonally averaged CO_2 latitude day-of-year surface obtained from the flask network for the dates and latitudes covered by the cruise track. This surface is obtained by smoothing the data from the CO_2 flask network to produce a representation of the variation of atmospheric CO_2 with latitude and time.

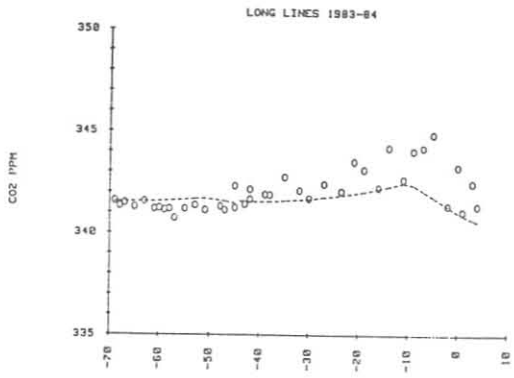

Figure 9.--Flask sample CO_2 data vs. latitude for the Long Lines Expedition. The dashed curve represents the CO_2 concentration interpolated in time and latitude from the smoothed distribution of atmospheric CO_2 calculated from the Flask Network data.

As seen in fig. 9, the agreement between the Long Lines flask sample data and the CO_2 latitude day-of-year surface is rather good. On the first leg of the cruise, the flask data are variable and tend to lie above the curve. This may be due to sample collection problems resulting in contaminated samples (most of the samples were bad pairs) or there may actually be high local concentrations of CO_2 over this area of the Atlantic. The proximity of the African continent suggests the possibility of biospheric effects contributing to the variability. On the second leg, the agreement between the cruise samples and the curve is excellent indicating that Southern Hemisphere air is well mixed and the assumption of zonality in constructing the surface is valid.

The samples from the DISCOVERER cruise are similarly compared to the CO_2 surface in fig. 10. Again the agreement with the curve is quite good. The data between 10-20°S tend to lie above the curve while those from 20-30°S are below the curve. This suggests the possibility that a steeper gradient of CO_2 concentration was sampled on the cruise than is detected by the network. From 40-60°S the agreement of the cruise data with the curve is excellent, again demonstrating the well-mixed nature of the atmosphere in the Southern Hemisphere.

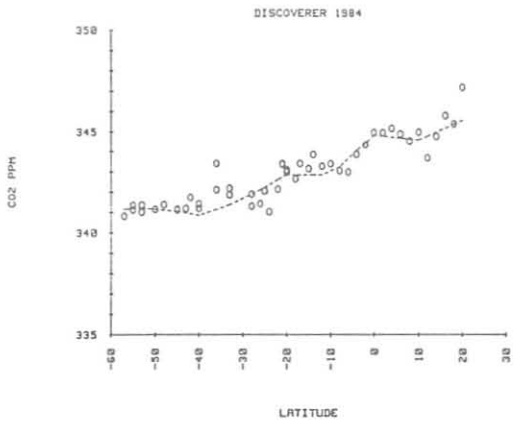

Figure 10.--Flask sample CO_2 data vs. latitude for the DISCOVERER 1984 cruise. The dashed line is as described in fig. 9, for the dates and latitudes of this cruise.

The samples collected on these two cruises provide further evidence for the representativeness of the CO_2 flask sampling network. The assumption of zonal averaging used in constructing the smoothed surface is also supported, particularly for the Southern Hemisphere. The data from both cruises demonstrate the existence of regional effects (near Africa and in the equatorial Pacific) which may not be detected by the network.

1984 OCEANOGRAPHIC ACTIVITIES ABOARD DISCOVERER

The Carbon Dioxide Group participated in the CO_2 Dynamics Cruise aboard the NOAA Ship DISCOVERER during 1984. The Weiss-design gas chromatograph was loaded aboard the ship in Seattle prior to the 14 February departure on Leg 1. The equipment was set up by Tom Conway and Lee Waterman while the ship was in Honolulu, 23-27 February. Lee Waterman operated the program on Leg 2 (Hawaii to Tahiti) and Leg 3 (Tahiti to American Samoa). On the return track,

the monitoring program was operated by Marilyn Roberts (PMEL) from Pago Pago to Honolulu, and by Glen Frick (NRL) from Honolulu to Seattle. The ship's track is shown in fig. 8 in connection with the description of shipboard flask sampling activities. A total of 1,256 hours of atmospheric air and 1,259 hours of air equilibrated with surface ocean water CO_2 measurements were obtained between 28 February and 6 May.

The 1984 monitoring program aboard the DISCOVERER was identical in most respects to the mode of operation aboard the AKADEMIK KOROLEV on the SAGA Expedition (GMCC Summary Report No. 12, 1983). Noteworthy differences are (1) a single atmospheric intake located at the bow of the ship was used for all measurements; (2) the surface ocean water was pumped from an intake located in an underwater observation chamber in the bow of the vessel; and (3) more frequent surface water temperature measurements were obtained than was possible on the Soviet ship. Preliminary results are graphically depicted in figs. 11 and 12. Each point represents the mean of all measurements of equilibrated air made over one degree of latitude. A correction has been applied to remove the increase in CO_2 concentration of the equilibrated air caused by warming the water in the transmission line between the seachest and the ship's laboratory. The mean atmospheric CO_2 concentration is represented by a straight line and is intended to be a reference level for illustrating the CO_2 undersaturation and supersaturation in the ocean surface waters.

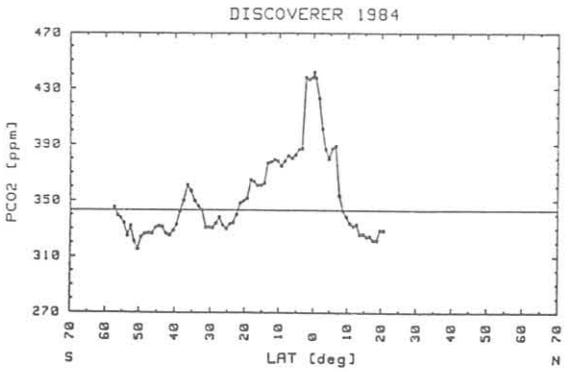

Figure 11.--pCO_2 along N to S track at 150°W long.

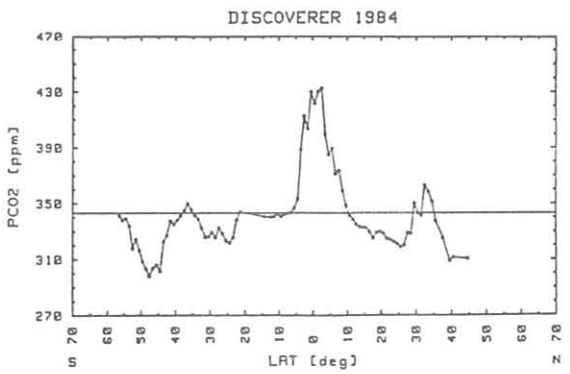

Figure 12.--pCO_2 along S to N track at 170°W long. and Honolulu to Seattle.

Figure 11 depicts the results for 18 February to 29 March from Hawaii to Tahiti and then to nearly 57°S, the track being mostly along 150°W longitude. The equatorial supersaturation feature is usually observed as rising abruptly to a region of maximum values, then declining abruptly to near equilibrium, Harris and Nickerson (1984). This time it has a shoulder between ~5°S and ~20°S, the approximate latitude of Tahiti. This shoulder disappears at 170°S longitude on return leg to Seattle, 29 March to 9 May (fig. 12). While north to south, the KOROLEV track shows the equatorial supersaturation feature shifted uncharacteristically southward by ~5°, the other three crossings made in 1983-84 bear close similarity. Likewise, on all four tracks, the surface ocean is undersaturated for most of the time between ~45°N

and ~57°S (see fig. 92 and 93, Harris and Nickerson 1984). Both the KOROLEV and DISCOVERER results, when compared with the SIO "Downwind" and "Monsoon" expeditions data, show the major features of the CO_2 distribution in the surface waters of the Eastern Pacific Ocean remain unchanged even as the atmospheric CO_2 continued to increase. For example, while the atmospheric CO_2 level has increased about 25 ppm in the past quarter century, the equatorial surface waters have maintained the 90-100 ppm supersaturation originally observed in 1957 (Keeling et al., 1965) indicating an uptake of industrial CO_2 and a rapid adjustment to maintain the status quo. These observations support the conclusions of Takahashi, et al. (1982) and Roos & Gravenhorst (1984), concerning similar adjustments in the surface waters of the North Atlantic Ocean.

RESULTS FROM A TWO-DIMENSIONAL CARBON CYCLE MODEL

The GMCC Carbon Cycle Model was designed to serve the interests of the GMCC effort in CO_2 research. It is focused largely on time scales of a year to a few years, on a global scale, and on having time resolution of 1 day. It is designed to provide comparison CO_2 concentration time series for specified locations and to develop (by comparison with CO_2) observations of the global-scale properties of the atmospheric reservoir of the global carbon cycle.

The model is two-dimensional, and has transport/diffusion as originally developed by Machta (1974). Spatial resolution is 20° latitude bands and 1- and 2-km layers. Coefficients were adjusted from Machta's original values to reproduce spatial distribution of CFC-11. A two-layer ocean simulation was added to the model, where the upper (mixed) layer has a depth that varies seasonally throughout the year. Ocean carbonate chemistry was that of Bacastow (1981), and the dissociation constants are as given by Weiss (1979) and Mehrbach et al. (1973). Salinity and alkalinity data were obtained from GEOSECS and TTO experimental data, and ice cover of the oceans data were obtained from the World Data Center in Boulder, Colorado. Wind stress and water temperature data were obtained from the literature (Hellerman, 1967; Defant, 1961). A theory of ocean-air exchange of CO_2 by Kerman (1984) was used to calculate CO_2 fluxes for the model.

One of the most innovative parts of the model was the use of carbon fluxes as calculated from the global biospheric models of E. Box (University of Georgia, Athens; personal communication, November 1983). Fossil fuel sources were obtained from the data of Rotty (1982). Carbon 13 as well as total carbon were considered by the model. Biospheric fractionation was that of Keeling (1973), oceanic fractionation was that of Siegenthaler and Münnich (1981), and fossil fuel isotopic data were obtained from Tans (1981).

The general results of the model gave pole-to-pole CO_2 differences of 3.4 ppm and pole-to-pole $\delta^{13}C$ differences of 0.35. The airborne fraction for the conditions of the base case was 51%, and the annual increase was 1.5 ppm for CO_2 and -0.096 permille for $\delta^{13}C$. (See the GMCC 1984 Annual Report for a discussion of $\delta^{13}C$).

The overall results of the model are shown in figs. 1 and 2. In these figures, the CO_2 and $\delta^{13}C$ values are plotted vs. DOY and latitude. Good general agreement with observations of CO_2 from the GMCC flask network was found.

Specific applications of the model have been made to answer questions, evaluate global estimates, and compare with questionable observations. Following are three examples of such applications. In examining these, one must remember that the model used to answer the questions is limited in dimension and represents only one approach to simulating the carbon cycle.

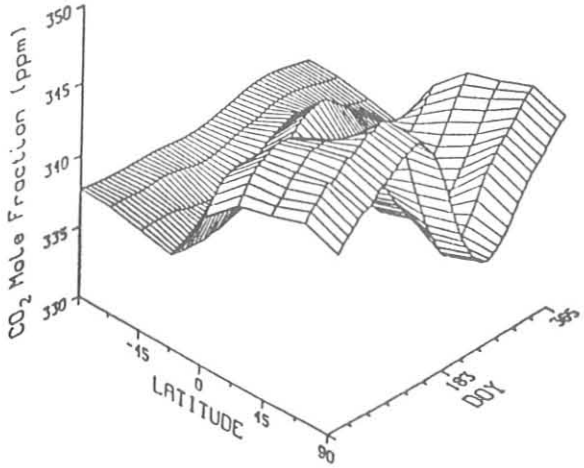

Figure 13.--Model CO_2 concentrations atmospheric CO_2 at sea level vs. latitude and day of year.

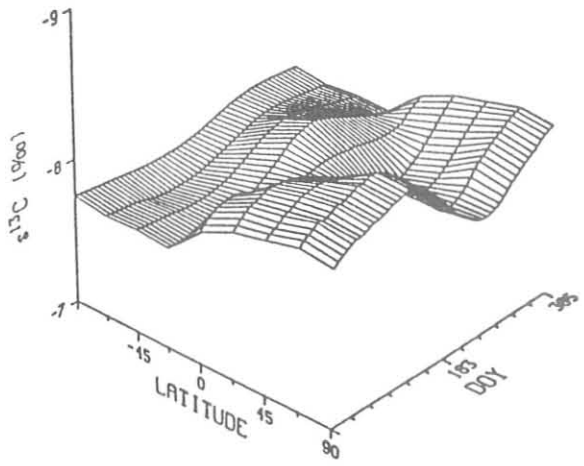

Figure 14.--Model $\delta^{13}C$ values for atmospheric carbon at sea level vs. latitude and day of year.

Example 1. Annual Fluctuation of CO_2 - What does it say about the biospheric activity in the latitudes north of 50°N?

From even a casual examination of fig. 13, the overall pattern of CO_2 concentration vs. time and latitude, the largest fluctuations of atmospheric carbon dioxide concentration occur in the latitude band of 50°-70°N. A logical question may be asked: Does the maximum biospheric activity also occur in this same latitude band?

The answer may be seen in terms of absolute change of carbon mass in the sea level box of the model for each of the latitude bands used. The causes for carbon mass change in the atmosphere are (in this model) anthropogenic sources, biospheric exchange, air-sea exchange, and atmospheric transport/diffusion. These changes are depicted in terms of bar graphs for each month of the year along with the net change for three latitude bands: 50°-70°N (fig. 15) and 10°-30°N (fig. 16). For the latitude band 50°-70°N we indeed see that the net change follows the biospheric change except for the months of May and September. In April, there is a considerable biospheric carbon change accompanied by almost no change in the net atmospheric carbon concentration. The two largest producers of atmospheric carbon change are the biospheric exchange and transport/diffusion. Anthropogenic carbon input is next in importance, followed by air/sea exchange. When we compare the biospheric flux at latitude band 10°-30°N with that of latitude band 50°-70°N, we see that there is a much larger flux of carbon into and out of the biosphere farther south. This contrasts to the equally much larger concentration changes for the more northern location, as shown in fig. 14. Again the net carbon change

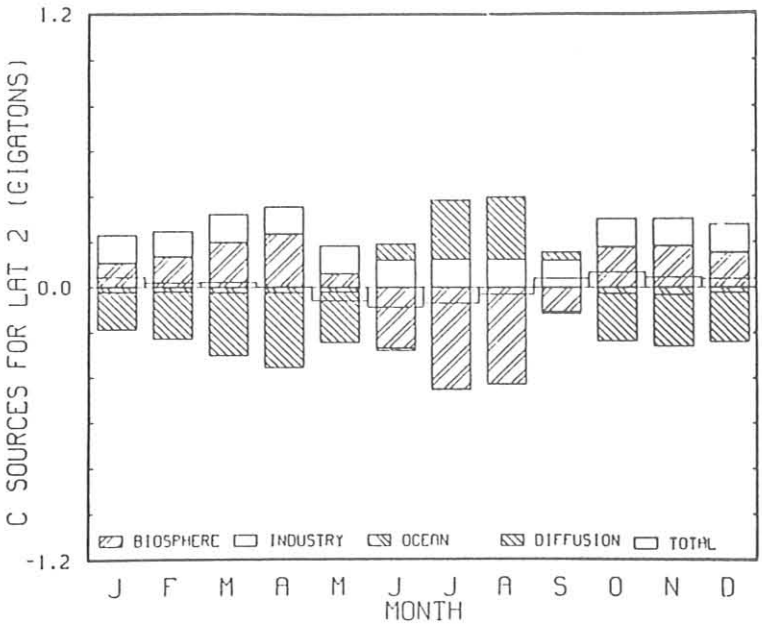

Figure 15.--Monthly carbon sources for latitude band 2 (50°-70°N). The net carbon source is a sum of the biospheric, industrial (anthropogenic), and oceanic sources and diffusive flux.

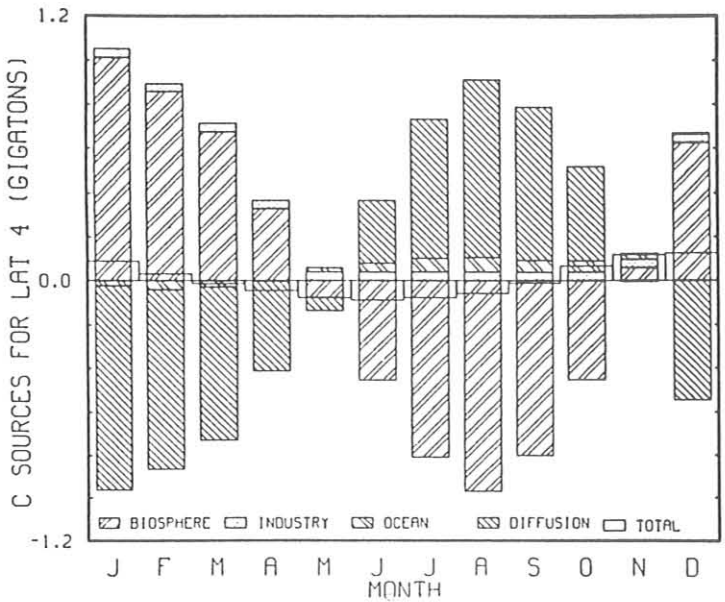

Figure 16.--Monthly carbon sources for latitude band 4 (10°-30°N). The net carbon source is a sum of the biospheric, industrial (anthropogenic), and oceanic sources, and diffusive flux.

in the atmosphere is much smaller than the change of carbon from the biospheric flux. The biospheric and transport/diffusion carbon changes are of roughly the same size, followed by air-sea exchange, and last by anthropogenic input. The total change of atmospheric carbon in the southern latitude band is larger than that in the northern latitude band. The difference in the resulting atmospheric concentrations comes about from two factors: the smaller amount of land and ocean area in the latitude band 50°-70°N than in the latitude band 10°-30°N (almost a factor of one half); and probably more important, the mixing of the CO_2 into the atmosphere. In the far north the vertical mixing is far less effective than it is farther south. In effect, the CO_2 is mixed into a smaller volume of air in the far north than it is in the south. The overall effect is then to create very much larger concentration differences from smaller absolute changes of atmospheric carbon mass.

Another example of the profound effect of the vertical mixing and smaller area of a latitude band, is the large concentration fluctuation in the latitude band 70°-90°N, which results from a relatively small change of atmospheric carbon mass. The strongest influences in carbon change in this farthest northern latitude band is air-sea exchange and diffusion. The small net change is thus not a biospheric signal in this latitude band as much as it is a transported signal from farther south, along with an oceanic CO_2 modification.

Example 2. Change of annual CO_2 increase by change of ocean-air exchange

As discussed in the interpretation of the Pt. Barrow CO_2 data in this volume, in the El Niño year of 1982 the annual increase of CO_2 in the air was significantly smaller than in the previous 2 years and, in the year following the El Niño the annual increase of CO_2 was larger than normal. The GMCC CO_2 Group set out to determine whether the GMCC Carbon Cycle Model would duplicate the anomalous 2 years of annual increases by making changes in the sea surface temperature at differing latitudes and by changing the wind speeds at differing latitudes in a similar way to that observed during the El Niño occurrence. Table 4 gives the details of the alteration of the model for three runs in addition to the base case. As is shown for the year of the El Niño, the changes to the base case for all three runs were that the sea surface temperature of the equatorial latitude band (10°N-10°S) was increased by 1° and the wind speed for the same latitude band was decreased to 75% of its base case value. At the other latitude bands, sea surface temperature was decreased by 1°. For the year following the El Niño, the three runs were changed as follows: (1) the equatorial latitude band SST was decreased to 0.5° above the base case, the wind speed was increased to 125% of the base case, and the conditions at the other latitudes were restored to these of the base case; (2) the equatorial SST was restored to the base case along with the winds and the SST at the other latitude bands; (3) the equatorial SST and winds were restored to those of the base case, along with the SST for the other latitudes except for 30°-70°N and 30°-70°S. Winds at other latitudes were changed as shown in the table.

Table 4.--Alterations of the model for El Niño conditions and conditions 1 year later

	1st Year			2nd Year			
	Change equat. SST (°C)	Equat. winds	Change SST at other latitudes	Change equat. SST (°C)	Equat. winds	Change SST at other latitudes	Wind at other latitudes
Base case	0	1	0	0	1	0	1
Run 1	+1	0.75	-1	+0.5	1.25	0	1
Run 2	+1	0.75	-1	0	1	0	1
Run 3	+1	0.75	-1	0	1	-0.5* (70°-30°) N and S	1.5

*Value is for 30°-70°N and 30°-70°S. At all other latitudes, the change is 0.

Results of the changes on the model are given in table 5. The base case gave an annual CO_2 increase of 1.5 ppm yr^{-1}. For the El Niño (1st) year, the disturbed model (Runs 1-3) gave a much smaller annual increase of 0.6 ppm yr^{-1}. For the first two disturbed runs in the year following the El Niño year, the increase went to 2.0 and 1.9 ppm yr^{-1}. For the third disturbed run, the increase was only 0.5 ppm yr^{-1}.

Although this simple simulation cannot be claimed as an accurate description of the complex El Niño phenomenon, it does point to the air-sea CO_2 exchange as being a strong possibility in explaining some of the El Niño effects.

Table 5.--Results of making the changes shown in Table 4.

	1st year mean annual increase (ppm)	2nd year mean annual increase (ppm)
Base Case	1.5	1.5
Run 1	0.6	2.0
Run 2	0.6	1.9
Run 3	0.6	0.5

Example 3. Are there any strong indicators that the biosphere is contributing to or taking away from the global CO_2 reservoir?

This question, of course, will be answered by long-term monitoring which will offset year-to-year changes in CO_2 concentration growth in the atmosphere. The evidence that we can look at before that long-term record is available is complicated with short-term effects and possibly inadvertent noise. One normal indicator of such a contribution of the biosphere (positive or negative) is the mean annual increase. When we compare data on mean annual increase with the model value for annual atmospheric CO_2 increase, we get comparable results. Figure 17 shows that the mean annual increase of CO_2 for the model falls well within one standard deviation of the mean for BRW and SPO CO_2 data for 1974-1982.

Likewise, in comparing the decrease of $\delta^{13}C$ values, the model shows general agreement with the data presented by Friedman (personal communication). The annual decrease of 0.096 is somewhat larger in magnitude than that of Mook et al. (1983).

Since the model has a balanced biospheric exchange budget, the above general agreement would not point to any obvious biospheric source or sink. It must be pointed out, however, that the present model will not be suitable for long-term comparisons with the data because it does not have deep ocean

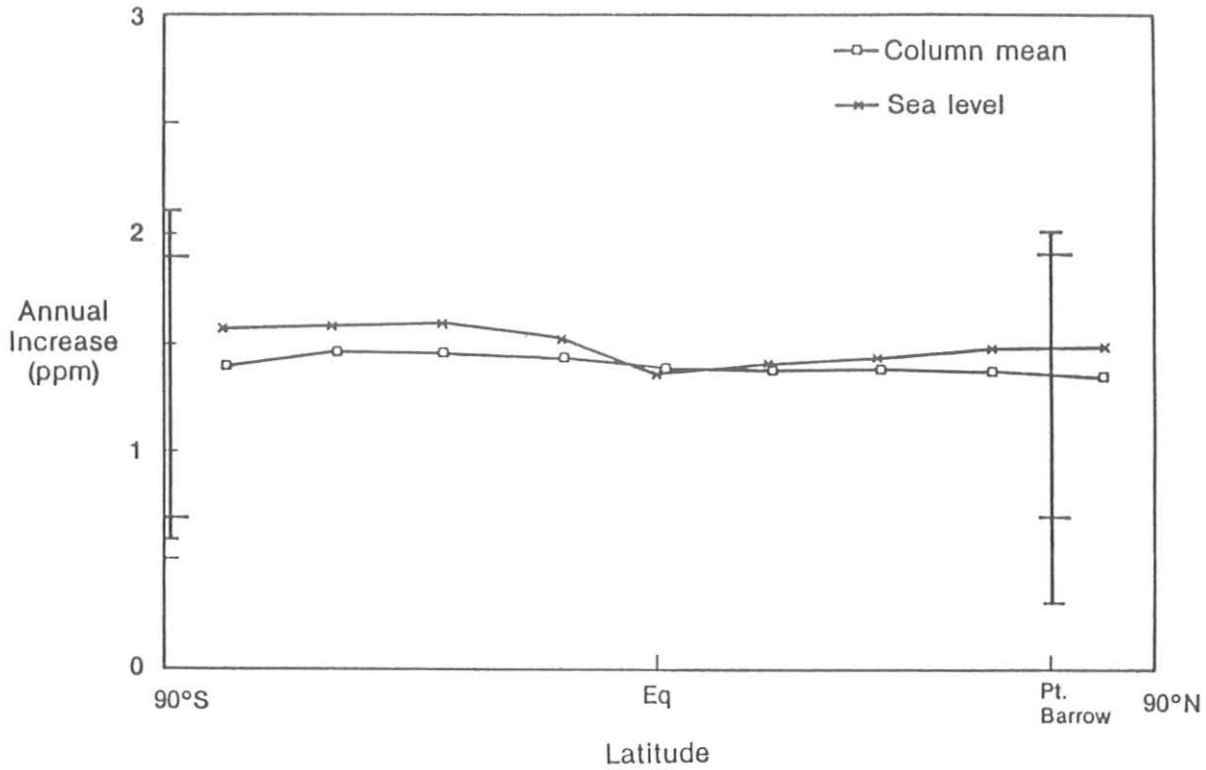

Figure 17.--Annual increase of atmospheric CO_2 concentration in the model for sea level and columnar mean. The mean and standard deviation of annual processes observed at SPO and BRW for 1974-1982 are shown.

circulation, an important component in a long-term carbon cycle model. It should also be pointed out that apparent agreement may also be fortuitous and that yet-unspecified mechanisms may have great importance for the short-term cycling of CO_2.

LABORATORY INTERCOMPARISON

A program was started in 1984 by GMCC in cooperation with WMO in order to assess the agreement between laboratories around the world making CO_2 measurements. A set of three CO_2-in-air reference gas tanks was prepared in 1984 and sent to SIO for initial calibration. Starting in 1985, these tanks will be circulated to over 15 participating laboratories around the world where each laboratory will determine the amount of CO_2 in each tank. A comparison of the results will indicate the level of agreement between different laboratories.

4.3 References

Bacastow, R., 1981. Numerical evaluation of the evasion factor.. In Carbon Cycle Modeling, SCOPE 16, B. Bolin (ed.), John Wiley and Sons, New York, 95-101.

Bacastow, R. B., 1976. Modulation of atmospheric carbon dioxide by the Southern Oscillation. Nature 261:116-118.

Defant, A., 1961. Phys. Oceanogr. Vol. 1, Pergamon Press, New York.

Fraser, P. J., M. A. K. Khalil, R. A. Rasmussen, and L. P. Steele, 1984. Tropospheric methane in the mid-latitudes of the Southern Hemisphere. J. Atmos. Chem. 1:125-135.

Gammon, R. H., W. D. Komhyr, L. S. Waterman, T. J. Conway, K. W. Thoning, and D. Gillette, 1984. The 1982/83 ENSO event: the response of the global atmospheric CO_2 distribution. Preprints, Conference on the Scientific Application of Baseline Observations of Atmospheric Composition, November 7-9, 1984, Aspendale, Australia.

Harris, J. M. and E. C. Nickerson (eds.), 1984. Geophysical Monitoring for Climatic Change, No. 12: Summary Report 1983. NOAA Environmental Research Laboratories, Boulder, CO. 184 pp.

Hellerman, S., 1967. An updated view of the wind stress on the world ocean. Mon. Weather Rev. 95:607-616. Corrigenda 1968, ibid 96:63-74.

Keeling, C. D., 1973. The carbon dioxide cycle: Reservoir models to depict the exchange of atmospheric carbon dioxide with oceans and land plants. Chemistry of the Lower Atmosphere, S. I. Rasool (ed.), Plenum Press, New York, 251-330.

Keeling, C. D., N. W. Rakestraw and L. S. Waterman, 1965. Carbon dioxide in surface ocean waters of the Pacific Ocean: 1, Measurements of the distribution. J. Geophys. Res. 70:6087-6097.

Kerman, B., 1984. A model of interfacial gas transfer for a well-roughened sea. J. Geophys. Res. 89:1439-1446.

Komhyr, W. D., L. S. Waterman, and W. R. Taylor, 1983. Semiautomatic nondispersive infrared analyzer apparatus for CO_2 air sample canalysis. J. Geophys. Res. 88(C2):1215-1322.

Komhyr, W. D., R. H. Gammon, T. B. Harris, L. S. Waterman, T. J. Conway, W. R. Taylor, and K. W. Thoning, 1985. Global atmospheric CO_2 distribution and variations from 1968-1982 NOAA/GMCC flask sample data. J. Geophys. Res. 90(D3):5567-5596.

Machta, L., 1974. Global scale atmospheric mixing. Turbulent Diffusion in Environmental Pollution, F. Frenkiel and R. E. Munn (eds.), Academic Press, New York, 33-56.

Mahrbach, C., C. Culbertson, J. Hawley, and R. Pytkowicz, 1973. Measurement of the apparent dissociation constants of carbonic acid in seawater at atmospheric pressure. Limnol. Oceanogr. 18:897-907.

Mook, W. G., A., M. Koopmans, A. F. Carter, and C. D. Keeling, 1983. Seasonal, latitudinal, and secular variations in the abundance and isotopic ratios of atmospheric carbon dioxide: 1, Results from land stations. J. Geophys. Res. 88(C15):10,915-10,933.

Ramanathan, V., R. J. Cicerone, H. B. Singh, and J. T. Kiehl, 1985. Trace gas trends and their potential role in climate change. J. Geophys. Res. 90(D3):5547-5566.

Reinsch, C. H., 1967. Smoothing by spline functions. Numerische Mathematik 10:177-183.

Roos, M. and G. Gravenhorst, 1984. The increase in oceanic carbon dioxide and the net CO_2 flux into the North Atlantic. J. Geophys. Res. 89:8181-3193.

Rotty, R., 1982. Distribution of and changes in industrial carbon dioxide production. Rep. ORAU/IEA-82-2(M), Oak Ridge Associated Universities/Institute for Energy Analysis, Oak Ridge, TN, 23 pp.

Siegenthaler, U., and K. O. Münnich, 1981. $^{13}C/^{12}C$ fractionation during CO_2 transfer from air to sea. Carbon Cycle Modeling, SCOPE 16, B. Bolin, (Ed.), John Wiley and Sons, New York, 249-257.

Steele, L. P., P. J. Fraser, R. A. Rasmussen, M. A. K. Khalil, T. J. Conway, A. J. Crawford, R. H. Gammon, K. A. Masarie, and K. W. Thoning, 1985. The global distribution of methane in the troposphere. Submitted to J. Atmos. Chem.

Takahashi, T., D. Chipman, T. Volk, 1982. Geographical, seasonal and secular variations of the partial pressure of CO_2 in surface waters of the oceans: the results of the North Atlantic TTO program. Proceedings of CO_2 Research Conference, Berkeley Springs, WV, 19-23 September 1982, CONF-820970, U. S. Dept. Energy, Washington, D.C.

Tans, P., 1981. $^{12}C/^{12}C$ of industrial CO_2. Carbon Cycle Modeling, SCOPE 16, B. Bolin (ed.), J. Wiley and Sons, New York, 127-129.

Weiss, R., 1974. Carbon dioxide in water and seawater; The solubility of a non-ideal gas. Mar. Chem. 2:203-215.

Weiss, R. F., 1981. Determinations of carbon dioxide and methane by dual catalyst flame ionization chromatography and nitrous oxide by electron capture chromatography. J. Chromatogr. Sci. 19:611-616

5. TRACE GASES GROUP

5.1 Continuing Programs

TOTAL OZONE

Routine total ozone observations were made with Dobson spectrophotometers during 1984 at 14 stations that comprise the U.S. total ozone station network (Table 1). Of the 14 stations, 4 are operated by GMCC personnel; 3 are foreign cooperative stations; 3 are domestic cooperative stations; and 4 are operated by the NWS.

Table 1.--U.S. Dobson ozone spectrophotometer station network for 1984

Station	Period of record	Inst. No.	Agency
Bismarck, ND	01 Jan 1963-present	33	NOAA
Caribou, ME	01 Jan 1963-present	34	NOAA
SMO	19 Dec 1975-present	42	NOAA
Tallahassee, FL	02 May 1964-present	58	NOAA; Fla. State Univ.
Nashville, TN	01 Jan 1963-present	79	NOAA
SPO	17 Nov 1961-present	80	NOAA
Wallops Is, VA	01 Jul 1967-present	86	NOAA; NASA
Huancayo, Peru	14 Feb 1964-present	91	NOAA; Huancayo Obs.
Fresno, CA	22 Jun 1983-present	94	NOAA
Boulder, CO	01 Sep 1966-present	61	NOAA
Poker Flat, AK	06 Mar 1984-present	63	NOAA; Univ. of Alaska
MLO	02 Jan 1964-present	76	NOAA
Perth, Australia	30 Jul 1984-present	81	NOAA; Aust. Met. Dept.
Haute Province, France	02 Sep 1983-present	85	NOAA; Obs. Haute Prov.

Daily 1984 total ozone amounts applicable to local apparent noon, for stations in the U.S. Dobson instrument network, have been archived by the World Ozone Data Centre, 4905 Dufferin Street, Downsview, Ontario M3H5T4, Canada, in Ozone Data for the World. Table 2 lists provisional monthly mean total ozone amounts for 1984 for the NOAA observatories and cooperative stations.

Table 2.--Provisional 1984 mean total ozone amounts (milli-atm-cm)

	Jan	Feb	Mar	Apr	May	Jun	Jul	Aug	Sep	Oct	Nov	Dec
Bismarck, ND	351	377	391	371	364	340	315	298	304	290	300	310
Caribou, ME	363	390	428	407	379	360	343	332	321	304	324	315
SMO	254	254	249	254	258	262	262	260	265	265	270	276
Tallahassee, FL	312	309	325	340	341	334	330	326	301	284	280	271
Boulder, CO	329	348	366	361	328	321	304	299	290	303	296	297
Poker Flat, AK			431	423	419	368	328	307	301	291		
MLO	249	273	264	301	290	277	277	274	269	262	244	246
Nashville, TN	326	358	374	381	369	355	347	333	310	293	305	274
SPO	304									216	271	303
Perth, Australia							337	322	341	324	311	294
Wallops Is, VA	338	352	367	371	361	343	326	317	300	282	293	275
Haute Province, France	373	360	400	381	401	366	326	330	320	300	296	312
Huancayo, Peru	258	258	250	252	242	238	248	255	259	259	258	252
Fresno, CA	317	331	345	365	333	344	319	311	298	297	287	309

NESDIS has designated a select set of 16 Dobson instrument stations whose total ozone data will be used for validation of SBUV ozone data obtained aboard the NOAA F satellite (and similar satellites to be flown in the future). The 16 select stations are shown in Table 3. In a cooperative endeavor, with funding provided by NESDIS, NOAA/GMCC has agreed to maintain the Dobson instruments at these sites highly accurately calibrated. Calibrations of each instrument will be performed at intervals of 3 to 4 years. The calibrations will be performed relative to primary standard Dobson instrument No. 83 which is maintained as the world total ozone standard by NOAA/GMCC in Boulder, Colorado.

Table 3.--Select NESDIS Dobson instrument stations

Arosa, Switzerland	Melbourne, Australia
Boulder, USA	New Delhi, India
Edmonton, Canada	Perth, Australia
Goose Bay, Canada	Poker Flat, USA
Huancayo, Peru	Pretoria, South Africa
Haute Province, France	Sapporo, Japan
Invercargill, New Zealand	Tateno, Japan
Mauna Loa, USA	Varanasi, India

As part of the calibration effort, NOAA/GMCC personnel conducted an international comparison of Dobson ozone spectrophotometers, sanctioned by the WMO, and hosted at Melbourne, Australia by the Australian Bureau of Meteorology,

November 19 to December 8, 1984. Countries, instruments, and scientists that participated in the comparisons are shown in Table 4. Instruments 105, 112, and 116 are operated, respectively, at Melbourne, New Delhi, and Tateno. Earlier in the year (August), R. D. Grass spent 3 weeks in Melbourne training Australian technicians in optically aligning, calibrating, and operating Dobson spectrophotometers. At that time major optical adjustments were performed on instruments 111 and 115.

Table 4.--International Dobson spectrophotometer comparison participants

Country	Instruments	Participants
Australia	105, 111, 115	J. Easson, D. Jenkins, S. Townsend
India	112	K. Chatterjee
Japan	116	R. Kajihara
New Zealand	82	E. Farkas
USA	83	R. Grass, W. Komhyr

Work was performed on several other Dobson instruments during 1984. New Zealand (Invercargill) Dobson instrument No. 17 was rebuilt and re-calibrated after having been in a flood. Boulder instrument No. 61 was re-calibrated. And instrument No. 81, that had been on loan to Australia, was re-called early in 1984, automated, calibrated, and re-installed at Perth, Australia in July for total ozone and Umkehr observations.

OZONE VERTICAL DISTRIBUTION

In late 1984, funding was obtained from NESDIS to conduct ozonesonde observations at 3 stations and Umkehr observations at 5 stations to obtain atmospheric ozone vertical distribution data for validation of SBUV ozone data obtained aboard the NOAA F satellite. The ozonesonde observations are made with balloon-borne ECC (electrochemical concentration cell) instruments (Komhyr, 1969), and the Umkehr observations are made with automated Dobson spectrophotometers (Komhyr et al., 1985).

Weekly ECC ozonesonde flights began at Boulder, Colorado, and Hilo, Hawaii, in January 1985. The sounding program was expanded later in 1985 to include observations at Edmonton, Alberta, in a cooperative endeavor with the Canadian Atmospheric Environment Service.

A list of the automated Umkehr observatories, operating in 1984, is given in Table 5. Stations yet to be implemented are: Huancayo, Peru (12°S, 76°W); Pretoria, South Africa (16°S, 28°E); and Lauder, New Zealand (45°S, 170°E).

Table 5.--Automated Dobson spectrophotometer Umkehr observatories

Station	Lat., Long.	Date observation began
Boulder, Colorado USA	40°N, 105°W	1-14-82
Haute Province Observatory, France	44°N, 6°E	9-02-83
Mauna Loa Observatory, USA	20°N, 156°E	3-12-84
Perth, Australia	32°S, 116°E	7-26-84
Poker Flat, USA	65°N, 148°W	3-05-84

Tests on ECC ozonesondes were continued in 1984 to assess their performance in the troposphere and at altitudes between 30 and 40 km. Eight ECC sondes were flown in March 1984 (Hilsenrath et al., 1985) from Palestine, Texas, aboard a balloon gondola carrying, also, Canadian and NASA Wallops Island ECC sondes, as well as UV ozone photometers from Harvard University, NOAA/AL, NASA/JSC, and NASA/GSFC. Additionally, ECC ozonesondes were flown at Palestine in March and October 1984 aboard a University of Minnesota balloon gondola that measured water vapor and ozone with a mass spectrometer.

Results of comparison ECC soundings made to nearly 40 km altitude in September 1983 at Aire-Sur-L'Adour, France, during the MAP/GLOBUS campaign are shown in Figure 1. Total ozone amounts deduced from the ozone profiles were 265 and 266 milli-atm-cm, respectively, for instruments 4A1031 and 4A1042. The total ozone amount measured that morning with Dobson spectrophotometer No. 85 at Haute Province Observatory, located 470 km to the east, was 371 milli-atm-cm.

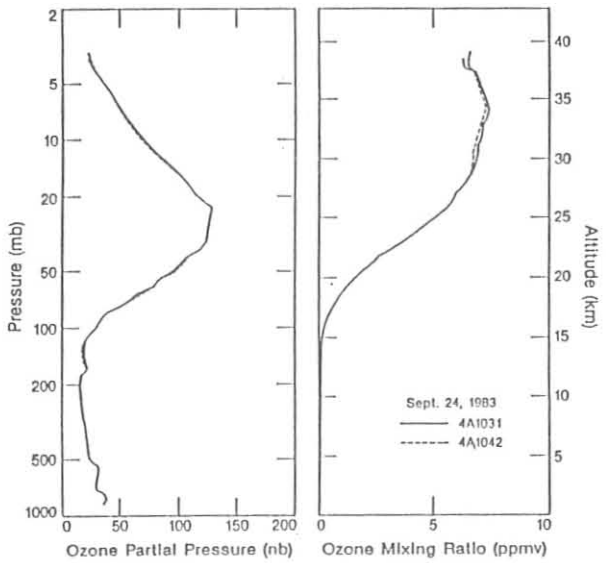

Figure 1.--Ozone profiles measured by a pair of ECC sondes in Air-Sur-L'Adour, France, during the Map/Globus Campaign.

SURFACE OZONE

The four-station GMCC surface ozone network operated throughout 1984. All of the station Dasibi ozone monitors were compared with the network standard instrument during the year. The return of Dasibi meter serial number 1316 from South Pole allowed for correction of data from this location back through 1981. The monthly mean data (Fig. 2) presented here supercede previously published results. Analysis of the surface ozone data through 1984 was completed with particular attention given to secular trends in the data. To investigate the long-term trends, seasonal cycles were removed from the monthly means by subtracting monthly normals to give the anomalies shown in Fig. 3. Included in Fig. 3 are least squares linear regression line fits to the data, along with calculated slope and 95% confidence intervals, in percent ozone change per year.

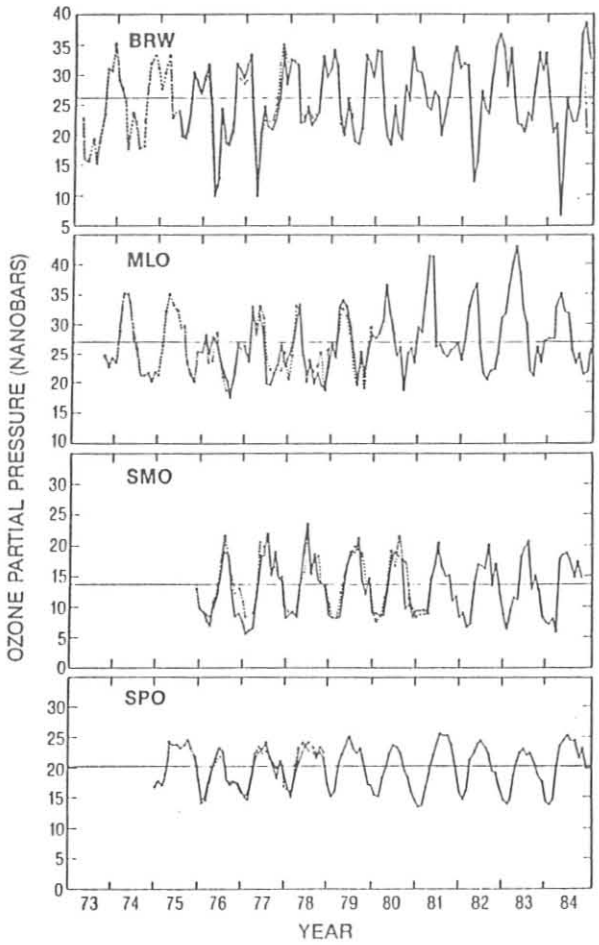

Figure 2.--Monthly mean surface ozone pressures at the GMCC observatories obtained from measurements with ECC ozone meters (•••••) and Dasibi ozone monitors (———).

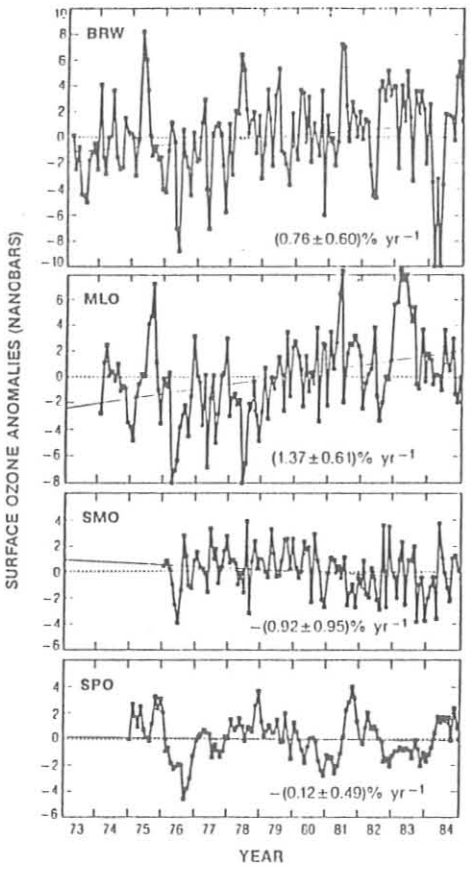

Figure 3.--Surface ozone anomalies (departures from monthly normals) at the GMCC observatories. Solid lines are linear least squares fits to the data. The printed values are linear trends with 95% confidence intervals, in percent per year.

The significant increase at BRW is a summer and autumn phenomenon, while at MLO the positive growth rate is strongest during the winter but still significant during the spring. In the Southern Hemisphere the overall decreases are not significant but a significant negative trend does appear during the summer months at both SMO and SPO.

Based on the general circulation model calculations of Levy et al. (1985), it appears that the winter and spring ozone rise each year in the troposphere at MLO is associated with the large buildup in ozone over the North Pacific. This strongly suggests that the long-term increase in tropospheric ozone since the late 1970's during these months may be tied to circulation changes and the subsequent altered transport by the circulation. Evidence for such circulation changes in the vicinity of Hawaii has been presented by Namias (1985). The role of anamolous circulation patterns may be evident in the very high surface ozone amounts observed at MLO in 1983 coinciding with the particularly strong ENSO event.

At Barrow during 1984 both the highest (November) and lowest (April) monthly means were recorded in the 12 years of observations. As can be seen in Fig. 2 the January-May 1984 period ozone amount (18.6 nb) was well below the 12-year normal (24.8 nb). In 1984, both February and April had the lowest values recorded for the months, while October and November had the highest values measured for those months. Departures from normal of this magnitude are most likely associated with anomolous circulation patterns.

STRATOSPHERIC WATER VAPOR

Ten stratospheric water vapor profiles were obtained in Boulder in 1984. Two soundings were also obtained at Laramie, Wyoming in November as part of the data validation program of the SAGE II satellite measurement system. Stratospheric mixing ratio profiles for the soundings in Boulder in 1984 are shown in Fig. 4. The lower stratospheric spring minimum in mixing ratio is very pronounced as seen especially in the April sounding.

As noted last year (Harris and Nickerson, 1984) the annual cycle in water vapor at 50 mb is small and thus this level is particularly useful in monitoring long-term changes. It has been noted previously (Mastenbrook and Oltmans, 1983) that there appears to be a relationship between tropical stratospheric winds and water vapor at 50 mb at mid-latitudes of the Northern Hemisphere. This relationship is observed in Fig. 5 where the smoothed water vapor and tropical winds are shown as the top and bottom curves, respectively. Also shown are the total ozone at Mauna Loa which exhibits a marked quasi-biennial oscillation (QBO), and temperatures near the tropopause and in the stratosphere at Ponape (7°N). The eruption of El Chichon in 1982 does not appear to have greatly altered the QBO wind oscillation at Ponape but had a marked effect on the temperature. The temperature increase at 100 mb appears to be especially pronounced. Based on the previously noted relationship of low water vapor mixing ratios associated with westerly tropical stratospheric winds it might have been expected that 1983 would have been a year of relatively lower water vapor amounts. In fact they are not much different from the 1982 and 1984 levels. This may be a confirmation of the role of the tropopause in the tropical western Pacific in

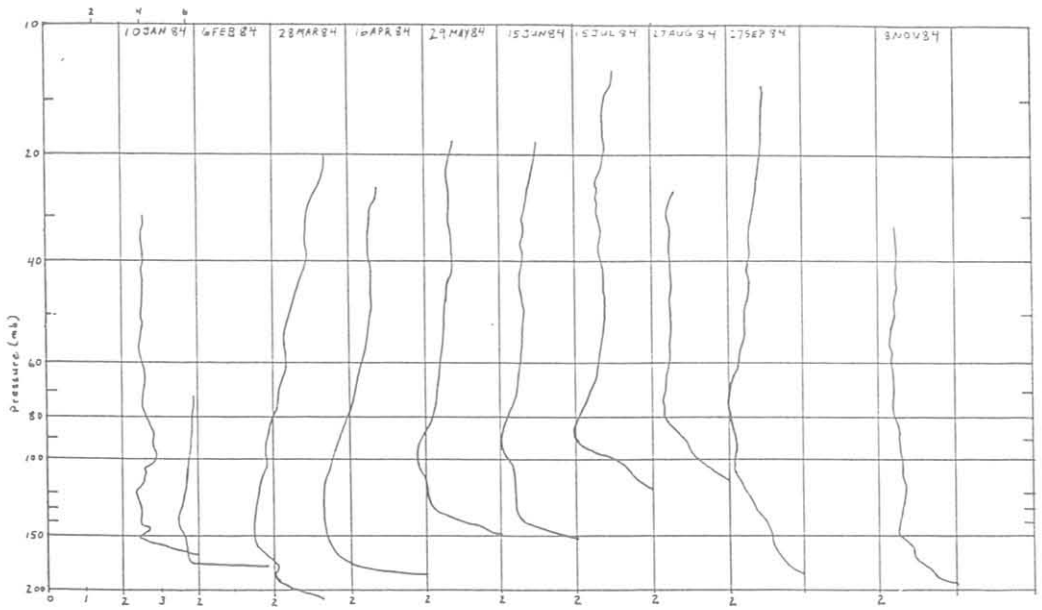

Figure 4.--Profiles of stratospheric mass mixing ratio in ppm at Boulder, Colorado for 1984. Numbers along the top of the plot for the first water vapor profile are volume mixing ratios in ppm.

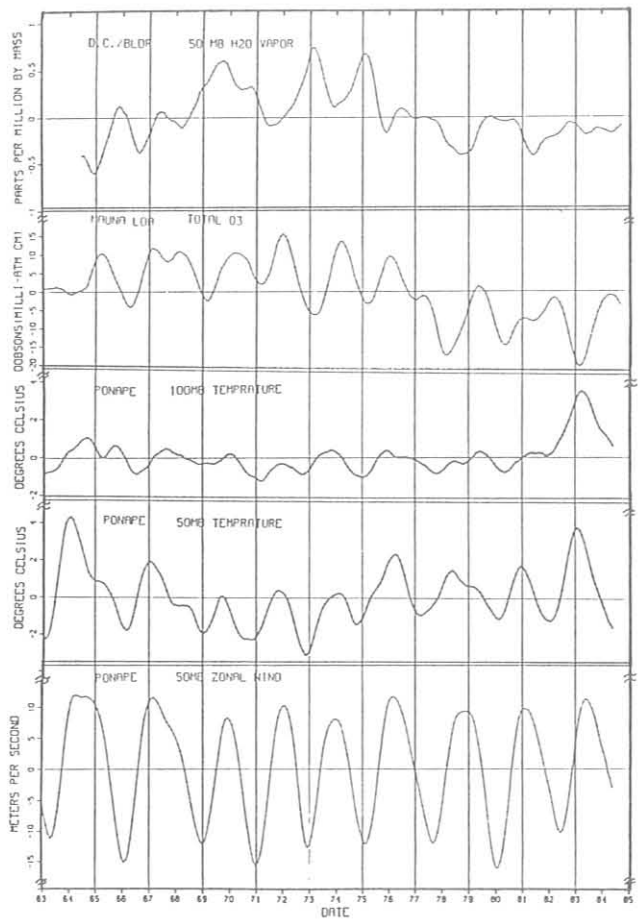

Figure 5.--Smoothed anomalies of water vapor, ozone, temperature and winds.

controlling the flux of water vapor into the stratosphere. Because of the high tropopause temperatures in the western Pacific the temperature of air entering the stratosphere would be warmer and moister than normal, thus counterbalancing the expected QBO effect on stratospheric water vapor over Boulder.

HALOCARBONS AND NITROUS OXIDE

Pair flask air samples continued to be collected weekly at BRW, NWR, MLO, and SMO, during 1984; and biweekly at SPO during January, November and December 1984. Sample analyses, for CCl_3F, CCl_2F_2, and N_2O concentrations continued to be made on a gas chromatograph in Boulder. From 1 January through 15 October 1984, a Shimadzu mini-2E gas chromatograph was operated at SPO, with CCl_3F, CCl_2F_2 and N_2O analyses made twice weekly. During October, calibration gas in cylinder 3081 was inadvertently lost, so that measurements could not continue. A new reference gas tank (No. 3083) was sent to SPO in early November, but did not arrive there until late December.

An additional Shimadzu mini-2E gas chromatograph was procured and set-up in Boulder for training and as a spare instrument. A power supply, temperature controller, and electrometer assembly were also procured and sent to SPO as spare parts.

With the eruption of Mauna Loa volcano and the subsequent loss of power at MLO, the sample collection location was transferred to Mauna Kea observatory during April 1984.

CCl_3F, CCl_2F_2, and N_2O data for 1973 to 1979 were archived in 1984 at the National Climate Data Center in Ashville, NC. A NOAA Technical Report (Thompson et al., 1985) describes in detail the sampling and analysis program since its inception in 1973, and presents all as well as selected data.

Selected CCl_3F, CCl_2F_2, and N_2O data for 1977 through 1 September 1984, for the NOAA/GMCC baseline stations and Niwot Ridge (NWR), Colorado, are shown in Figs. 6, 7 and 8. Solid lines fitted to the data are least squares linear regressions. Errors associated with indicated growth rates are 95% confidence intervals. All concentrations shown are expressed in the Oregon Graduate Center CCl_3F, CCl_2F_2, and N_2O calibration scales (Rasmussen, 1983). Results for N_2O are tentative, since analyses of the air samples for N_2O may have been adversely influenced by atmospheric CO_2. The extent of the CO_2 interference has yet to be determined.

January 1 CCl_3F and CCl_2F_2 concentrations for 1978 through 1984, derived from the linear regression analyses, are shown in Table 6. Because the growth rates of these two trace gases has remained nearly constant in recent years, the Northern Hemisphere/Southern Hemisphere annual concentration differences for CCl_3F and CCl_2F_2 have decreased by about a factor of 2 during 1978 to 1984.

Preliminary analysis of the data have yielded a best estimate atmospheric life-time for CCl_3F to be 79.9 year, and that for CCl_2F_2 94.8 years. Taking into account systematic errors in estimates of release rates of these halocarbons, and systematic and random concentration measurement errors, the atmospheric lifetimes for CCl_3F and CCl_2F_2 are calculated to range from a minimum of 35 years to a maximum of ∞ years.

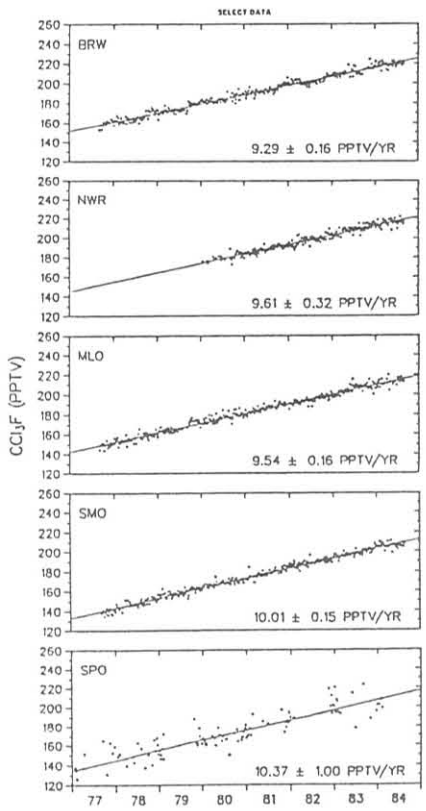

Figure 6.--Selected CCl_3F data obtained from chromatographic analyses of pressurized air samples collected in pair flasks.

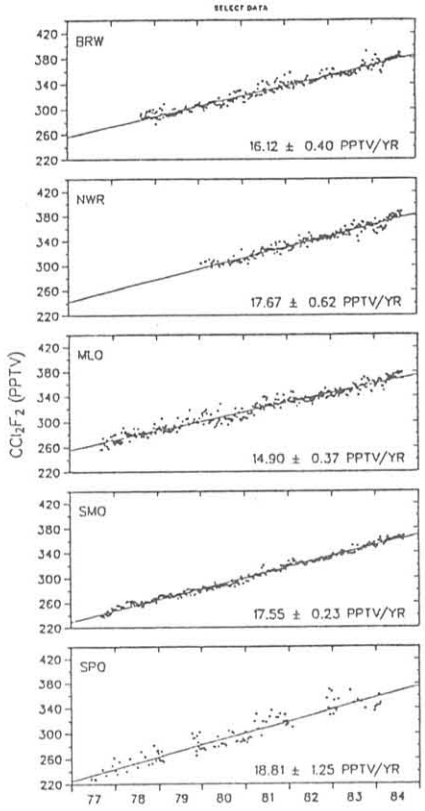

Figure 7.--Selected CCl_2F_2 data obtained from chromatographic analyses of pressurized air samples collected in pair flasks.

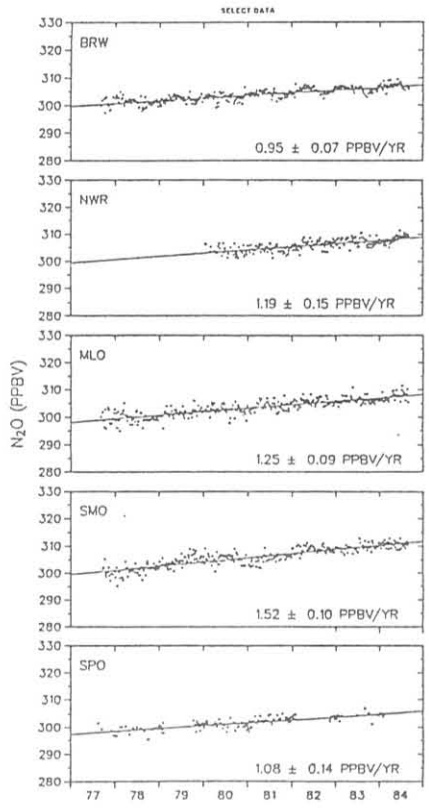

Figure 8.--Tentative, selected N_2O data obtained from chromatographic analyses of pressurized air samples collected in pair flasks.

Table 6.--CCl_3F and CCl_2F_2 Northern Hemisphere, Southern Hemisphere, and Global concentrations* in PPTV

	Year	N.H.	S.H.	Globe	% Diff: NH-SH
CCl_3F	1979	281.5 ± 1.1	264.5 ± (6.1)	273.0 ± (3.6)	6.2
	1980	297.4 ± 1.0	282.3 ± (5.2)	289.8 ± (3.1)	5.2
	1981	313.4 ± 0.9	300.0 ± (4.2)	306.7 ± (2.6)	4.4
	1982	330.1 ± 1.0	317.2 ± (3.3)	323.7 ± (2.2)	4.0
	1983	346.2 ± 1.1	335.0 ± (2.5)	340.6 ± (1.8)	3.3
	1984	362.9 ± 1.2	352.3 ± 1.8	357.6 ± 1.5	3.0
CCl_2F_2	1978	154.2 ± 0.8	145.0 ± 1.0	149.6 ± 0.9	6.2
	1979	163.6 ± 0.7	155.0 ± 0.9	159.3 ± 0.8	5.4
	1980	173.4 ± 0.6	165.0 ± 0.8	169.2 ± 0.7	4.9
	1981	182.6 ± 0.5	175.0 ± 0.8	178.8 ± 0.7	4.3
	1982	192.2 ± 0.4	184.9 ± 0.7	188.6 ± 0.6	3.9
	1983	201.8 ± 0.5	194.9 ± 0.9	198.3 ± 0.7	3.5
	1984	211.0 ± 0.6	205.0 ± 1.5	208.0 ± 1.1	2.9

*Concentrations are given for 01 January of each year, derived from least squares linear regression fits to the data. Indicated uncertainties are 95% confidence interval measurement errors.

5.2 References

Harris, J. M., and E. C. Nickerson (eds), 1984. Geophysical monitoring for climatic change, No. 12: Summary Report, 1983. NOAA Environmental Research Laboratories, Boulder, CO, 184 pp.

Hilsenrath, E., J. Ainsworth, A. Holland, J. Mentall, A. Torres, W. Attmannspacher, A. Bass, W. Evans, W. Komhyr, K. Mauersberger, A. J. Miller, M. Proffitt, D. Robbins, S. Taylor, and E. Weinstock, 1985. Results from the balloon ozone intercomparison campaign (BOIC). In Atmospheric Ozone, Proceedings of the Quadrennial Ozone Symposium held in Halkidiki, Greece, 3-7 September 1984, D. Reidell, Dordrecht, Holland, 454-459.

Komhyr, W. D., R. D. Grass, R. D. Evans, R. K. Leonard, and G. H. Semeniuk, 1985. Umkehr observations with automated Dobson spectrophotometers. In Atmospheric Ozone, Proceedings of the Quadrennial Ozone Symposium held in Halkidiki, Greece, 3-7 September 1984, D. Reidel, Dordrecht, Holland, 371-375.

Komhyr, W. D., 1969. Electrochemical concentration cells for gas analysis. Annales de Geophysique 25(1):203-219.

Levy II, H., J. D. Mahlman, W. J. Maxim, and S. C. Liu, 1985. Tropospheric ozone: the role of transport. Journal of Geophysical Research 90:3753-3772.

Mastenbrook, H. J., and S. J. Oltmans, 1983. Stratospheric water vapor variability for Washington, DC/Boulder, CO: 1964-82. Journal of Atmospheric Science 40(9):2157-2165.

Namias, J., 1985. Remarks on the potential for long range forecasting. Bulletin of the American Meteorological Society 66:165-173.

Rasmussen, R. A., and J. E. Lovelock, 1983. The atmospheric lifetime experiment; 2. Calibration. Journal of Geophysical Research 88:8369-8378.

Thompson, T. M., W. D. Komhyr, and E. A. Dutton, 1985. Chlorofluorocarbon-11, -12, and nitrous oxide measurements at the NOAA/GMCC baseline stations (16 September 1973 to 31 December 1979). NOAA Technical Report ERL 428-ARL-8 124 pp.

6. ACQUISITION AND DATA MANAGEMENT GROUP

6.1 Continuing Programs

STATION CLIMATOLOGY

Introduction

The interpretation of measurements of trace gases, aerosols and atmospheric turbidity, including an assessment of the influence of local pollution sources, requires the measurement of ancillary meteorological variables including wind direction, speed, station pressure, air temperature and moisture content. Where appropriate, common, off-the-shelf instrumentation was chosen and WMO-recommended exposure standards were used. Table 1 contains the serial number and altitude or elevation of each instrument as of December 1984. At this time the new instrumentation control and monitoring system (CAMS) had been installed at each station.

With the installation of the CAMS to manage the meteorological data, a number of changes were made to the measurement and reporting of meteorological conditions. Specifically a second thermometer was added at the top of the sampling tower to measure the gradient in the boundary layer. At those sites where a representative temperature gradient can be measured, BRW, MLO and SPO, this measurement will be used with the surface wind to determine the bulk Richardson Number. On request, the CAMS also supplies a complete listing of the hourly average values for the previous 24-hr period. This is used in conjunction with a daily observation to monitor data quality. A CAMS system was installed in BRW in August, SMO in October, SPO and MLO in November. This period also marked the end of a 2-year project to recalibrate all the sensors in the network. The serial numbers reported in table 1 represent new or recalibrated instrumentation. The listing of sensors in the GMCC Summary Report for 1983 (Harris and Nickerson, 1984) describes the complement of sensors as they were up to the time the CAMS were installed With one exception, platinum resistance thermometers (Yellow Springs Inst. Co.) were used at SPO throughout 1984.

Hourly average values, scaled in metric units, are processed, checked for quality and reported for each measurement listed in table 1. The values are stored on microfiche and magnetic tape. The microfiche listings are organized by station, date, time and variable. The files are usually available 6 to 9 months after the end of the year.

Barrow

A description of the Barrow site, its surroundings, and climatology can be found in previous GMCC Summary Reports. Wind roses of the hourly average resultant wind direction and speed are presented in 16 direction classes and 4 speed classes. The wind rose for 1984 shows significant deviations from the 1977-1983 period average (fig. 1). The predominant wind direction is northeasterly for 1984 as opposed to north-northeasterly for the longer term. At the same time, easterly winds (NE-SE) occurred 50% of the time in 1984 as compared with 61% for the previous 7 years. This is consistent with deviations observed in 1983. The main differences are in the relatively large occurrence of winds in the northeasterly and southwesterly direction.

Table 1.--GMCC meteorological sensor deployment

Sensors	BRW serial No.	BRW elev (m)	MLO serial No.	MLO elev (m)	SMO serial No.	SMO elev (m)	SPO serial No.	SPO elev (m)
Primary Wind								
Aerovane*	576	16.7	931	8.4	782	13.7	585	12.2
Station Pressure								
Pressure transducer†	2366	9	109	3397	752	30	117	2841
Mercury barometer	641	9‖	278	3397		30		2841
Air Temp. A								
Linearized thermistors¶	2	2.5	10	1.6	8	9	703	2.0 **
Air Temp. B ††								
Linearized thrmistors	4	15.3	11	1.6	7	2.3 ‖‖	704	23.2
Air Temp. C								
Linearized thermistors		N/A	N/A		9	2.3 ‖‖	836	-0.1
Dew Point Temp.								
Dew point hygrometer¶¶	7162	2.5	182	1.6	592	9	N/A	

*Aerovane, serial no. 141, Bendix, Inc. Environmental Science Div., Baltimore, MD.

†Pressure transducer, serial no. 1201F1B, Rosemount, Inc. Mineapolis, MN.

‖The altitude of the instrument above MSL is reported.

¶Linearized thermistors, serial no. 44212, Yellow Springs Inst. Co., Yellow Springs, Ohio.

**Platinum resistance thermometers, S/N 139AP, Yellow Springs Inst. Co., Yellow Springs, Ohio. Installed in a naturally ventilated radiation shield no. 43103C, R. M. Young Co., Traverse City, Michigan.

††This thermometer is positioned at the top of the local sampling tower to facilitate an estimation of boundary layer stability.

‖‖This thermometer is used to measure the air temperature under the photovoltaic arrays.

¶¶General Eastern model no. 1200 ASP, General Eastern Instrument Co., Watertown, Massachusetts, an E.G. & G. model no. 911, E.G. & G. Newton, Massachusetts at SMO.

Referring to table 2, the deviation from the NE direction occurred primarily during the winter and spring months. In 1984, 17% of the wind speeds were equal or greater than 10 ms^{-1} in comparison to a long-term average of about 9%. The maximum wind speeds in August, September, October and December 1984 equal or exceeded the previous 7-year average. The December 1984 value of 24.8 ms^{-1} is almost equal to the 25.0 value measured in December 1983.

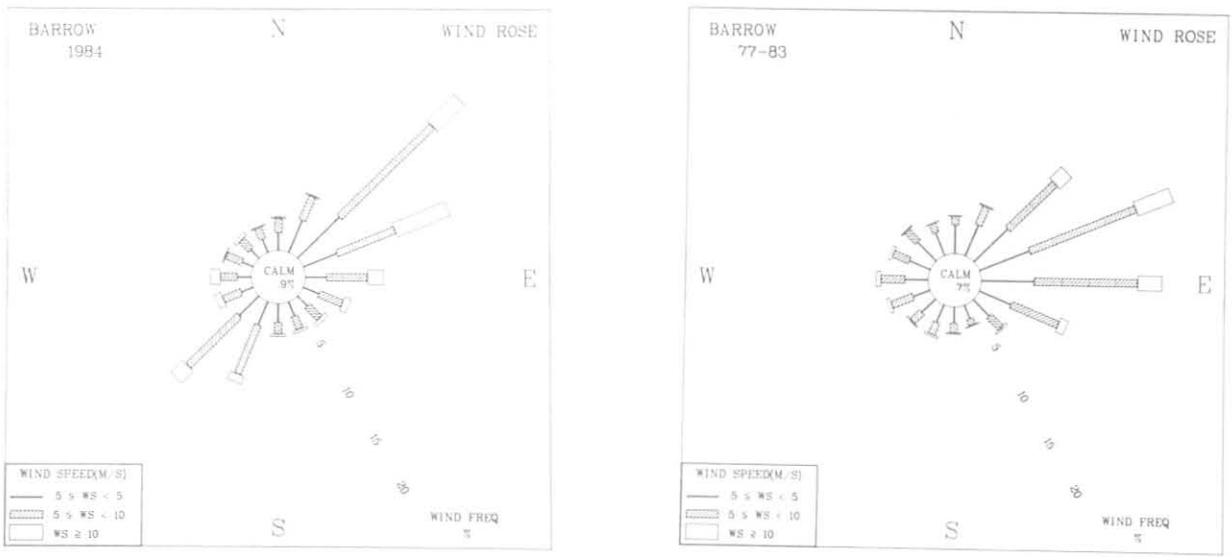

Figure 1.--Wind rose of surface winds for BRW for (left) 1984 and (right) 1977-1983. The distribution of the sesultant wind direction and speed are in units of percent occurrance for the year and 7-year period, respectively. Wind speed is displayed as a function of direction in three speed classes.

The winter and spring of 1984 was significantly colder than normal. The average temperature for January was 11°C below the average for the previous 7 years. A new minimum of -48°C was reported. In February the average was 13° below the station average and a new all-time record minimum temperature of -50°C was reported. The all-time minimum reported at the NWS station in Barrow is -49°C. The warmest temperature reported in February was only -24°C. March through June were also significantly below normal. This condition in BRW is consistent with a substantially colder than normal spring observed over the continental U.S. (Wagner, 1985). The average temperature for the year was almost 4°C below normal. For the first time, table 2 contains the dew point measurements. All frost points have been converted to dew point. Too many periods of prolonged outages due to instrumentation problems have precluded the inclusion of this data in the past. The average pressure for the year was 1015.9 mb which is 2.7 mb above the 7-year average.

Table 2.--BRW 1984 monthly climate summary*

	Jan	Feb	Mar	Apr	May	Jun	Jul	Aug	Sep	Oct	Nov	Dec	1984
Prevailing wind direction	NE	SW	NE	SW	SSW	NE	SW	W	E	ENE	NE	ENE	NE
Average wind speed ($m\ s^{-1}$)	7.1	6.1	6.8	5.6	6.8	5.7	5.8	6.0	6.6	8.5	7.8	7.5	6.8
Maximum wind speed† ($m\ s^{-1}$)	17	13	16	13	13	11	12	18	19	19	20	25	25
Direction of wind† (deg.)	43	229	70	76	222	189	214	228	73	73	50	262	262
Average station pressure (mb)	1015.3	1019.8	1022.9	1016.6	1013.5	1013.6	1009.8	1009.3	1015.4	1018.2	1015.7	1015.8	1015.9
Maximum pressure† (mb)	1039	1041	1037	1031	1026	1025	1021	1028	1031	1043	1033	1039	1043
Minimum pressure† (mb)	999	1001	1012	1002	1003	1004	994	988	993	997	989	984	984
Average air temperature (°C)	-34.0	-39.2	-30.2	-26.8	-11.7	-1.5	-1.0	2.2	-0.7	-8.7	-22.5	-25.9	-16.8
Maximum temperature† (°C)	-22	-24	-13	-12	-3	5	5	13	9	2	-9	-5	13
Minimum temperature† (°C)	-48	-50	-41	-42	-32	-6	-5	-3	-4	-22	-33	-36	-50
Average dew point temperature (°C)	-37	-45	-39	-36	-21	-10	-10	-1	-1	-10	-23	-27	-22
Maximum dew point† temperature (°C)	-14	-33	-21	-22	-11	-1	-1	8	5	0	-9	-6	8
Minimum dew point† temperature (°C)	-49	-50	-47	-47	-41	-15	-16	-13	-6	-22	-33	-36	-50

*Instrument heights: wind, 17 m; pressure, 9.5 m (MSL); air and dewpoint temperature, 3 m. Wind and temperature instruments are on a tower located 25 m northeast of the main building.
†Maximum and minimum values are hourly averages.

Mauna Loa

A description of the MLO site and its climatology can be found in previous GMCC Summary Reports. The wind distribution for the period 1977-1983 (fig. 2) shows a greater frequency of occurrence of southerly winds than would be expected from synoptic-scale flow analysis. The effect of the Mauna Loa volcano is to redirect stronger, predominately easterly or westerly winds aloft, down the slope with a more southerly component. The wind distribution for 1984, also shows pronounced deviations with southeasterly direction winds occurring in excess of 24% of the year compared to a long-term average of about 12%. At the same time the remainder of the southerly components show a lower percentage of occurrence than in the longer-term average. The distribution of wind speed in four classes in 1984 was similar to the 7-year averages. The greatest occurrence of higher winds was in March when 19% were equal to or greater than 10 ms^{-1}. This indicates a series of storms occurring in March when most of the southwesterlies are observed. Unlike 1983 when no spring storms were reported at MLO and no rain fell between January and March 1984 a few storms were experienced and a modest amount of precipitation was reported in each of the winter and spring months, see table 3. Otherwise the average values for wind, pressure, temperature and humidity for the year were very close to normal. Bear in mind that in most respects average values are not representative of median values due to the bimodel distribution of wind, temperature and humidity, dependent upon the time of day or wind direction.

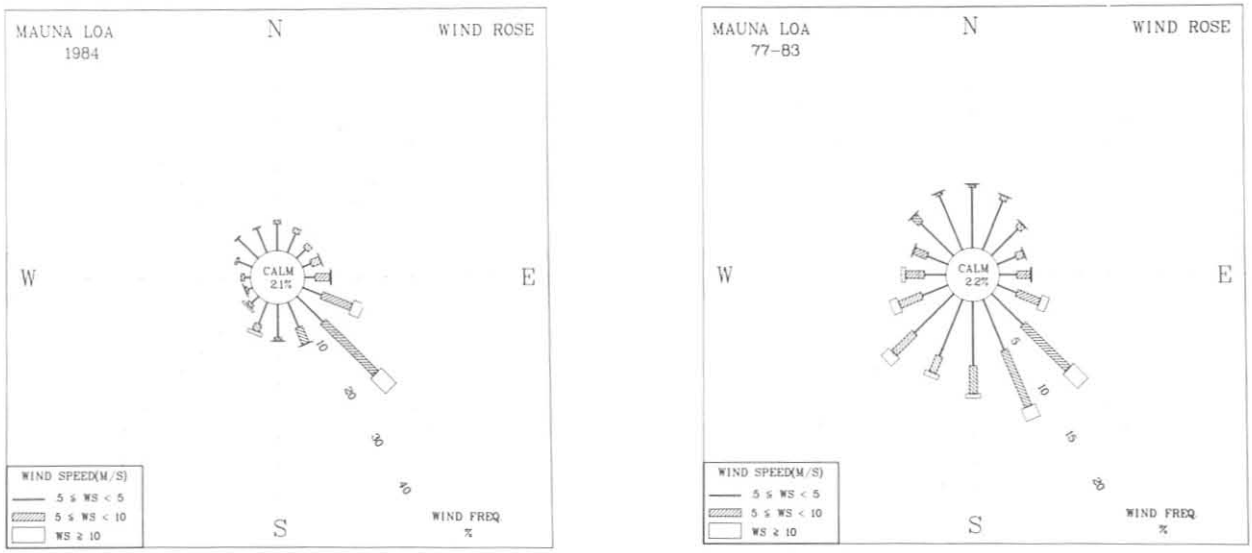

Figure 2.--Wind roses of surface winds for MLO for (left) 1983 and (right) 1977-1983. The distribution of the resultant wind direction and speed are in units of percent occurrance for the year and 7-year period, respectively. Wind speed is displayed as a function of direction in three speed classes.

Table 3.--MLO 1984 montlhly climate summary*

	Jan	Feb	Mar	Apr	May	Jun	Jul	Aug	Sep	Oct	Nov	Dec	1984
Prevailing wind direction	SE	SE	SSW	--	SE	SE	SE	SE	SE	SE	SE	SE	SE
Average wind speed (m s^{-1})	5.3	5.9	6.1	--	5.2	5.6	4.3	3.6	3.2	4.4	4.9	5.6	4.9
Maximum wind speedt (m s^{-1})	14	13	15	--	15	14	15	11	9	14	14	14	15
Direction of max. windt (deg.)	205	195	197	--	142	134	131	134	145	135	122	136	131
Average station pressure (mb)	680.9	680.3	681.5	--	682.2	682.5	681.7	682.1	681.7	682.7	682.5	678.6	681.6
Maximum pressuret (mb)	685	683	686	--	686	686	685	686	685	686	685	683	686
Minimum pressuret (mb)	675	676	674	--	679	680	679	679	679	680	680	675	674
Average air temperature (°C)	4.4	4.7	6.9	--	7.4	10.2	7.7	8.7	7.4	7.4	6.2	4.3	6.9
Maximum temperaturet (°C)	13	14	17	--	18	19	15	18	18	18	14	14	19
Minimum temperaturet (°C)	-2	-3	0	--	-1	-1	1	3	1	1	0	-3	-3
Average dewpoint temperature (°C)	-10.0	-15.7	-16.5	--	-11.0	-14.8	-7.1	-8.2	-6.7	-5.8	-5.0	-5.0	-9.9
Maximum dewpointt temperature (°C)	6	5	5	--	5	8	8	8	8	8	8	5	8
Minimum dewpointt temperature (°C)	-29	-32	-36	--	-33	-34	-33	-33	-28	-31	-25	-21	-36
Precipitation (mm)	10	7	9	--	6	0	10	27	17	14	40	35	183

*Instrument heights: wind, 10 m; pressure, 3397 m (MSL); air and dewpoint temperature, 1.6 m. Wind and temperature sensors are located approximately 15 m southwest of the main building on a tower. Pressure sensors are located in the observatory building.

†Maximum and minimum values are hourly averages.

Samoa

Southeasterly winds (ESE-SSE) occurred only 58% of the time in 1984 compared to an average of 63% for the 1977-83 period. This is an even more pronounced decrease when compared to the 72% occurrence in 1983. Part of the deficit in the occurrence of southwesterlies was made up by an increase in northwesterlies (NWW-NNW) of 18% over the long-term average of 11%, fig. 3. The increase in northwesterly wind occurrence is primarily in the first 4 months of the year and in December. Northwesterly winds occurred a significant proportion of February, March and December to constitute the prevailing direction for the month, table 4. The unusually high occurence of northerly winds in February and March is caused by the presence of the intertropical convergence zone (ITCZ) in the vicinity of Samoa for much of the period. The ITCZ is not usually found this far south. During the remainder of the year the trade wind directions prevail. The average wind speed for the year is about 1 ms^{-1} above normal, beginning in May and continuing throughout the year. The May monthly average wind speed equals or exceeds the long-term average for the individual month. This increase coincides with the thinning of the vegetation on the eastern extent of Lauagae Ridge. The prevailing easterlies would be affected the most. There also appears to be a slight shift in the prevailing direction from SSE to SE. A storm in December established new maximum wind speed, 19 ms^{-1} and low pressure readings, 990.8 mb for that month. No significant deviations from normal temperatures were reported during the year. The 2.7 m of precipitation reported in 1984 was 1 m more than that reported in 1983.

The exposure of the meteorological instrumentation at SMO is significantly different from that at other GMCC stations. Since February 1977, the anemometer has been located at a height of 13.7 m on a sampling

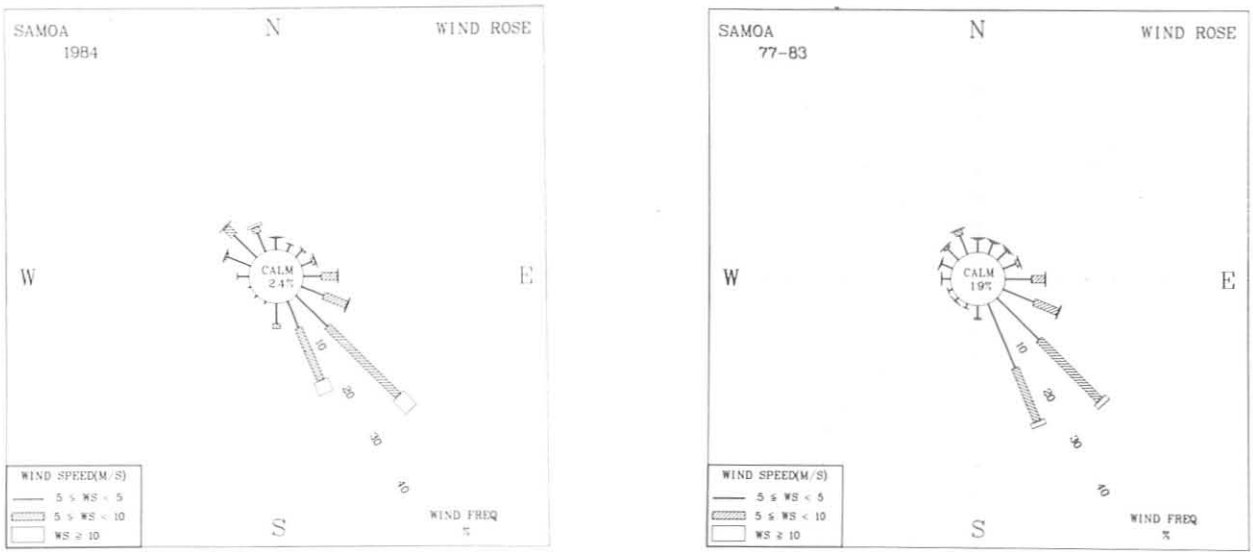

Figure 3.--Wind roses of surface wind for SMO for (left)1983 and (right) 1977-1983. The distribution of the resultant wind direction and speed are in units of percent occurrance for the year and 7-year period, respectively. Wind

Table 4.--SMO 1984 monthly climate summary

	Jan	Feb	Mar	Apr	May	Jun	Jul	Aug	Sep	Oct	Nov	Dec	1984
Prevailing wind direction	SE	NW	NW	SE	SE	SE	SE	SE	SE	SSE	SSE	NW	SE
Average wind speed ($m\ s^{-1}$)	2.8	2.9	2.9	3.5	6.6	8.6	7.5	5.6	5.7	6.4	5.1	5.0	5.3
Maximum wind speed† ($m\ s^{-1}$)	7	13	13	10	11	16	13	13	12	14	14	19	19
Direction of max. wind† (deg.)	313	326	313	142	139	149	149	136	149	155	6	327	327
Average station pressure (mb)	1000.1	999.9	1000.4	1001.8	1002.6	1002.9	1003.5	1003.2	1003.5	1002.7	1001.6	997.0	1001.6
Maximum pressure† (mb)	1004	1003	1005	1005	1006	1007	1008	1009	1008	1007	1005	1004	1009
Minimum pressure† (mb)	997	994	996	997	999	998	1000	998	998	998	999	991	991
Average air temperature (°C)	26.8	27.7	27.2	27.7	27.3	26.5	25.7	25.8	26.1	26.0	26.8	27.1	26.7
Maximum temperature† (°C)	30	32	31	31	29	30	29	29	30	30	31	35	35
Minimum temperature† (°C)	23	23	23	24	24	24	23	23	23	22	22	23	22
Average dewpoint temperature (°C)	24.9	25.1	25.7	25.6	--	--	--	--	--	--	--	--	25.2
Maximum dewpoint† temperature (°C)	28	29	29	28	--	--	--	--	--	--	--	--	29
Minimum dewpoint† temperature (°C)	22	22	23	23	--	--	--	--	--	--	--	--	22
Precipitation (mm)	224	105	365	194	162	111	64	46	354	420	134	613	2692

*Instrument heights: wind, 14 m; pressure, 30 m (MSL); air and dewpoint temperature, 9 m. Wind and temperature sensors located atop Lauagae Ridge, a distance 110 m northeast of the station. Pressure sensors are located in the station.
†Maximum and minimum values are hourly averages.

tower atop Lauagae Ridge. In this location the shape of the bluff displaces the prevailing trade winds from the southeast to a more southerly direction, but there are no major obstacles to the winds from the westerly direction as there was at the previous location on the point. Temperature is measured at a height of 9 m on the same tower. Dew point temperature is measured at the same elevation. Station pressure is measured in the main building located about 100 m west of the sampling tower. During April 1984, a significant amount of vegetation was removed from the bluff to the east of the sampling tower. The immediate result of this cleanup was to increase the air flow across the upper half of the sampling tower. The missing dew point temperatures are the result of instrumentation failure.

South Pole

Following a year when the wind speed seldom exceeded 10 ms^{-1}, 1984 showed a return to normal with 2.5% of the winds reported to be equal or in excess of 10 ms^{-1}, fig. 4. This is in comparison to the 7-year average of 3.5%. The absence of winds from the contaminated grid southwesterly directions (S through W), that make long-term sampling of trace atmospheric constituent possible, is clearly illustrated, occurring only 74 hours in the year. The prevailing wind in every month is from the grids northeast quadrant. At the SPO grid, north is defined as being along the prime meridian. The full extent of the austral winter, often termed a "coreless winter" on the Antarctic Plateau is evident by the fact that for 8 months of the year the monthly average temperature is below the annual average. Regardless, the average for 1984 of -47.7°C is the warmest in the past 8 years.

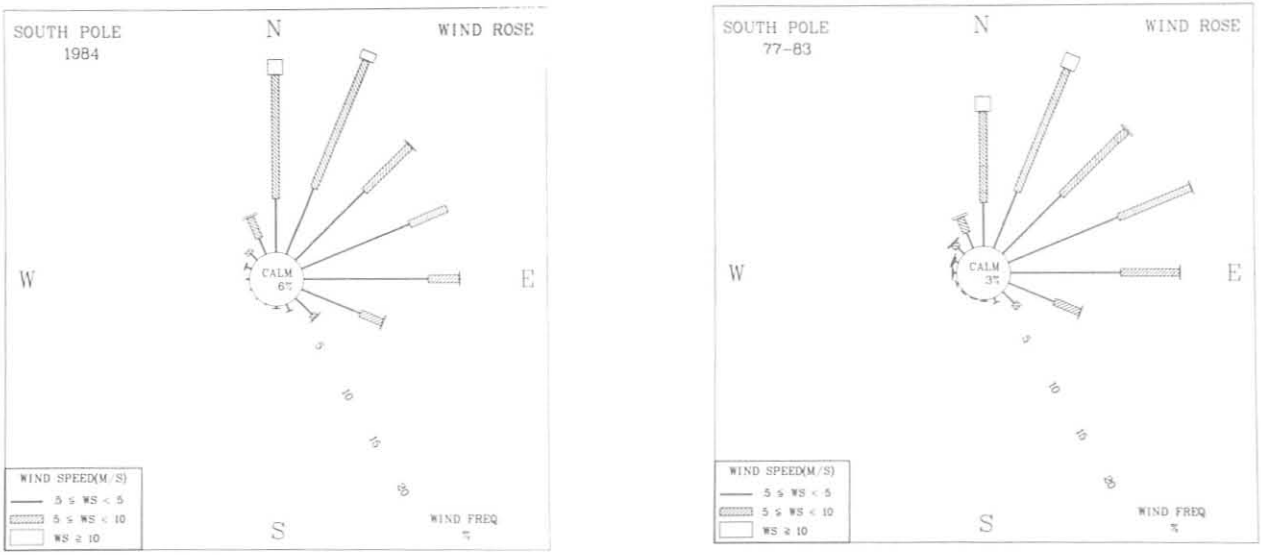

Figure 4.--Wind roses of surface winds for SPO for (left) 1983 and (right) 1977-1983. The distribution of the resultant wind direction and speed are in units of percent occurrance for the year and 7-year period, respectively. Wind speed is displayed as a function of direction in three speed classes.

Table 5.--SPO 1984 monthly climate summary*

	Jan	Feb	Mar	Apr	May	Jun	Jul	Aug	Sep	Oct	Nov	Dec	1984
Prevailing wind direction	NNE	N	ENE	E	NE	ESE	NNE	NNE	NNE	E	NNE	N	NNE
Average wind speed (m s^{-1})	4.2	4.7	4.6	4.5	5.8	4.3	7.5	5.6	6.1	3.9	4.4	4.2	5.0
Maximum wind speedt (m s^{-1})	8	10	9	8	13	9	14	11	13	9	8	11	14
Direction of max. windt (deg.)	17	357	7	12	20	128	18	8	12	343	339	359	18
Average station pressure (mb)	692.3	683.8	679.4	679.7	683.2	676.2	674.7	677.7	675.4	672.9	680.7	693.9	680.8
Maximum pressuret (mb)	707	699	698	691	704	696	694	691	697	683	690	703	707
Minimum pressuret (mb)	679	666	666	666	669	659	664	660	665	663	670	677	659
Average air temperature (°C)	-28.5	-39.0	-50.0	-58.6	-54.7	-62.9	-53.0	-58.4	-55.0	-51.4	-35.9	-22.5	-47.7
Maximum temperaturet (°C)	-22	-19	-28	-41	-35	-45	-38	-45	-33	-34	-27	-14	-14
Minimum temperaturet (°C)	-34	-57	-63	-68	-69	-75	-67	-72	-72	-66	-50	-32	-75

*Instrument heights: wind, 12 m; pressure, 2841 m (MSL); air temperature, 2 m. The anemometer and thermometer are located on a tower 100 m grid ESE of CAF. Pressure measurements are made inside CAF.
†Maximum and minimum values are hourly averages.

DATA MANAGEMENT

ICDAS Operation

With regard to the operation of ICDAS in 1984, the major event of consequence was the interruption to the supply of power at MLO. For 29 days in April, the power was off. Generator power was implemented near the end of April. For the remainder of the year MLO experienced ICDAS failures that accounted for 96 hours. The ICDAS at BRW was decommissioned during the 4th week of July to allow renovations of the station interior. CAMS was started August 9, 1984. Early in the year BRW experienced 214 hours of down time caused by tape drive failures. For the remainder of the year only 24 hours were reported. Samoa reported 73 hours of ICDAS down time during the first quarter of 1984 and none until the unit was replaced by CAMS, October 15, 1984. While brownouts continue to plague the SPO GMCC measurements causing intermittent interruptions to the data flow, longer-term outages were avoided.

CAMS Testing and Deployment

At the beginning of the year the software for the Aerosol and Solar Radiation (ASR) CAMS and Meteorology and Ozone (MO3) CAMS was complete, but for the most part untested. The software to operate the carbon dioxide CAMS was incomplete at that time. Due to excessive transmission lengths between the ozone monitoring instrumentation and the CAMS in Samoa, it was decided to implement an RS-422 port which required software changes and further testing. No further hardware changes were made. A complete listing of the subcomponents that make up CAMS can be found in Summary Report No. 12 (Harris and Nickerson, 1984). Most of the serious bugs in the software were located and corrected by late spring. The testing of the four CAMS, (a spare unit is maintained at each station) for BRW was begun in May and the units were certified and shipped at the end of July. The new CAMS's were installed without difficulty the first week in August. Testing of the 4 CAMS destined for SMO began with the removal of the BRW set. This phase was completed without difficulty and the units were sent to SMO the end of August. The installation in SMO was completed during the second week of October.

A third set of CAMS were installed for testing with the removal of the SMO unit. The electronics were removed at the end of September and shipped to SPO. The enclosures were sent during the previous austral summer to avoid shipping delays common at the beginning of the session. The remaining period from October through mid-November was used to test the four CAMS for MLO. The installation at SPO was hindered by missing components, specifically connectors to attach the printer. As a result it was not possible to complete the installation of the ASR CAMS. Parts arrived a couple of weeks later and the installation was completed by the staff early in December. The CO2 and MO3 CAMS began operation at SPO during the 3rd week of November. The CAMS at MLO were installed during the 4th week of November. Two problems arose during this installation. The first involved the accurate acquisition of voltages from the CO_2 analyzer. It was solved by increasing the gain for the analog-to-digital converter. The second involved a faulty memory board in the MO3 CAMS which was causing certain files not to be written to tape and, therefore, inhibiting tape recording of all data. The problem was not correctly diagnosed and corrected until the end of December. It resulted in the missing

of data for the weekends in December. Due to noise problems, it was necessary to add preamplifiers to the solar radiation channels, later in the year. This changeover was not completed until early in 1985.

Figure 5.--Photographs of the CAMS installation in BRW, showing both the MO3 and ASR CAMS on the left and the CO2 CAMS on the right.

6.2 Atmospheric Trajectories

Descriptions of various atmospheric trajectory programs developed within GMCC have appeared in previous summary reports (Bodhaine and Harris, 1982, pp. 71-74; Harris and Bodhaine, 1983, pp. 67-75; Harris and Nickerson, 1984, pp. 73-80). This section describes trajectory work done during 1984, including improvements made to the isentropic model and an example comparing isobaric and isentropic trajectories for an AGASP case study.

Table 6 lists most of the isobaric trajectories produced in GMCC in 1984. Another year (1983) was added to the MLO and SMO climatologies, and many trajectories were produced for Arctic locations in support of AGASP (March and April 1983). Several years of trajectories were provided for precipitation chemistry studies at various sites. A problem in the system for producing trajectories in the Southern Hemisphere was finally traced to a switch of tapes for the Northern and Southern Hemispheres. Once the problem was solved, we were able to produce trajectories in the Southern Hemisphere for the CSIRO conference (Katherine and Cape Grim, Australia). To prevent a recurrence of the same problem, a hemisphere flag was added to the identification array for each record.

Most of the trajectories produced in GMCC are isobaric; that is, the winds are traced along surfaces of constant pressure. The isentropic model developed during the past 2 years traces the winds on surfaces of constant

Table 6.--GMCC Trajectories Calculated in 1984

Destinations	Dates
Amsterdam Island	1981-1983
Katherine, Australia	1980-1983
Cape Grim, Australia	1982-1983
SMO	1983
Western Mediterranean	1982-1983
Bermuda	1983
Caribou, Maine	1979-1983
MLO	1983
White Face Mountain, New York	Summer 1983
Hong Kong	1979-1980
Miscellaneous Arctic locations	Spring 1983
Equatorial Pacific cruise	1982-1983
North Atlantic cruise	1983
Korolev cruise	1983

potential temperature, approximating adiabatic flow. This is a kinematic model that does not account for moisture or diabatic effects. We use the isobaric trajectories for most of the production work because they only require the wind data on the selected pressure surface, whereas calculation of isentropic trajectories requires height, temperature, and wind data at all mandatory levels because this type of trajectory may travel across several mandatory pressure levels. The programs that produce isentropic trajectories are also considerably more complex and costly to run. For these reasons, isentropic trajectories, at least for the time being, are used on a case study basis only. The AGASP example shown later demonstrates that in certain situations isentropic trajectories are quite useful because, compared with isobaric trajectories, they give more information about heights of transport and source areas.

Two main improvements were made to the isentropic model during 1984. The first improvement extended the lower limit of the isentropic surface from 850 to 1000 mb. To find the location of the isentropic surface when it falls between 1000 and 850 mb, we need to know the temperature at 1000 mb (T_{1000}). Since NMC does not provide 65 × 65 grids of temperatures at 1000 mb (only the wind and height information), we used a slightly different form of the following equation for z_j, the height of the isentropic surface:

$$z_j = z_i + \frac{c_p}{g}\left[\frac{(T_i\Pi_j - T_j\Pi_i)}{\Pi_j - \Pi_i}\ln\frac{\Pi_i}{\Pi_j} + T_i - T_j\right] \quad (1)$$

where z_i is the height of the mandatory pressure level below z_j, c_p is the specific heat of dry air at constant pressure, g is the acceleration of gravity, T_i is temperature at the mandatory pressure level, T_j is the temperature on the isentropic surface, $\Pi = \left(\frac{P}{1000}\right)^{\kappa}$, P is pressure (mb), and κ is $\frac{R}{c_p}$ or ≈ 0.286, where R is the gas constant for dry air at constant pressure. Eq. (1) is derived by integrating the hydrostatic equation from height z_i.

Since we have T_{850} and the heights at 850 and 1000 mb, we solve (1) for T_i to get a good approximation of T_{1000} based on the thickness of the layer and the temperature at 850 mb:

$$T_i = \frac{(\Pi_j - \Pi_i)\left[(z_j - z_i)\frac{g}{c_p} + T_j\right] + T_j\,\Pi_i\ln\frac{\Pi_i}{\Pi_j}}{\Pi_j\ln\frac{\Pi_i}{\Pi_j} + \Pi_j - \Pi_i}$$

where $T_i = T_{1000}$, $T_j = T_{850}$, $z_i = z_{1000}$ (height at 1000 mb), and $z_j = z_{850}$, (height at 850 mb).

The second improvement to the isentropic program was the capability to produce forward trajectories, which could be used to investigate transport of pollutants or tracers from a known source. Figure 6 shows a forward trajectory computed for 71.32°N, 156.67°W, a location in the Ural industrial region of the U.S.S.R. Note that the 275-K "A" trajectory that departed on 9 March 1983 at 0000 GMT arrived at BRW after five days of travel. The start location for the forward trajectories was chosen because it corresponded to the position 5 days back on the 275-K back trajectory shown in fig. 7. Note that the forward A trajectory in fig. 6 agrees well with the corresponding back trajectory in fig. 7 as it should. This transport to BRW occurred during the AGASP experiment and is discussed in detail next.

The advantages of isentropic trajectories over isobaric ones are emphasized by comparing the isentropic trajectories for 14 March 1983 at 0000 GMT (fig. 7) to the isobaric trajectories for the same time (fig. 8). Figure 8 shows the 850-, 700-, and 500-mb trajectories (Harris, 1984) during an AGASP haze event. These levels were chosen because Schnell and Raatz (1984) found that the densest aerosol concentration during the event was located between 800 and 600 mb. The 700- and 500-mb trajectories show transport over the Ural region after looping around from Central Europe and beyond. The 10-day endpoints are arbitrary and do not indicate the source of the haze event.

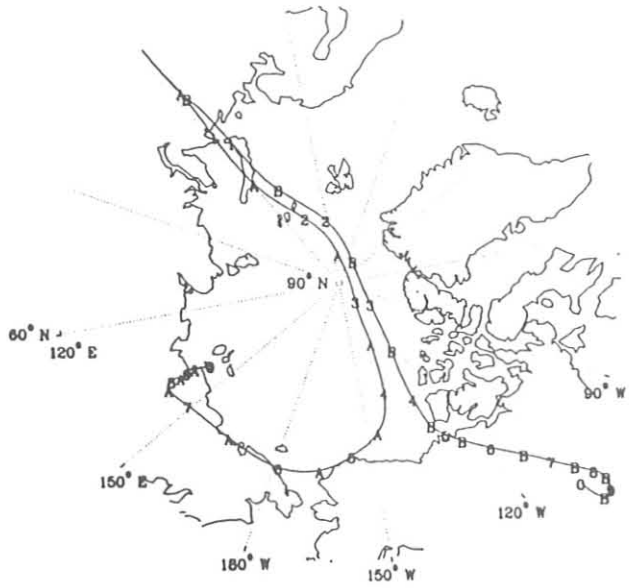

Figure 6.--Forward 275-K isentropic Trajectories from 71.32°N, 156.67°W on 9 March 1983 at 0000 and 1200 GMT.

With isobaric trajectories such as these, we can only surmise that industrial areas anywhere along the tracks could have contributed to the haze. Figure 7 shows the isentropic trajectories for this case arriving at BRW along the 270-, 275-, and 280-K isentropic surfaces. The heights and pressures upon arrival at BRW were the following: for 270 K, 1.8 km and 807 mb; for 275 K, 2.4 km and 742 mb; and for 280 K, 3.2 km and 665 mb. These heights roughly bracket the level of highest aerosol concentration mentioned previously. The important information added by these isentropic trajectories is the termination of each back trajectory marked in fig. 7. Because the isentropic surfaces are domed, as each trajectory is traced back from BRW, it rises about 100 mb towards the pole then descends to the boundary layer where the trajectory terminates (specifically, the endpoint of the next trajectory segment would fall below 1000 mb, hence is undefined.) The termination point is an estimate of the source region for air traveling to BRW along the isentropic surface.

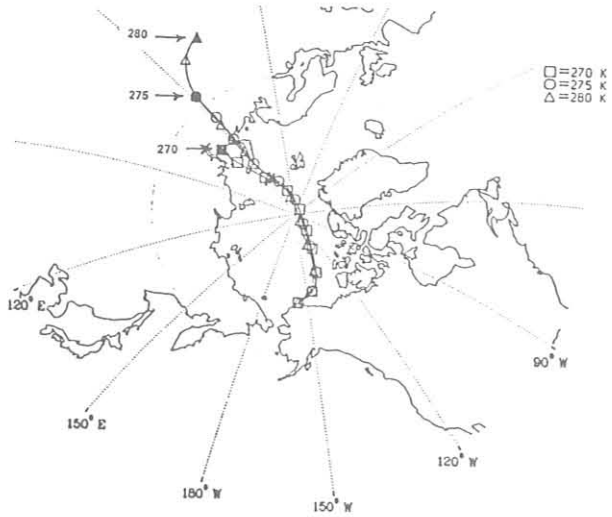

Figure 7.--BRW isentropic trajectories arriving 14 March 1983 at 0000 GMT on the 270-, 275-, and 280-K

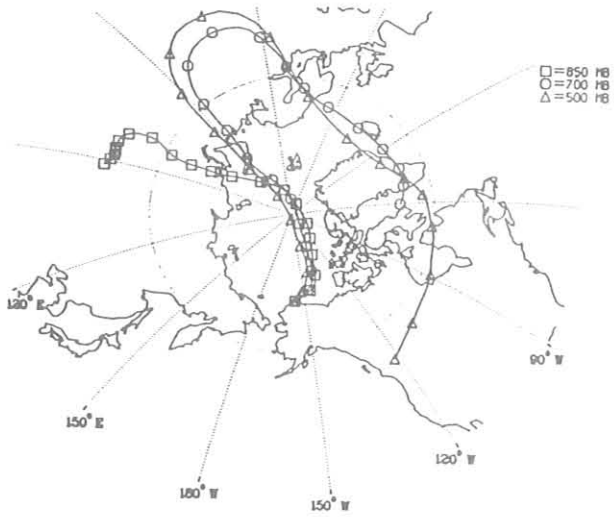

Figure 8.--BRW isobaric trajectories arriving 14 March 1983 at 0000 GMT on the 850-, 700-, and 500-mb isentropic surfaces.

6.3 References

Bodhaine, B. A., and J. M. Harris (eds.), 1982. Geophysical Monitoring for Climatic Change, No. 10: Summary Report 1981. NOAA Environmental Research Laboratories, Boulder, CO, 158 pp.

Harris, J. M., 1984. Trajectories during AGASP. Geophys. Res. Lett. 11(5): 453-456.

Harris, J. M., and B. A. Bodhaine (eds.), 1983. Geophysical Monitoring for Climatic Change, No. 11: Summary Report 1982. NOAA Environmental Research Laboratories, Boulder, CO, 160 pp.

Harris, J. M., and E. C. Nickerson (eds.), 1984. Geophysical Monitoring for Climatic Change, No. 12: Summary Report 1983. NOAA Environmental Research Laboratories, Boulder, CO, 184 pp.

Schnell, R. C., and W. Raatz, 1984. Vertical and horizontal characteristics of Arctic haze during AGASP: Alaskan Arctic. Geophys. Res. Lett. 11(5): 369-372.

Wagner, A. J., 1985. The climate of spring 1984 - An unusuallly cold and stormy season over much of the United States. Mon. Weather Rev. 113:149-169.

7. DIRECTOR'S OFFICE

7.1 Continuing Programs

PRECIPITATION CHEMISTRY

Richard S. Artz
Air Resources Laboratory, NOAA
Silver Spring, MD 20910

INTRODUCTION

Routine and special precipitation chemistry measurements continued at the GMCC sites of MLO and SMO and at the regional sites. Samples were also measured approximately twice-monthly at SPO and BRW. Special studies continued at MLO using the ion chromatograph for anion analysis for the six-site network, and plans were undertaken to purchase an additional Dionex ion chromatograph to measure cations and possibly organic acids. The Washington, D.C. network was terminated.

BASELINE MEASUREMENTS

The five-site special network on the island of Hawaii and a sixth site on Kauai continued to operate on approximately a weekly schedule. (Site locations are discussed in previous GMCC reports.) As seen in fig. 1, three of the stations (Kumukahi, MLO and Kulani Mauka) show strong concentration increases in March or April, probably caused by highly acidic small black particles in the precipitation samples caused by volcanic eruption. The October peak at 22 Mile Site cannot currently be explained. Agreement for SO_4 at Halai Hill and Kauai, sites with similar elevation and orientation to the trade winds, was very good throughout the year although Halai Hill values were routinely about 10 μeq/1 higher.

The normal trend of decreasing $SO_4^=$ concentration with elevation was not seen in 1983 except for during the winter months. However, the removal of the seawater component yielded the typical result where $SO_4^=$ is quite constant for all five sites, with the exception of the very high spikes attributed to volcanic activity (fig. 2).

At MLO and SMO three independent pH measurements have been made for several years and as explained in previous GMCC reports, the GMCC H^+ values should be highest in concentration, followed by NADP field values, and finally NADP laboratory values. MLO values were not plotted due to a limited data set. However, SMO values indicate that while the expected trend was found for January through May and December, intervening months were not in the expected order (see fig. 3).

Precipitation values for the six-station Hawaiian network are shown in fig. 4. While 1984 was wetter than 1983 for all sites, both 1983 and 1984 were much drier than normal.

Snow sample data for BRW and SPO are shown in fig. 5. Except for a few samples high in sulfate at BRW (probably sea-salt sulfate) concentrations of H^+ and $SO_4^=$ tend to be less than 20 μeq/1.

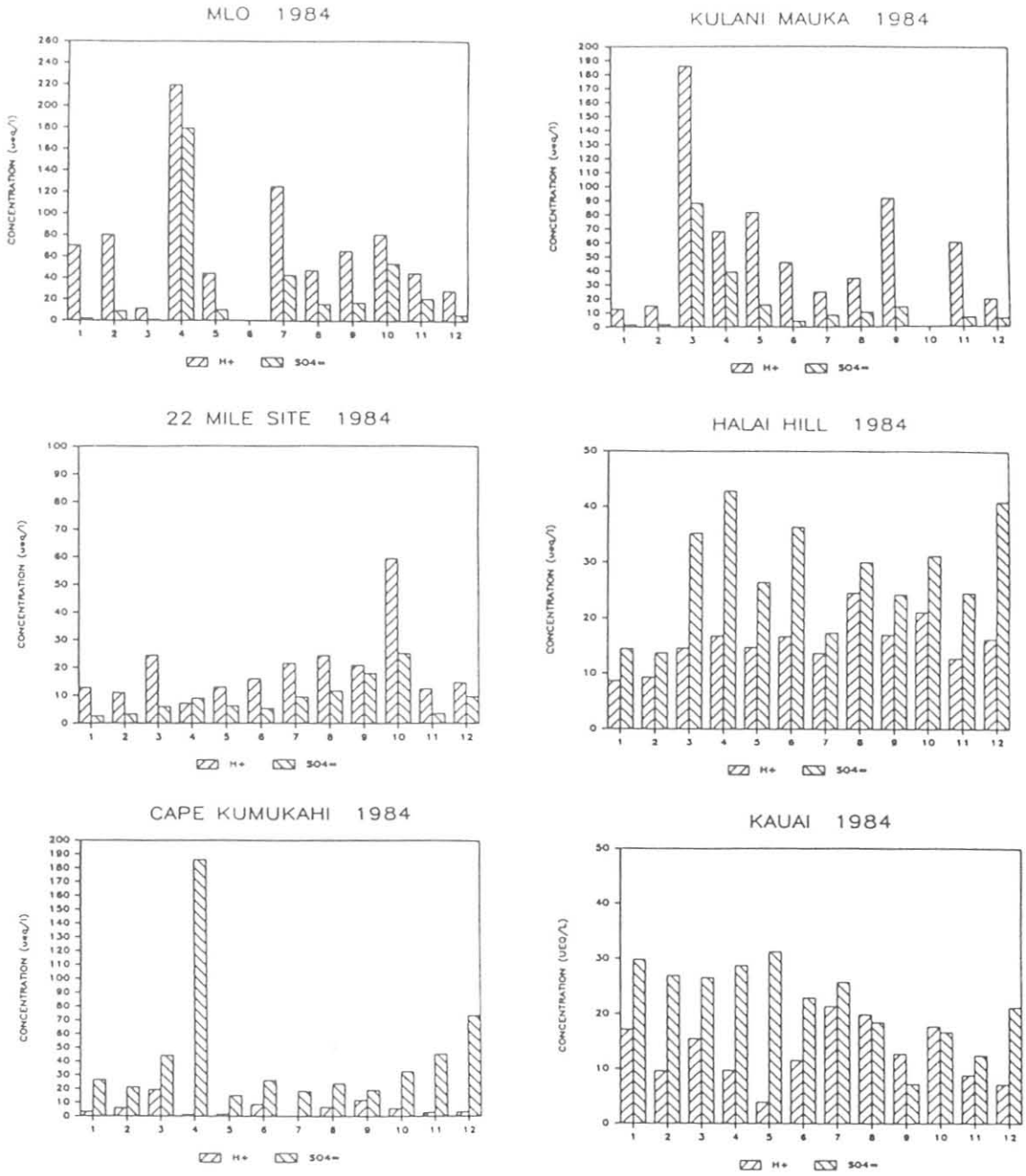

Figure 1.--Monthly precipitation weighted means for six sites on the islands of Hawaii and Kauai during 1984.

REGIONAL MEASUREMENTS

Two new NOAA NADP/NTN regional precipitation sites were opened in 1984; all of the old sites remained in operation. A second site, Presque Isle, was established in northern Maine near an existing site in Caribou. A second Texas site, Beeville, was established near an existing site in Victoria.

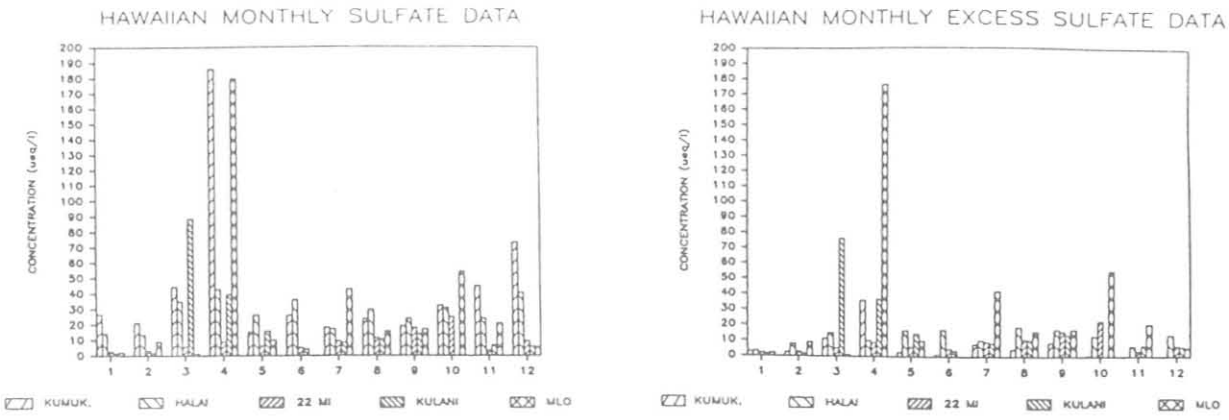

Figure 2.--Monthly precipitation weighted (left) sulfate means and (right) excess sulfate means for five sites on the island of Hawaii.

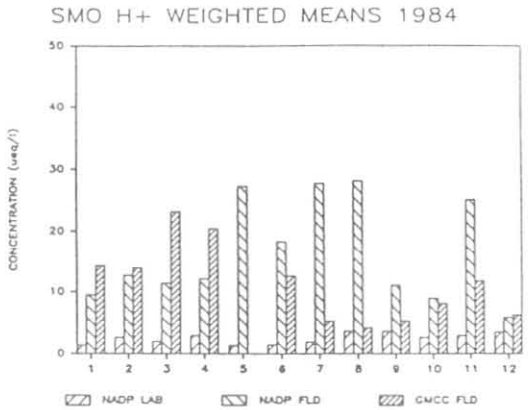

Figure 3.--Monthly precipitation weighted pH at SMO. Values vary as a function of time between sample collection and measurement.

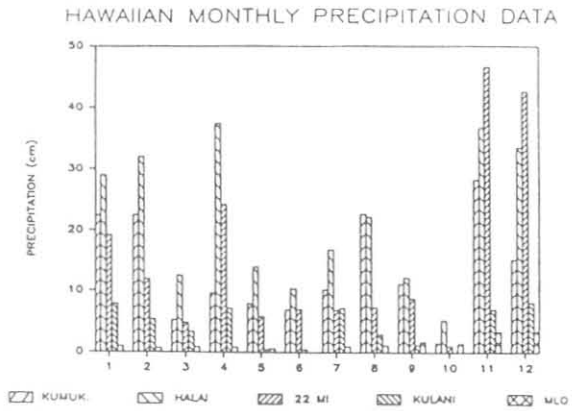

Figure 4.--Monthly precipitation at Hawaiian sites for 1984.

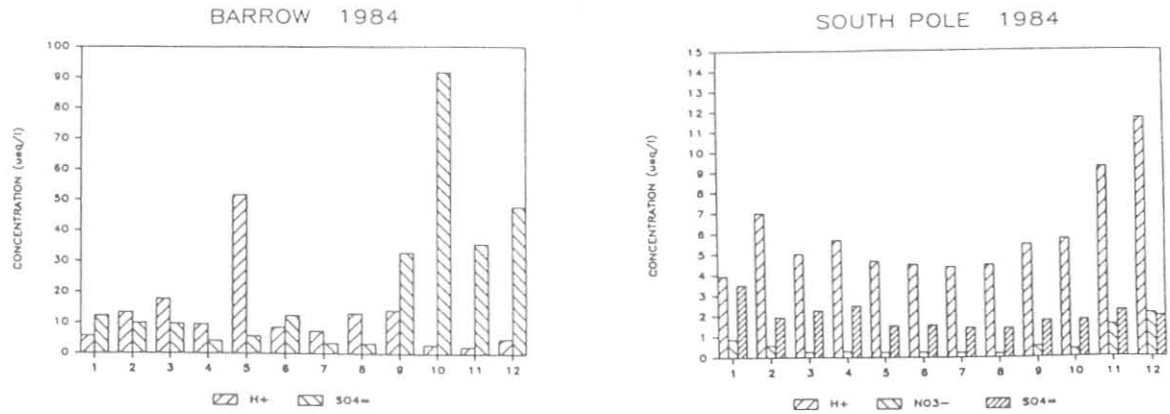

Figure 5.--Snow sample ion concentrations for BRW and SPO during 1984.

PRECIPITATION AMOUNTS ON ALASKA'S NORTH SLOPE

George P. Clagett
Soil Conservation Service
Anchorage, Alaska 99501

INTRODUCTION

Barrow and Barter Island have been National Weather Service first-order weather stations for 43 and 37 years, respectively. The mean annual precipitation derived from these records and published by the National Weather Service is 4.4 inches for Barrow and 6.4 inches for Barter Island. As a result, the widely held belief is that the Arctic is a "frozen desert". Articles, reports, scientific documents and educational institutions nearly all refer to this belief right up to the present.

Precipitation gauges equipped with "Wyoming Windshields" are now into the tenth year on the North Slope. Of the seven locations, two are at Barrow and Barter Island. Data from these instruments indicate that the mean annual precipitation is nearly 10 inches at Barrow and 12 to 13 inches at Barter Island.

PRECIPITATION AMOUNTS CONTROVERSY

Precipitation data from sites equipped with Wyoming windshields is a controversy among some groups that have reviewed the data:

1. Correct Catch. Rechard (et al., 1973, 1975) who developed the design of the Wyoming windshield, reported a correlation coefficient, R, of 0.98 with a standard error, S, of 0.07 for 160 separate storms between a Wyoming shield gauge and the standard (forest protected site). The storms covered a three winter period, November through March between the fall of 1972 through the spring of 1975.

2. Undercatch. Sturges (1984), reported that over a 7-year study period, the gauge caught only 48% of the standard (forest protected site) during the midwinter (November-March) months. Also, the amount of undercatch is correlative with windspeed. Their data indicate undercatch begins at winds of about 3 mph and can exceed 80% of the storm total if winds exceed 20 mph.

3. Overcatch. The National Weather Service's comment concerning the wide discrepancy between their data and the Wyoming gauge data at Barrow and Barter Island is that the Wyoming windshield erroneously "loads up" the catch and, therefore, makes it much greater (E. Diemer, Chief Meteorologist, National Weather Service, Anchorage; personal communication, 1984). They do not officially recognize their data as differing from a true or 100% catch, even though their gauges are not equipped with even so much as an Alter Shield.

NORTH SLOPE PRECIPITATION INVESTIGATIONS

A fair amount of research and analysis has been directed toward resolving this conflict. This includes analysis of the Weather Service's historical records at Barrow and Barter Island; measurements of the actual water-content of the tundra snowpack and the volume of water held in enormous drift catchments. The results of these investigations include:

1. Tundra snow measurements. Snow pack water-content measured on the tundra are a minimum estimate of winter precipitation because the remaining snow is, in itself, less than the amount precipitated. Some of the total amount of snow is always relocated by wind and either evaporated or deposited in drifts. Measurements near Barrow by Black (1954) and Benson (1982) indicate the NWS winter catch of precipitation is at least 40% less than the snow water-content on the tundra. Similarly, U.S. Geological Survey measurements of tundra snow in 1977, 1978, 1982, and 1983 near Barrow made during mid to late April indicate the NWS data is 36% less than snowpack water-content (Sloan et al 1979, 1980, 1982, 1983). The USGS snow measurements averaged 30% less than nearby Wyoming gauge precipitation data for the same periods of time.

2. Drift catchments. Measurement of snow in huge drift catchments was conducted along the banks of the Meade River near Atkasook, approximately 60 miles SSW of Barrow between 1961 and 1979. The amount of snow caught in the drifts, if it could be redeposited back upwind onto the fetch area, leads to an estimate of the amount of snowfall it would have taken to produce the drift. Benson (1982) estimated that an average 7.68 inches of moisture fell as snow, of which 4.45 inches remained on the tundra, while 3.23 inches were relocated. A portion of the relocation moisture was sublimated, while the rest accounted for the drifts which averaged 72 tons of moisture per meter of river bank from east winds and 31 tons from west winds. The analysis also shows that during heavy snow years, the NWS gauge catches a much higher percent of the Wyoming gauge catch.

3. Complications due to "traces". Another source of error in weather station records comes from the slow rates of snowfall in Arctic areas. This frequently results in a run of "traces" which are not entered quantitatively in the records (Jackson, 1960). At both Barrow and Barter Island there are a large number of "traces" in the precipitation records. During the calendar year 1978 at Barrow, there were 282 days with recorded precipitation, but 192 of these days (60%) showed only "T" (for trace). These 192 entries of T add up to zero in the annual precipitation record, and the error introduced by this is unknown (Benson, 1982).

4. Precipitation records analysis. Comparison of precipitation records at Barrow and Barter Island between NWS and Wyoming gauge data show Wyoming gauges catch an average three times as much snow from September 1 to May 31 (Benson, 1982). Individual years vary considerably from the average, however. During very low snowfall winters, the NWS standard gauge catch may be as low as 10% of the Wyoming gauge catch. In 1983, for instance at Barter Island, the NWS catch was only 16% of the tundra snowpack water-content in the near vicinity measured by the USGS and only 11% of the Wyoming gauge catch.

5. Summer precipitation. National Weather Service records during the summer months (June, July, and August) are also deficient due to the high frequency of "trace" entries. Brown et al. (1968) concluded an adequate overall correction is obtained by multiplying the summer record by a factor of 1.1.

CONCLUSION

Benson's estimates (1982) of 9.8 inches of mean annual precipitation at Barrow and 12.5 inches at Barter Island were arrived at through analysis of drift catchments and Tundara snow measurements. These analyses make the Wyoming gauge data appear about right. Wyoming gauge data is, however, far from a precise measure of precipitation. These data should only be considered as today's best available estimate of rain and snowfall in wind blown, exposed locations.

It is important to continue operation of the Wyoming gauges on the Arctic Slope. In particular, the gauges at Barrow and Barter Island need to be maintained in comparison with the unshielded gauges operated by the National Weather Service so that refinements can be made in our correction of existing precipitation records. The Barrow, Wyoming-shielded gauge is maintained by NOAA, GMCC, while the one at Barter Island is maintained by the U.S. Fish and Wildlife Service.

REFERENCES

Benson, C. S., 1982. Reassessment of winter precipitation on Alaska's Arctic slope and measurements on the flux of windblown snow. Geophysical Institute, University of Alaska Report UAG R-288, September 1982.

Black, R. F., 1954. Precipitation at Barrow, Alaska, greater than recorded. American Geophysical Union Transactions, 35:203-206.

Brown, J., S. L. Dingman, and R. I. Lewellen, 1968. Hydrology of a drainage basin on the Alaskan Coastal Plain. CRREL Research Report 240.

Glude, W., and C. Sloan, 1980. Reconnaissance snow survey of the National Petroleum Reserve in Alaska, April-May 1979. U. S. Geological Survey, Water Resources Investigations.

Jackson, C. I., 1960. Snowfall measurements in Northern Canada, Quart. J. Roy Meteorol. Soc., 6:(368)273-275.

Rechard, P. A., R. E. Brewer, and A. Sullivan, 1973. Measuring snowfall, a critical factor for snow resource management. Paper presented at Symposium on Advanced Concepts and Techniques in the Study of Snow and Ice Resources. Monterey, Calif., December 1973.

Sloan, C., D. Trabant, and W. Glude, 1979. Reconnaissance snow survey of the National Petroleum Reserve in Alaska, April 1977 and April-May 1978. U.S. Geological Survey, Water Resources Investigations Open-file Report 79-1342.

Sloan, c. E., 1982. Reconnaissance snow survey and spring inventory, North Slope, Alaska, 1982. U.S. Geological Survey, Water Resources Investigations trip report, May 1982.

Sloan, C. E., 1983. Reconnaissance snow survey and spring inventory, North Slope, Alaska, 1983. U.S. Geological Survey, Water Resources Investigations trip report, May 1983.

Sturges, D. L., 1984. Comparison of precipitation as measured in gages protected by an Alter Shield, Wyoming Shield, and stand of trees. 52nd Proceedings, Western Snow Conference, Sun Valley, Idaho, April 1984. Proc. WSC 1984, 57-67.

δC^{13} IN ATMOSPHERIC CO_2

Irving Friedman, Jim Gleason, John Stacey
U.S. Geological Survey
Denver, CO 80225

INTRODUCTION

With the encouragement of Lester Machta and with financial support from GMCC, we have been monitoring the δC^{13} of atmospheric CO_2. Sampling began in 1981 at South Pole, Samoa, Mauna Loa and Point Barrow. Initially, the frequency of collection varied from one sample a month at South Pole Station and Barrow, to once a week at Mauna Loa, and twice monthly at Samoa. Later, the frequency at Barrow was increased to twice monthly and Mauna Loa was decreased to twice monthly.

EXPERIMENTAL

Samples were collected in 10 l. stainless steel flasks that were pre-treated to remove carbon from the steel surface by heating them in air for 24 hours at 450°C. The flasks are sealed at both ends with stainless steel diaphram values. The samples were collected by drawing air through two flasks connected in series with copper tubing. The bottom side of the flasks were heated to ~ 60°C during sampling to aid in convective mixing of the inflowing gas. The sample air was obtained from the station sampling stack. Upon receipt in Denver, the air from each 10 l. flask was passed through a trap cooled with liquid nitrogen to condense CO_2 and water. The trap was then warmed to dry ice temperature and the CO_2 and H_2O separated. The δC^{13} and δO^{18} of the CO_2 is measured on a specially constructed 12" radius, triple collector mass spectrometer. Replicate air samples from a high pressure tank has been processed and analyzed for δC^{13} with a two sigma of $.02^{o}/oo$. The δC^{13} results are reported in per mill compared to P.D.B. We report a δ^{13} of -28.00 for NBS-21 (spectrographic graphite) as well as $-1.95^{o}/oo$ for NBS-19. No corrections have been applied for N_2O, inasmuch as the N_2O content of the air has been reported to be relatively constant over the time interval that we have been sampling.

RESULTS

Fig. 1 are plots of the δC^{13} versus time for the four stations. A linear regression of all of the data shows a decrease in C^{13} at all stations sampled. Point Barrow, Samoa and Mauna Loa show a decrease of $.1 \pm .02^{o}/oo$ per year. South Pole shows a much smaller decrease of $.02^{o}/oo$ per year. If we eliminate a number of samples collected in early and mid 1983 that show a large deviation from the average, then the yearly change at South Pole is reduced to $.01^{o}/oo$ per year.

Keeling, et. al (1984) published δC^{13} data on samples collected during 1981 at South Pole and 1981 to early 1982 at Mauna Loa. Fig. 2 shows plots in which their data and our data are compared. In general, the agreement is good, although occasional sample dates show significant disagreement.

DISCUSSION

The seasonal variation in δC^{13} in atmospheric CO_2 from samples collected at Point Barrow is higher than at the other three stations. There is also a decrease in δC^{13} from south to north (see Fig. 3). these changes parallel those found by Mook, et al. (1983). However, we find a smaller change in δC^{13} with time at the South Pole than that reported by Mook, et al.

Mook, W. G., Koopmans, M., Carter, A. F., and Keeling, C. D., 1983. Seasonal, latitudinal, and secular variations in the abundance and isotope ratios of atmospheric carbon dioxide. Journal of Geophysical Research 88: 10915-10933.

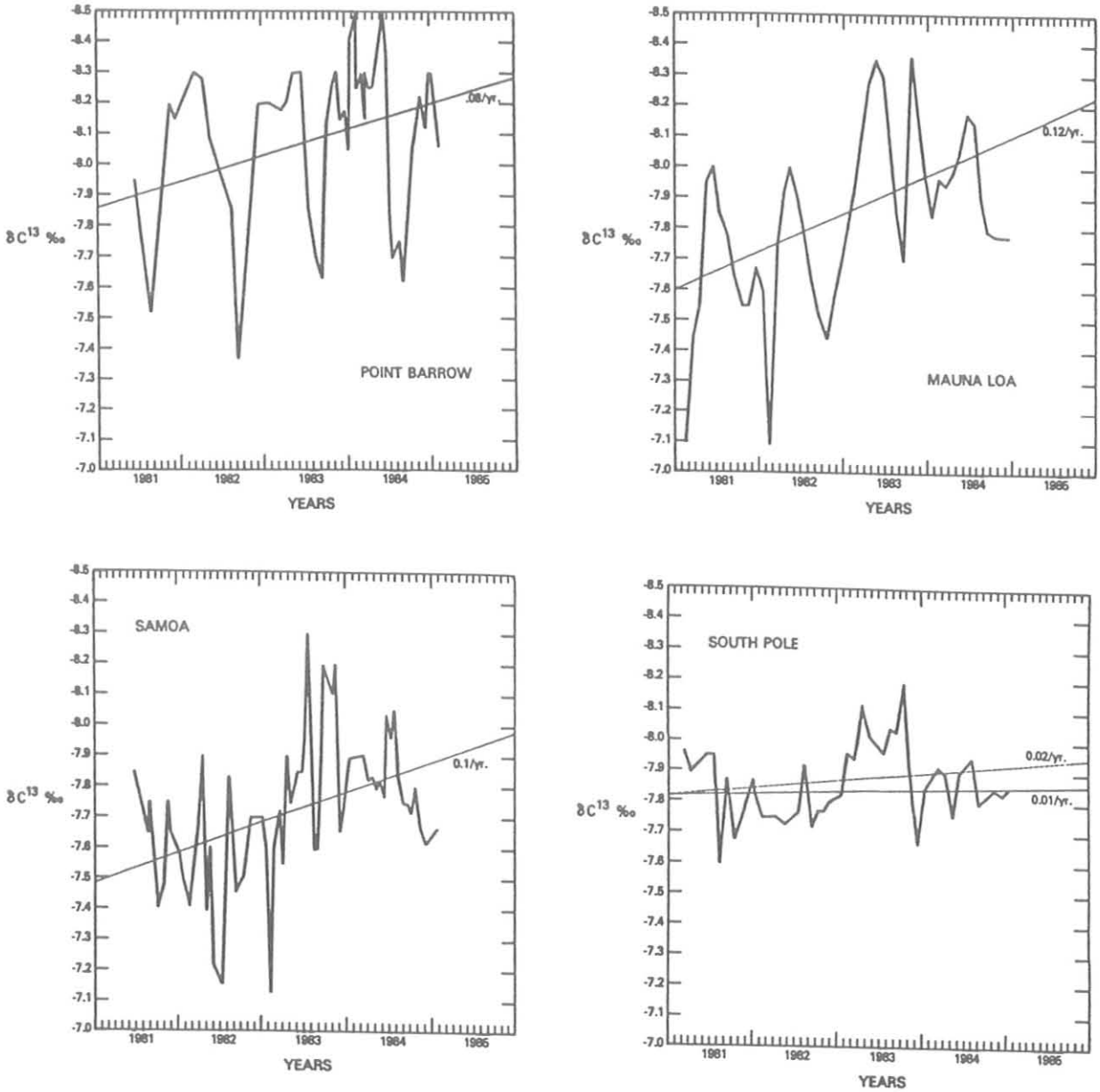

Figure 1.--Plots of δC^{13} versus time.

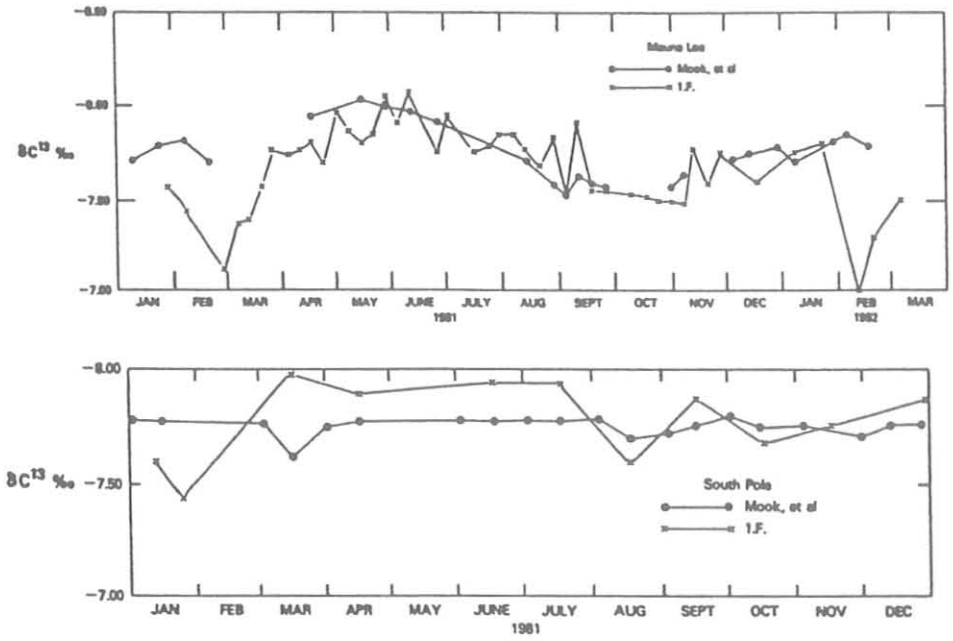

Figure 2.--Comparison of the data of Mook, et al. and this paper.

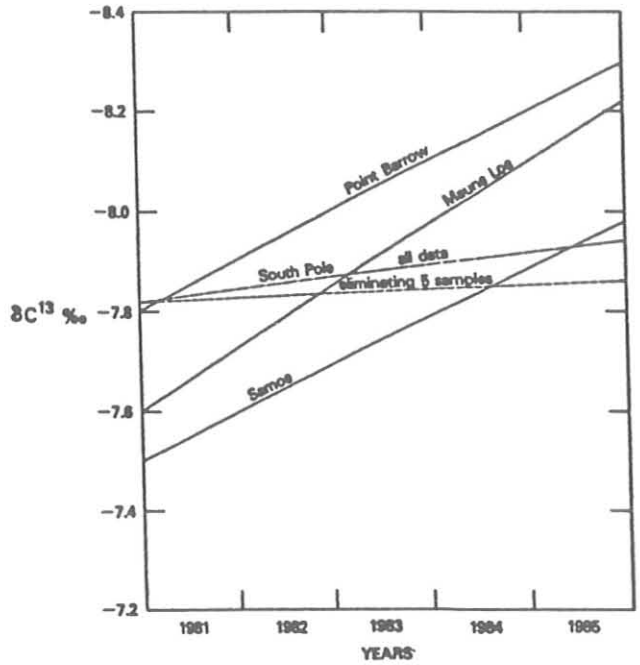

Figure 3.--Variation of δC^{13} with time. These lines are linear regression plots of the data plotted in Figure 1.

MEASUREMENT OF ULTRAVIOLET IRRADIANCE BETWEEN 290 nm AND 325 nm

Bernard Goldberg
Smithsonian Institution
12441 Parklawn Drive, Rockville, MD 20852-1773

Since August 1984 there has been a high precision scanning ultraviolet radiometer taking data in eight 5 nm wide bands. These bands are nominally centered at 290 nm, 295 nm, 300 nm, 305 nm, 310 nm, 315 nm, 320 nm and 325 nm. The instrument was developed at the Smithsonian and a good description of it has been published by Goldberg (1985).

The data are global, i.e., they contain both the beam and sky component. This makes it very difficult to do exact computations for ozone, however, a simple relationship between the various bands allows us to compute with a high degree of accuracy, the changes in ozone. The relationship assumes equal effects on all bands by aerosols and other pollutants. Figure 1 shows a comparison between our calculated values and the Dobson values for ozone. Both data sets are raw values.

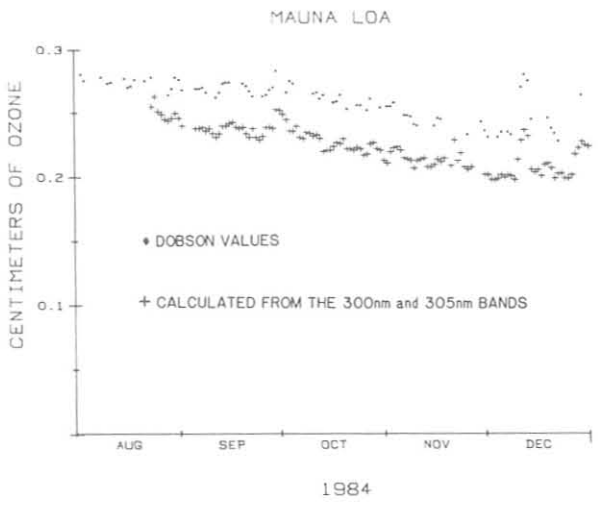

Figure 1. Comparison of Dobson values and computed values from the scanning radiometer. Although the computed values are lower, they track with the Dobson readings.

Although the purpose of the data are not to study ozone changes, the fact that the simple computation allows us to do so is important for checking the consistancy of the data and also helps to determine drifts in calibrations. A sample set of data are shown in Figures 2 and 3 for a fixed solar zenith distance in the morning. The data have a positive slope because the ozone has a negative slope. From all three Figures we see that two "solar events" took place in December of 1984.

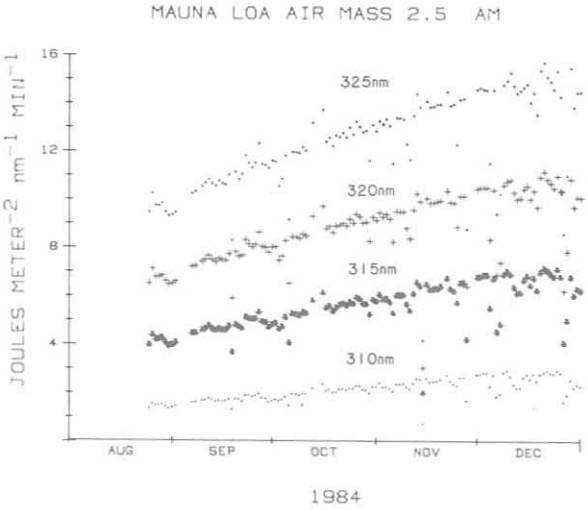

Figure 2. Variability at fixed solar angle in the longer wavelengths of the UVB.

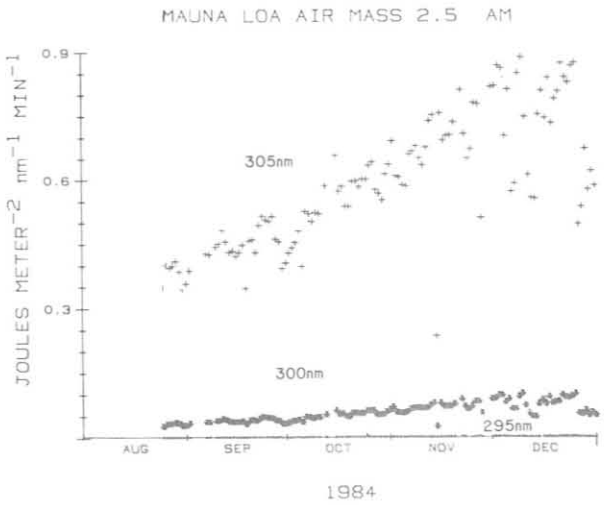

Figure 3. Variability at the shorter UVB wavelengths. Notice the low level of 295 nm, and the absence of 290 nm irradiance.

Although there is no 290 nm energy at this particular solar angle or at air mass 1.5, there is energy at noon when the sec z is less then 1.3. A more sensitive unit will be used to replace the one now in operation to better detect changes in the lowest two wavelength bands.

REFERENCE

B. Goldberg, et al. 1985. Instrumentation for performing spectral measurements in a marine environment. Marine Tech. Soc. J. 18: 4.

RECENT CONTRIBUTIONS OF THE GLOBAL PRECIPITATION CHEMISTRY PROJECT

W. C. Keene and J. N. Galloway
Department of Environmental Sciences
University of Virginia, Charlottesville, VA 22903

G. E. Likens
Institute of Ecosystems Studies
Cary Arboretum, Millbrook, NY 12545

J. M. Miller
Air Resources Laboratory
NOAA, Silver Spring, MD 20910

INTRODUCTION

Anthropogenic emissions of SO_2 and NO_x has resulted in widespread acidification of precipitation and subsequent environmental damage in Eastern North America and Northern Europe. Of numerous research questions posed by this phenomenon, two are of special interest: (1) What was the composition of precipitation prior to the advent of fossil-fuel combustion; and (2) To what degree does the long-distance transport of sulfur and nitrogen species influence the composition of precipitation in remote regions of the world? The Global Precipitation Chemistry Project (GPCP) was initiated in 1979 to address these questions. Principal objectives are to measure the chemical composition of precipitation in remote areas of the world and to determine major processes controlling measured composition. Earlier reports of the GPCP include a preliminary assessment of the composition of precipitation in remote areas of the world (Galloway, 1982), an analysis of organic acidity in precipitation from remote regions (Keene et al., 1983) and an evaluation of the long distance transport of anthropogenic pollutants from North American to Bermuda (Jickells et al., 1982; Church et al., 1982). In this report, we will summarize current research and review more recent contributions of the project.

MATERIALS AND METHODS

Samples of precipitation are collected by event in scrupulously washed polyethylene containers. Immediately after collection, pH is measured, samples are treated with $CHCl_3$ to prevent biological activity and aliquots are susequently sent to the University of Virginia for analyses for major organic and inorganic chemical constituents. To-date we have analyzed 1,247 samples of precipitation collected at 12 land-based sites and during 4 oceanic cruises.

RESULTS AND DISCUSSION

Composition of Precipitation and Influence of Air Mass Source Region

Amsterdam Island, Southern Indian Ocean. Precipitation on Amsterdam Island has two components, seawater and acid (Galloway and Gaudry, 1984). Using Mg^{2+} as the seawater tracer, there were no significant differences between the K^+/Mg^{2+}, Cl^-/Mg^{2+}, Na^+/Mg^{2+} and Ca^{2+}/Mg^{2+} ratios of the rain and those of seawater. The SO_4^{2-}/Mg^{2+} ratio was significantly larger than the

seawater ratio although the non-seasalt component was substantially smaller than the seasalt component. The volume weighted pH of the precipitation samples was 5.06 with primary donors being H_2SO_4, organic acids (HCOOH and CH_3COOH) and HNO_3. The maximum contributions of these acids to precipitation acidity were 30, 25 and 15%, respectively. The alkaline seawater component reacted with the acid component neutralizing 10% of the original volume weighted free acidity. Specific samples ranged from 10 to 50% neutralization, depending on the relative magnitude of the acid and seawater components. ^{222}Rn was used as a tracer to estimate the influence of the long range transport of continental material on the composition of Amsterdam Island precipitation. Only NO_3^- was found to have a possible continental source.

Alaska. The chemical composition of precipitation collected at Poker Flat, Alaska and at Point Barrow, Alaska was analyzed in conjunction with backward air trajectories to evaluate temporal variations in, and the influence of source regions on precipitation chemistry in Alaska (Dayan et al., 1985). The free acidity of precipitation generally decreased from spring through autumn at both sites. Three major sources of air were associated with precipitation events at Poker flat. Southwesterly flow from the Pacific Ocean generated 42% of the storms (volume weighted H^+ = 9.8 ueq/l); localized flow generated 25% (volume weighted H^+ = 12.7 ueq/l); and northerly flow from the arctic generated 19% (volume weighted H^+ = 7.8 ueq/l). H_2SO_4 was the most important source of a acidity contributing between 46 and 80% of free H^+. Organic acids contributed a maximum of 33%, and HNO_3 contributed a maximum of 20% of free H^+ in samples. Pacific and local storms were similar in composition, suggesting a similar mix of sources. Arctic storms exhibited higher SO_4^{2-} but lower H^+ concentrations, suggesting long-distance transport and neutralization of anthropogenic acids from the Polar region.

Organic Acidity in Precipitation

Extending previous work, Keene and Galloway (1984) measured organic anions in 16 precipitation events sampled in central Virginia between 25 April and 1 October 1983. HCOOH and CH_3COOH contributed 16% of volume weighted free acidity. The decrease in free acidity in stored aliquots was directly proportional to the disappearance of dissociated $HCOO^-$ and CH_3COO^-. The loss of free acidity between pH measured at field sites and at central laboratories was used to estimate dissociated organic acidity in samples collected by the National Atmospheric Deposition Program (NADP) and the MAP3S Precipitation Chemistry Project. Based on the arithmetic means of the volume weighted averages for each site, it was estimated that organic acids contributed 18-35% of free acidity in NADP samples and 16% of free acidity in MAP3S samples. The loss of free acidity in MAP3S samples was three times greater during the growing season than it was during the rest of the year. Because they are rapidly assimilated by microbes, organic acids are unimportant in the long-term acidification of the environment. The nature of organic acidity in precipitation is, however, an important consideration for analytical techniques such as Gran's titrations which are commonly used to differentiate strong and weak acidity in precipitation (Keene and Galloway, 1985).

Natural Versus Anthropogenic Components in Precipitation

The concentrations of H^+, SO_4^{2-}, and NO_3^- in the precipitation of eastern North America are greater now than they were historically as a result of

fossil-fuel combustion. Because of a lack of data prior to 1950, the absolute increases in the concentrations of these three ions are unknown. This problem can be addressed by comparing the composition of precipitation from impacted areas with that of precipitation from remote areas. An analysis of precipitation data indicates that many areas of eastern North America receive precipitation with substantially greater H^+, SO_4^{2-}, and NO_3^- concentrations than remote areas. For example, SO_4^{2-}, the most ecologically significant indicator of change, is enriched 2 to 16 times in eastern North American precipitation relative to its concentration in remote areas (Galloway et al., 1985).

ONGOING RESEARCH

Research efforts which are currently underway within the GPCP include:

- o A rigorous evaluation of assumptions involved in correcting precipitation chemistry for the influence of seasalt.
- o A reanalysis of process controlling precipitation chemistry on Bermuda.
- o Analysis of processes controlling precipitation chemistry at Katherine, Australia.
- o Development of a sampler for organic acids in the gaseous and particulate phases.

REFERENCES

Church, T. M., J. N. Galloway, T. D. Jickells, and A. H. Knap, 1982. The chemistry of western Atlantic precipitation at the mid-Atlantic coast and on Bermuda. Journal of Geophysical Research 87: 11013-11018.

Dayan, U., J. M. Miller, W. C. Keene, and J. N. Galloway, 1985. A meteorological analysis of precipitation chemistry from Alaska. Atmospheric Environment 19: 651-657.

Galloway, J. N. and A. Gaudry, 1984. The chemistry of precipitation on Amsterdam Island, Indian Ocean. Atmospheric Environment 18: 2649-2656.

Galloway, J. N., G. E. Likens, W. C. Keene, and J. M. Miller, 1982. The composition of precipitation in remote areas of the world. Journal of Geophysical Research 87: 8771-8786.

Galloway, J. N., G. E. Likens, and M. E. Hawley, 1985. Acid precipitation: Natural versus anthropogenic components. Science 226: 829-830.

Jickells, T. C., A. H. Knap, T. M. Church, J. N. Galloway, and J. M. Miller, 1982. Acid precipitation on Bermuda. Nature 297: 55-56.

Keene, W. C., J. N. Galloway and D. H. Holden, Jr., 1983. Measurement of weak organic acidity in precipitation from remote areas of the world. Journal of Geophysical Research 88: 5122-5130.

Keene, W. C. and J. N. Galloway, 1984. Organic acidity in precipitation of North America. Atmospheric Environment 18: 2491-2497.

Keene, W. C., and J. N. Galloway, 1985. Gran's titrations: Inherent errors in measuring the acidity of precipitation. Atmospheric Environment 19: 199-202.

TRICHLOROTRIFLUOROETHANE (F-113): TRENDS AT PT. BARROW, ALASKA

M. A. K. Khalil and R. A. Rasmussen
Department of Chemical, Biological, and Environmental Sciences
Oregon Graduate Center, Beaverton, OR 97006

The production and uses of trichlorotrifluoroethane ($C_2Cl_3F_3$; F-113) have been increasing rapidly. Since the atmospheric lifetime of F-113 is quite long, its atmospheric concentration is also increasing rapidly. Although at present the atmospheric levels are only around 30 pptv, it constitutes some 90 pptv of anthropogenic gaseous chlorine. In the future increased levels of F-113 may deplete the stratospheric ozone layer. Here we will report on the rate of increase of F-113 observed at Barrow and the precision of measurement of F-113 in flask samples.

Starting in January 1983 we have taken measurements of F-113 at Pt. Barrow, Alaska. Triplicate air samples were collected in 0.8 L stainless steel flasks and sent to the Oregon Graduate Center where the concentrations of trace gases were measured (Rasmussen & Khalil, 1980). In all, some 115 weeks of data have been obtained thus far, constituting a total of nearly 350 samples of air. The concentration of F-113 was measured with a gas chromatograph equipped with an electron capture detector (EC/GC).

The concentrations of F-113 were found to be almost the same in the three flasks that constituted a weekly sample. The standard error (est $\sigma/\sqrt{n}$; $n = 3$) of the concentrations in the three cans of the triplicate sample may be interpreted as the combined precision due to short-term atmospheric variability, and the sampling and analytical methods. Figure 1a shows the frequency distribution of the standard deviations of the concentrations observed each week in the triplicate samples. In Figure 1b these data are expressed as the percent of time the standard deviation exceeded the value on the horizontal axis. For instance, according to Figure 1a the standard deviation was most often (mode) between 0.07 pptv and 0.33 pptv (37% of the time in 113 weekly samples). According to Figure 1b, 50% of the time the standard error of the triplicate samples was less than 1% of the mean value, 90% of the time it was less than 2.5%, and it never exceeded 5%. These results demonstrate that in our method of flask sampling and EC/GC analysis the variability of F-113 is extremely small and that flask samples can be used to accurately determine the long-term trend of F-113 at Barrow, Alaska.

From the observations of F-113 at Barrow it is apparent that the concentrations are increasing at a relatively rapid rate caused by the increasing emissions and the long atmospheric lifetime. In Figure 2 the monthly averaged concentrations of F-113 are plotted. The rate of increase was determined by using the equation $C = \alpha e^{\beta t}$. According to the results shown in Table 1, F-113 increased at a rate of 13% per year between January 1983 and early 1985 (27 months). Over the past 21 months the rate of increase is about 14% per year. It is probable that the rate of increase of F-113 is also increasing. In Table 1 the results obtained at Barrow, Alaska, are compared with previously published results of the increase of F-113 observed at the South Pole (Rasmussen & Khalil, 1982). The time series of measurements of F-113 at Barrow and the South Pole are for different times.

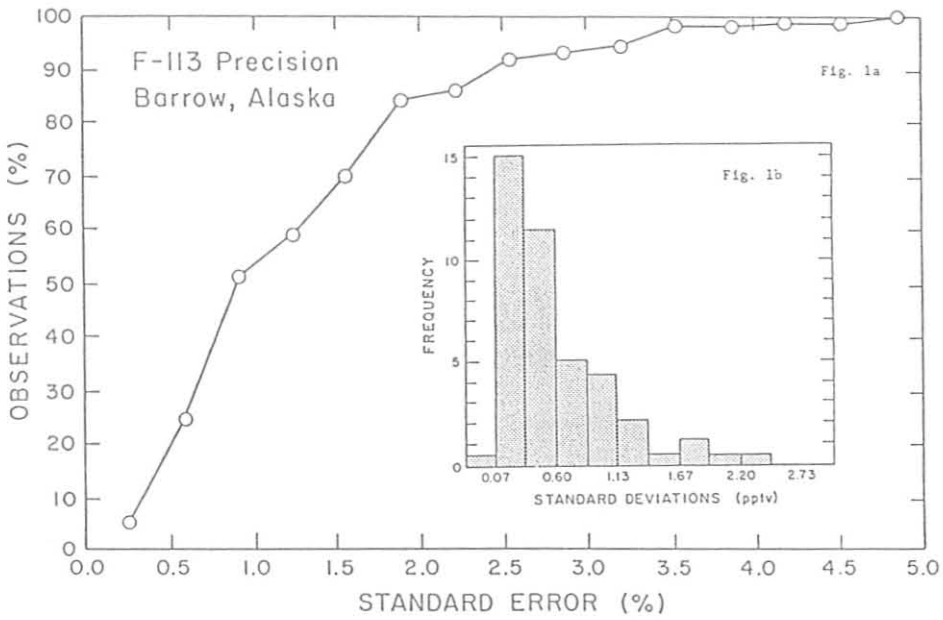

Figure 1a.--Precision of measured concentrations of F-113 shown as the distribution of standard deviations of the concentrations of F-113 at Barrow, Alaska, in each week's triplicate samples.
Figure 1b.--Cumulative frequency distribution of the Standard Error of the concentrations of F-113 in triplicate flask samples collected at the same time. The variability of the short-term atmospheric concentrations, sampling and analytical methods is $\leq$ 2.5% 95% of the time (based on 113 sets of triplicate samples).

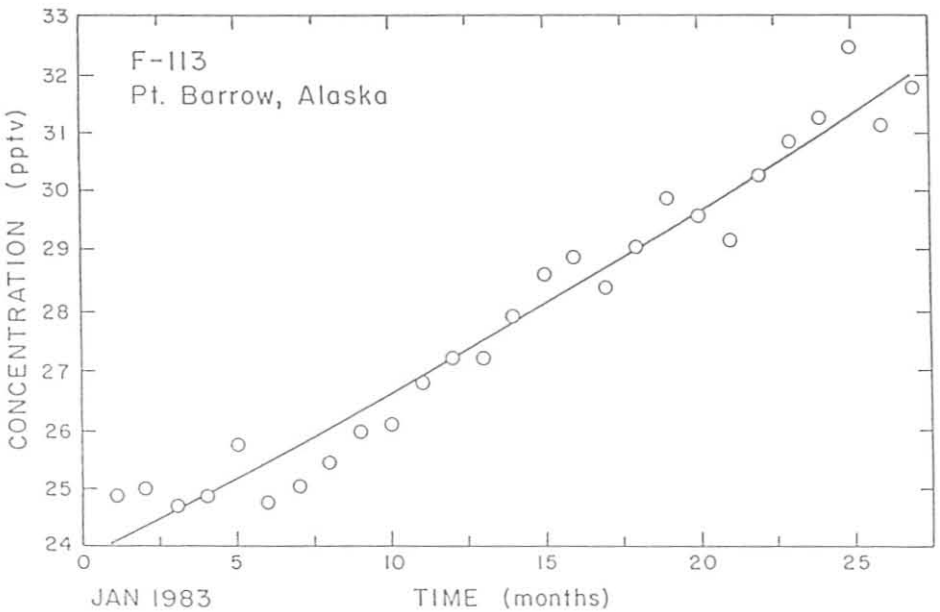

Figure 2.--The increase of trichlorotrifluoroethane ($C_2Cl_3F_3$; F-113) at Barrow, Alaska. The first datum is for January 1983.

At the South Pole the measurements were reported from 1979-1982, while the Barrow data are for 1983-1985. The rates of increase are comparable, and the difference may be due to the acceleration of the accumulation of F-113 in the atmosphere. The calculations of the increase based on the linear equation $C = A + bt$ are also given in Table 1.

We conclude that (1) the trends of F-113 can be accurately measured by using weekly flask sampling procedures; (2) the concentration of F-113 is increasing relatively rapidly at a rate of about 14% per year in response to the long atmospheric lifetime and the increasing uses of F-113; and (3) the F-113 may be increasing at a faster rate now than a few years ago.

Table 1.--The rate of increase of F-113 observed at Pt. Barrow, Alaska

	Exp. (Barrow)		Lin. (Barrow)	Exp. (South Pole)
	All data	21 months		
β (%/yr)	13.0 ±0.1	14.3 ±1.1	--	10
b (pptv/yr)	--	--	3.7 ±0.3	--
α (pptv)	23.9	23.4	--	12
A	--	--	23.7	
r	0.98	0.98	0.98	0.99
N (months)	27	27	21	4

α and β refer to the (exponential) model $C = \alpha e^{\beta t}$, and A and b refer to (linear) $C = A + bt$. The ± values are the 90% confidence limits. r is the correlation coefficient. N is the number of months data during which measurements were taken. At the South Pole measurements are taken only during the austral summer of each year. Exp. refers to the exponential case and Lin. to the linear case. The data for the South Pole are for 1/1979-1/1982 and those for Barrow are from 1/1983-3/1985.

REFERENCES

Rasmussen, R. A., and M. A. K. Khalil, 1983. Atmospheric fluorocarbons and methyl chloroform at the South Pole. Antarctic Journal of the United States, Volume XVII, No. 5:203-205.

Rasmussen, R. A., and M. A. K. Khalil, 1980. Atmospheric halocarbons: measurements and analyses of selected trace gases. Proceedings, NATO Advanced Study Institute on Atmospheric Ozone: Its Variation and Human Influences, Algarve, Portugal, October 1-13, 1979. A. C. Aikin (Ed.), U.S. DOT, Washington, D.C., 209-231.

DETECTION OF ATMOSPHERIC TRACERS IN ANTARCTICA

E. J. Mroz, M. Alei, J. H. Cappis, P. R. Guthals,
A. S. Mason, T. L. Norris, J. Poths, and D. J. Rokop
Los Alamos National Laboratory
Los ALamos, New Mexico 87545

The Antarctic Tracer Experiment is designed to aid scientific understanding of meridional atmospheric transport processes in Antarctica. Meridional transport is responsible for bringing pollutants, both natural and man-made, to Antarctica from the lower latitudes. These materials then become part of the record of climate history that is frozen in the polar ice cap. The experiment consists of releasing unique gases into the atmosphere at a time and place of our choosing and subsequently sampling the antarctic atmosphere in search of the tracer gases. Figure 1 shows the experimental concept and the location of the stations where sampling for the tracer is being conducted.

The tracers used are $^{13}CD_4$ and $^{12}CD_4$. These gases are isotopic analogs of methane and are called "heavy methanes" because they are composed of the heavy isotopes of carbon and hydrogen, namely, ^{13}C and deuterium. These gases can be detected in the atmosphere at a level of a few parts in 10^{17} in air. This extremely low level of detection means that the gases can be detected over four thousand kilometers from the point of release.

1984 Field Activities

During the austral spring of the 83/84 season samplers were deployed to eight stations on the antarctic continent. The stations included the US stations at McMurdo, Palmer, and Amundsen-Scott. Samplers were also

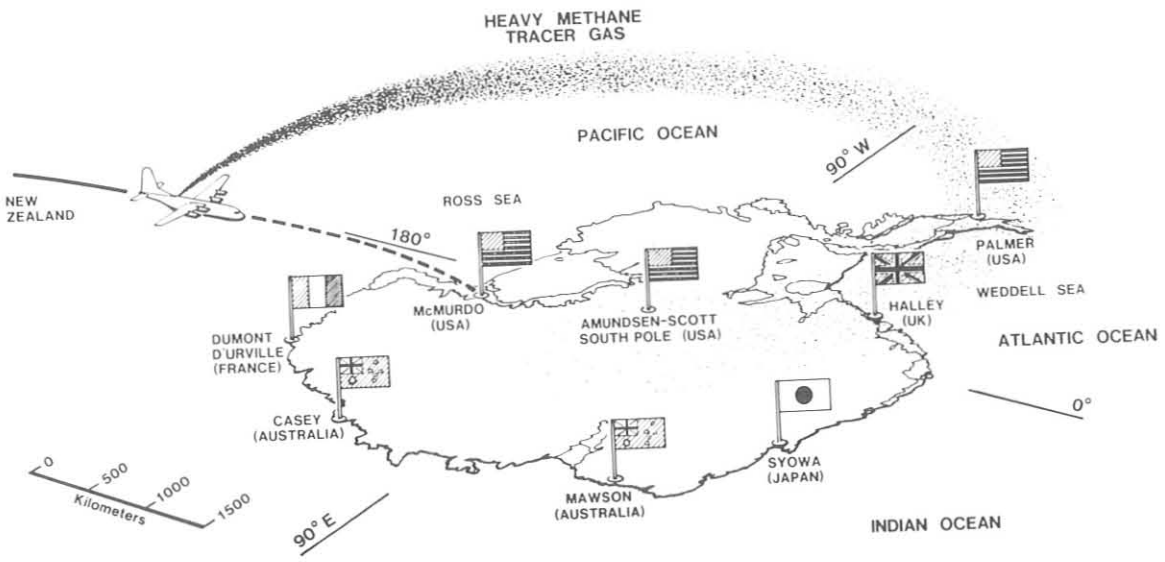

Figure 1. Conceptual view of the Antarctic Tracer Experiment.

installed at Halley Bay (UK), Dumont D'Urville (FR), Syowa (Japan), and Casey and Mawson (AUS). Sampling at these locations is being conducted with the cooperation of personnel stationed there.

After the sampling network was established we conducted the first release of the tracer gas. This took place at 55° 00'S and 167° 47'E at 18,000 ft MSL on 9 January 84 (0015Z). One kilogram of $^{13}CD_4$ was released from a NSF LC-130 aircraft flying from Christchurch, NZ, toward McMurdo Station. Upon release of the tracer, all sampling stations were notified to begin sampling. The sampling protocol consists of collecting one sample continuously over a three day period. This is followed for 60 days after the release. Thus, twenty samples are collected by each station following each release.

Following the January release, additional samples were collected by a cryogenic sampler developed for use on board LC-130 aircraft. Samples were collected on a nearly daily basis from 9 January to 15 February by taking advantage of the normal flight operations of VXE-6. Samples were collected on flights between McMurdo and Siple, Byrd, Amundsen-Scott stations as well as between McMurdo and Christchurch. Other flights on which samples were collected included flights to the Siple coast, Martin Hills, Mt. Smart, and the Ohio Range areas. About one hundered samples were collected by this means.

A second release of 1 kg of $^{13}CD_4$ was made on 8 June 1984. This release was conducted with the assistance of the US Air Force using a WC-135 aircraft and was made at 59° 40'S and 160° 45'W at 18,000 ft MSL. Sampling was conducted at the Antarctic stations in the manner described above. Of course no airborne sampling could be conducted during the austral winter.

The third and final release took place on 18 October 1984. This release was comprised of two releases of different tracer gases at 62° 15'S, 172° 10'E but at different altitudes. The release of 1 kg of $^{13}CD_4$ was made at 5,000 ft while 20 kg of $^{12}CD_4$ was released at 18,000 ft. The releases were made from a USAF C-141 aircraft enroute from McMurdo to Christchurch, NZ. Following this release we again collected samples during LC-130 aircraft flights in the same manner as after the January release.

Trajectory Analysis

Understanding the path by which the tracer travels is an important aspect of this research. A trajectory forecast of the first tracer release in January 1984 has been performed by meteorologists of the US Air Force, British Antarctic Survey, and National Oceanic and Atmospheric Administration (NOAA).

The results are shown in Figure 2. Trajectories A through D were forecast by Mr. David Limbert of the British Antarctic Survey while Trajectory E was forecast by the US Air Force. The forecast by Dr. Elmer Robinson of NOAA is essentially the same as trajectory C. The dearth of meteorological observations in the high southern latitudes exacerbates the uncertainties associated with trajectory forecasting. The plotted trajectories of the tracer show a wide divergence of possible paths after

just a few days. However, all of the trajectories agree that the initial path was toward the east and south. Similar trajectory analyses have been performed for the other releases.

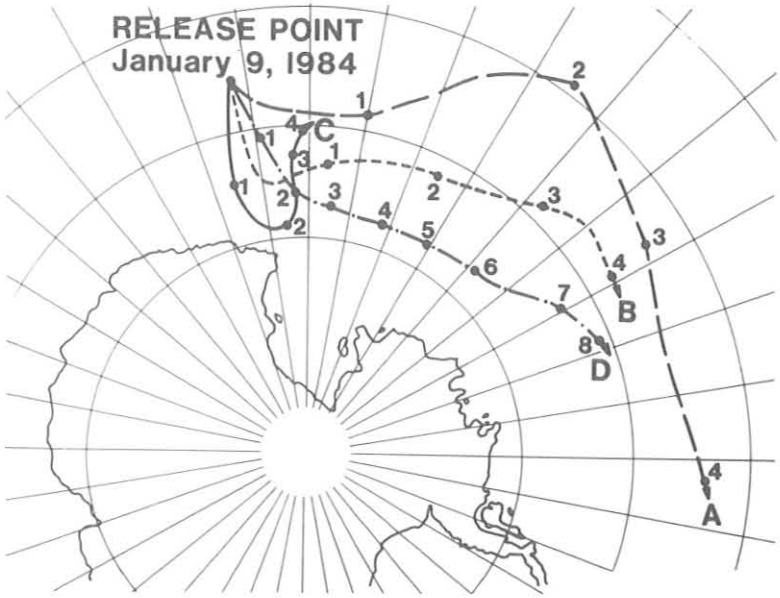

Figure 2. Forecast Tracer Trajectories Following the Release on 9 January 1984.

We are currently analyzing the samples that were obtained following the January release for the presence of heavy methane. We have detected heavy methane in samples collected at 24,000 ft over the Ross Ice Shelf 26 hours after the release. The tracer was found to have persisted in this region for several days following the release. This finding indicates that southward transport from the release point was much faster and further than had been predicted from trajectory analysis. Small amounts of tracer have been detected in samples collected at the South Pole and at Halley Bay within about a week to 10 days after the release. However, during this same time interval no tracer was detected at McMurdo. This suggests that the heavy methane did not mix down to the surface until after passing over McMurdo.

This work was supported in part by National Science Foundation grant OPP 81-18562. Los Alamos National Laboratory is operated by the University of California for the United States Department of Energy under contract W-7405-ENG-36.

FURTHER STUDIES OF DATA COLLECTED DURING THE ARCTIC GAS AND AEROSOL SAMPLING PROGRAM (AGASP)--SPRING 1983

R. C. Schnell
Cooperative Institute for Research in Environmental Sciences
University of Colorado, Boulder, CO 80309

INTRODUCTION

The NOAA Arctic Gas and Aerosol Sampling Program (AGASP) is a study of a type of anthropogenic air pollution commonly known as Arctic haze. In spring 1983, a NOAA WP-3D research aircraft, flown for 144 hours across the Arctic, measured Arctic haze in relation to similar measurements at surface baseline stations such as those at Barrow, Alaska; Alert, Northwest Territories; and Ny Alesund, Svalbard. The initial results from these flights and the companion cooperative programs conducted by scientists from Canada, Norway, Sweden, United Kingdom, and the Federal Republic of Germany have been published in a special issue of Geophysical Research Letters, Vol. 11, May 1984 (28 papers). Some subsequent analyses and future research plans are presented below.

PARTICULATE SULFUR IN ARCTIC HAZE

Sulfur in various forms is a large component of the haze aerosols. On the AGASP flights, particulate sulfur was captured on a variety of filter media for various exposure volumes both in and out of visible haze layers. Some samples were integrated over a total flight.

In fig. 1 are presented the concentrations of particulate S as measured by five separate groups using different sampling systems on the AGASP flights. For the FSU impactors, like the CNL filters, integrations are over periods from 4.5 to 9.5 h and usually include up to 3 h of high-altitude ferry time in air with little or no haze. The measurements by the LBL group are from filters exposed for periods ranging from 0.5 to 2 h in either haze or clear-air target zones. The NCAR filters were exposed mainly in haze layers for periods of from 1 to 2 h. The NOAA sample for flight 6 was obtained from impactor grids and in situ aerosol probes; this is discussed by Shapiro et al. (1984).

The highest S values plotted in fig. 1 were from the haze layer measurements and the lowest values for "clean air" zones. The S values obtained from the flight-integrated filters (FSU and CNL) fall within the lower portion of the two extremes, as would be expected. With respect to the highest S values measured during the AGASP program, Hansen and Rosen (1984) have shown that they occurred in haze layers restricted to the lower 2 km of the Arctic atmosphere and that the S concentrations measured aloft were greater than those measured at the surface near sea level at the Barrow GMCC Baseline Station.

With respect to the flight-integrated samples, it is worthy of note that on flights 7 and 9 the CNL filter and FSU impactor began and ended sampling relatively close in time of each other; they also produced comparable S concentration values. The CNL system ran at 10.5 L min^{-1} and the FSU system at

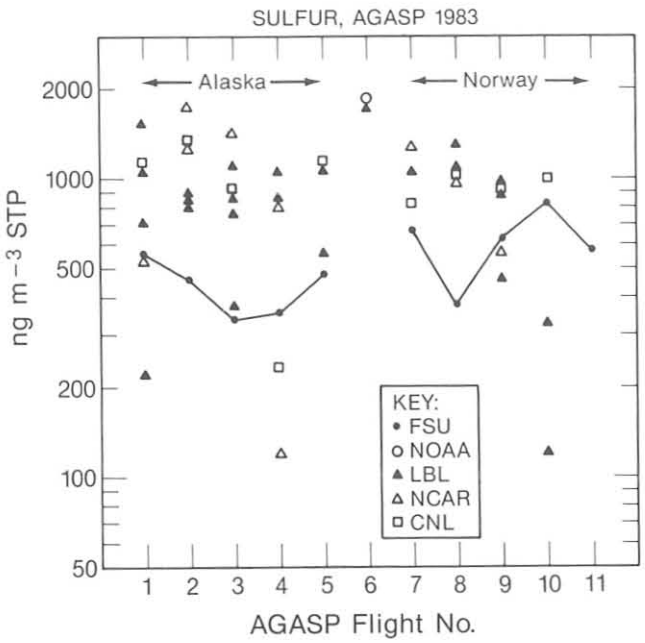

Figure 1.--Particulate sulfur concentrations measured during the AGASP program. Flight numbers and dates are 1, 11 March; 2, 13 March; 3, 15 March; 4, 17 March; 5, 21 March; 6, 23 March; 7, 28 March; 8, 31 March, 9, 4 April; 10, 5 April; and 11, 10 April, 1983. The sulfur measurements were conducted by LBL (Hansen and Rosen, 1984), NCAR (Lazrus and Ferek, 1984), CNL (Cahill and Eldred, 1984), FSU, and NOAA. All concentrations are in STP units.

1.6 L min^{-1}. On flight 4, the CNL filter was run for a 30% longer period on the ferry leg (clean air) than the FSU impactor, which is reflected in higher per unit volume S concentrations observed on the FSU impactor. On flight 5, the exposure times were reversed (40% longer clean-air exposure on the FSU impactor), with the result that higher average S concentrations were observed on the CNL filter.

Both the comments in the flight observers' logs and the gas and aerosol profiles collected during AGASP leave an overall impression that the haze in the Alaskan Arctic was much more stratified and layered than in the Norwegian Arctic. For instance, on flights 1 and 2 in the Alaskan Arctic, up to six haze layers interspersed with extremely clean air were observed (Schnell and Raatz, 1984). On flights 7 and 8 in the Norwegian Arctic, when the aircraft was in haze, the haze appeared to be more well mixed throughout the troposphere, and fewer clean zones were observed between haze bands (Raatz and Schnell, 1984). These observations could explain the greater variation in measured S concentrations in the Alaskan Arctic than in the Norwegian Arctic.

Sulfur measured in stratospheric air within a tropopause fold (flight 6) is also plotted in fig. 1. From these data it may be observed that S was measured in concentrations similar to those measured in Arctic haze layers. This S is thought to be in the form of pure H_2SO_4 produced by the El Chichon eruption. Shapiro et al. (1984) have published electron micrographs of these sulfur-containing droplets.

Finally, it is of interest to note that within the haze, S values at various altitudes on both sides of the Arctic cluster at about 1000 ng m^{-3} STP in concentration. This suggests that S is dispersed fairly evenly throughout the polluted Arctic troposphere and that there were no major sinks for S over the Arctic ice cap during the period of these measurements (March-April 1983).

TRANSPORT OF POLLUTION OVER THE NORWEGIAN ARCTIC

On two research flights in the Norwegian Arctic, the horizontal and vertical variability of the Arctic haze was probed using the NOAA WP-3D research aircraft and dropwindsondes. The results from a flight on 4 April 1983 are presented here.

As shown in fig. 2, the aircraft flew north at 426 mb and descended to 1000 mb at 69.75°N, 10.7°E through the southern frontal boundary of a polluted continental polar air mass. The dry, haze-laden zone of haze transport was traversed between 680 and 820 mb (Raatz and Schnell, 1984).

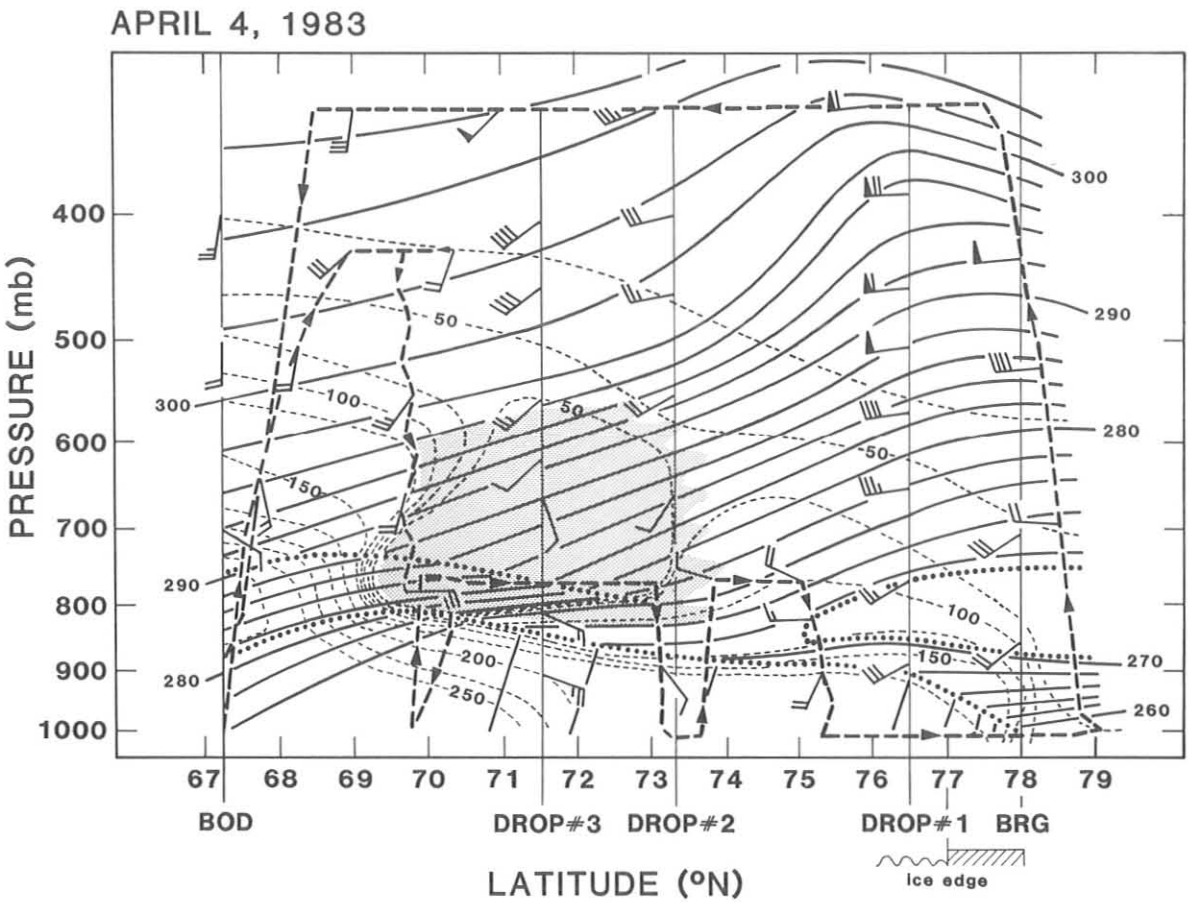

Figure 2:--Latitude-altitude cross section of potential temperature (K, solid lines) and water vapor mixing ratio (x 10^{-2} g kg^{-1}, thin broken lines) for 4 April 1983. The aircraft flight track is indicated by the thick broken line; wind speeds are in knots. The approximate core of the haze transport zone is indicated by shading. The top of the marine boundary layer is indicated by the dark dotted line.

After completing the profile, the aircraft probed the horizontal variability of the main haze transport zone characteristics. Between 1011 GMT (69.95°N, 11.42°E) and 1127 GMT (73.02°N, 23.73°E) the aircraft flew at a constant pressure of 770 mb northbound. Within the haze transport zone of heavy aerosol loading (~1030 GMT), the aircraft passed into a patch of relatively cleaner and drier air at the northern edge of the transport zone. At 1118 GMT the core of the haze transport zone was reentered east of the earlier exit point.

For a portion of the flight, the aircraft flew in the haze transport zone and made two descents through the marine boundary layer to just above the ocean. Toward the end of the flight, the aircraft flew through the ice edge baroclinic zone to a point 175 km north over the pack ice. On the climb out, at 79°-78°N for the return leg, the bottom of the haze was observed at 790 mb and the top of the main haze zone at 610 mb. On that day the northern boundary of the haze zone was not determined, but it was north of 79°N.

The boundaries of the core of the haze transport zone on 4 April were well defined at the top and bottom, determined in general terms on the southern edge, and extended beyond 78°-79°N, the limit of the aircraft flight path. These boundaries are shown in fig. 2 by the shaded area.

These and other measurements document the transport of heavy concentrations of anthropogenic aerosols (within well-defined dry continental air masses) out of Eurasia into the Norwegian Arctic. Such haze transport zones had been suggested as being in existence by Raatz and Schnell (1984).

AGASP-II, MARCH-APRIL 1986

In spring 1986, Arctic haze will be studied both at the surface and aloft in a comprehensive international program. Surface measurements of gases, aerosols, solar radiation, and meteorology will be conducted from baseline stations located at Barrow, Alert, and Ny Alesund. Upward-pointing lidar measurements of the haze layers will be obtained at Alert, and ozonesondes will be released from both Alert and Barrow. The NOAA WP-3D, University of Washington C-131A, and Max-Planck-Institute Hawker Siddeley 125 aircraft will operate together out of Thule, Greenland, flying research patterns above and upwind of the Alert baseline station. Similar patterns will be flown by the NILU Piper Navajo in relation to the Ny Alesund baseline station, both above and in conjunction with the NOAA WP-3D and Max-Planck Hawker Siddeley. The NOAA WP-3D will fly solo research flights in conjunction with ground measurements at the Poker Flat Optical and Atmospheric Chemistry Facility and the Barrow baseline station. The planned flight paths and surface locations are shown in fig. 3.

In addition to the above program, heavy methane tracers and constant-level balloons will be released from Europe to trace the pollution across the polar region.

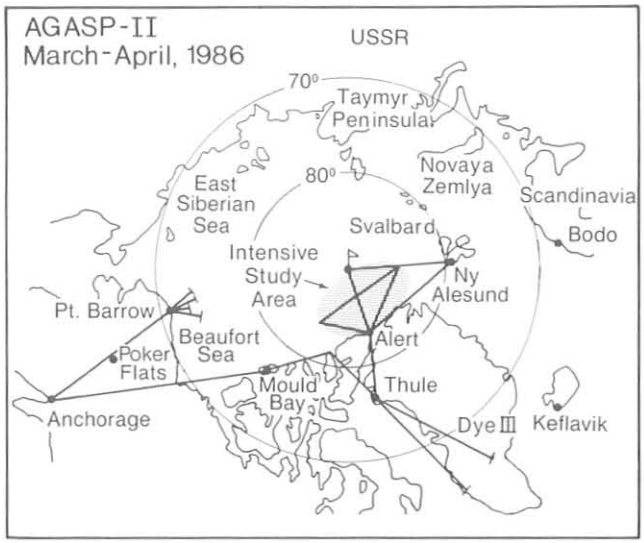

Figure 3.--Operational area, flight tracks, and surface sampling and base operations for the 1986 Arctic haze research project.

REFERENCES

Cahill, T. A., and Ellred, R. A.. 1984. Elemental composition of Arctic particulate matter. Geophysical Research Letters 11:413-416.

Hansen, A. D. A., and H. Rosen, 1984. Vertical distributions of particulate carbon, sulfur, and bromine in the Arctic haze and comparison with ground-level measurements at Barrow, Alaska. Geophysical Research Letters 11:381-384.

Lazrus, A. L., and R. J. Ferck, 1984. Acidic sulfate particles in the winter Arctic Atmosphere. Geophysical Research Letters 11:417-419.

Raatz, W. E., and R. C. Schnell, 1984. Aerosol distributions and an Arctic aerosol front during AGASP: Norwegian Arctic. Geophysical Research Letters 11:373-376.

Schnell, R. C., and W. E. Raatz, 1984. Vertical and horizontal characteristics of Arctic haze during AGASP: Alaskan Arctic. Geophysical Research Letters 11:369-372.

Shapiro, M. A., R. C. Schnell, F. P. Parungo, S. J. Oltmans, and B. A. Bodhaine, 1984. El Chichon volcanic debris in an Arctic tropospheric fold. Geophysical Research Letters 11:421-424.

ATMOSPHERIC SUBMICRON PARTICLE COLLECTION AT THE SOUTH POLE OBSERVATORY

R. E. Witkowski and W. A. Cassidy
University of Pittsburgh
Pittsburgh, PA 15260

G. W. Penney
Carnegie-Mellon University
Pittsburgh, PA 15213

INTRODUCTION

In a continuing effort as part of the University of Pittsburgh Antarctic Search for Meteorites Project, an atmospheric particle collector has been in operation at the South Pole Observatory's Clean Air Facility (Witkowski, et al., 1984). To date, more than 12,000 hours of collection time has been logged; a total of 27 specimen plates have been exposed and returned to the laboratory for study using scanning transmission electron microscopy coupled with energy dispersive spectrometry and selected area diffraction for particle morphology, elemental composition and crystallographic structure determinations. Particles now have been collected throughout the entire year (December 1983 to the end of November 1984) with detailed laboratory studies being carried out on specific specimen plates exposed for time intervals as low as 24 hours and as high as 4000 hours. These studies have shown that collection periods of 1000 hours during the austral summer and 4000 hours during the austral winter will produce collections that are ideal for individual particle analysis, i.e., high particle density per unit area, without such high densities that agglomerates form.

RESULTS AND DISCUSSION

Submicroscopic particles from contaminating sources are very abundant in the atmosphere at the South Pole. Even though this site is a location where airborne particles of artificial, natural and terrestrial contamination are expected to have low abundance, particularly during the austral winter, particles resulting from fossil fuel burning (fly ash alumino-silicate spheres) and volcanic and marine origin (sulfuric acid and a fragment of a siliceous radiolarian shell) have been found.

In addition to these particles, which can be identified as terrestrial contaminants, a number of particles whose terrestrial origin cannot be confirmed have been isolated and studied. These include rod-shaped grains, typically 0.1 micrometer long that give Ca and S elemental signatures and, although rather rare in number, another group of submicron size grains that apparently consists of single metallic elements (or, for example, their oxides, hydroxides, carbides or carbonates) that give single-element signatures of Mg, Ti, Cr, Fe, and Co. In some special cases, selected area electron diffraction measurements could be obtained, with the resulting diffraction patterns giving some clue to the chemical and crystallographic make-up of a particle. For example, the fluffy aggregate of needle-like crystals (Figure 1) that gives an appearance of extreme fragility, and the plate-like crystals (Figure 2), yielded a pattern that suggests the mineral species magnetite or goethite. While these particles have the

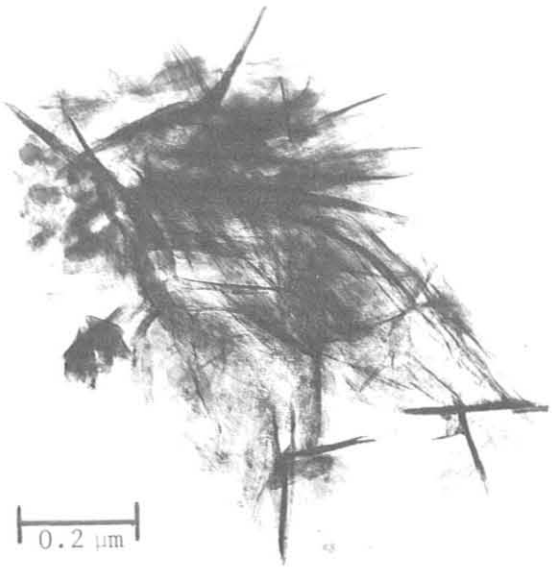

Figure 1.--Needle-like crystals. (Plate #14, 1032 hours.)

Figure 2.--Plate-like crystals. (Plate #14, 1032 hours.)

simple compositions and small physical sizes that would be expected of extra-terrestrial dust grains, they cannot be positively identified as such; the possibility of terrestrial contamination sources or condensation smokes of stratospheric origin (see, for example, Hunten, et al., 1980) still must be considered.

FUTURE PROGRAM

The particle collector will remain in operation throughout the 1984-85 austral season. An additional set of nine collector specimen plates will be exposed. Laboratory studies will continue in the identification and characterization of material already returned from the previous year.

ACKNOWLEDGMENTS

We acknowledge LTJG Frank Migaiolo, NOAA-GMCC Station Chief, who maintained this experiment throughout the winter season. This work is made possible by NSF grant DPP 83 14496; the electron microscope facilities were made available by the Westinghouse R&D Center.

REFERENCES

Hunten, D. M., R. P. Turco, and O. B. Toon, 1980. Smoke and dust particles of meteoric origin in the mesosphere and stratosphere. Journal of the Atmospheric Sciences, 32:1342-57.

Witkowski, R. E., W. A. Cassidy and G. W. Penney, 1984. The search for particles of cosmic origin at SPO. Geophysical Monitoring for Climatic Change Summary Report No. 12, December 1984, J. M. Harris and E. V. Nickerson (Ed.), NOAA Environmental Research Laboratories, Boulder, Colorado, 149-150.

8. INTERNATIONAL ACTIVITIES

From June 1984 to January 1985, the CO_2 group had use of a Siemens Ultramat III infrared gas analyzer on loan from N. Trivett of Atmospheric Environment Service, Canada. This analyzer was tested as a possible replacement for the aging URAS analyzers currently in use at the GMCC observatories.

Collection of flask samples for CO_2 and CH_4 analyses was begun in April 1984 at Cape Grim Observatory, Tasmania in cooperation with the Australian CO_2 group at CSIRO. Flask sampling was also begun at Christmas Island, Republick of Kiribati in cooperation with J. Bryden of Christmas Island and SIO.

In April 1984, L. Waterman of the CO_2 group visited the CO_2 group at CSIRO, Australia, and made a trip to the Cape Grim Observatory.

B. Bodhaine participated in the Third Symposium on Arctic Air Chemistry, 7-9 May, at Downsview, Ontario, Canada. He presented the GMCC aerosol record obtained at BRW, and an analysis of some aerosol measurements from the AGASP flight program in March-April 1983.

B. Bodhaine participated in the Scientific Application of Baseline Observations of Atmospheric Composition meeting, 7-9 November, at Aspendale, Australia. He presented an analysis of the GMCC aerosol record obtained at SMO. Many of the attendees at this meeting had the opportunity to visit the Australian baseline station located at Cape Grim, Tasmania.

On 9-13 April, J. DeLuisi participated in a WMO-sponsored Meeting of Turbidity Experts at Tenerife, Canary Islands, to commemorate the opening of a Spanish baseline observatory. The meeting was attended by nine experts representing the United States, W. Germany, Switzerland, Italy, Canada and Spain. The deliberations of the meeting were concerned with applications of sunphotometery, including measurement of O_3, NO_2, and H_2O, besides aerosol optical depth. The participants recommended nine standard wavelengths for sunphotometery. DeLuisi described GMCC's baseline station sunphotometer measurements and plans for upgrading of the U. S. turbidity network. He also offered the MLO GMCC solar radiation facility as an ideal site for calibration of primary standard sunphotometers used by various countries making BAPMoN turbidity measurements. WMO subsequently issued a memorandum designating the site as a World Sunphotometer Calibration site.

R. Grass and R. Evans visited Perth, Australia during July and August 1984 to install automated Dobson ozone spectrophotometer No. 81 for operation at the Australian Bureau of Meteorology Weather Office. The Perth station is one of seven global sites where Umkehr observations will be made on a long-term basis to monitor possible future stratospheric ozone depletion by man-made pollutants such as the chlorofluorocarbons.

R. Grass spent 3 weeks at Melbourne, Australia, in August 1984, training Australian technicians in Dobson spectrophotometer operating procedures. Instructions were provided also, in optically aligning and calibrating the Dobson instruments.

W. Komhyr and R. Grass convened an International Comparison of Dobson spectrophotometers at Melbourne, Australia, 19 November to 10 December 1984, under auspices of the WMO. Participating countries were Australia, India, Japan, New Zealand, and the U.S.A.

J. Peterson headed a U.S. delegation of five scientists to Vilnius, Lithuania, U.S.S.R., during August 1984. The delegation participated in the Symposium on atmospheric trace gases affecting climate hosted by the U.S.S.R. under Working Group VIII of the U.S.-U.S.S.R. bilateral agreement on protection of the environment. He gave talks on "The NOAA halocarbon and nitrous oxide measurement program," and "Results from AGASP."

J. Peterson, (B. Mendonca, E. Dutton, G. Herbert, R. Gammon, P. Steele, and B. Bodhaine) participated in the conference "The Scientific Application of Baseline Observations of Atmospheric Composition" at Aspendale, Australia, in November 1984. He presented a paper on "Measurements of atmospheric CO_2 at Barrow, Alaska, from the U.S. NOAA/GMCC program."

P. Steele, visiting scientist from Australia, continued his appointment at GMCC as an NRC-NOAA Research Associate up to 14 September 1984. He took over full management of the cooperative program between CSIRO, NOAA/GMCC, and OGC to measure CH_4 and CO_2 concentrations by gas chromatography in flask air samples from the GMCC cooperative flask sampling network. He traveled to the SABOAC Conference held at the CSIRO Division of Atmospheric Research during 7-9 November 1984 where he presented a paper on results from this cooperative program. While en route to this conference, visits were made to the New Zealand Meteorological Service (Atmospheric Physics and Chemistry Section) in Wellington, and to the cooperative flask sampling site located at Kaitorete Spit near Christchurch. Seminars were presented at the following institutions: Centre for Resource and Environmental Studies, Australian National University, Canberra; Meteorological Department, Bangkok, Thailand; Department of Environmental Sciences, University of Lancaster, Lancaster, England.

R. Schnell attended the 3rd Arctic Haze Symposium in Toronto, Canada, May 1983 where he presented a paper on the AGASP results. At the same time, plans for the 2nd AGASP program were developed with Canadian counterparts.

June 6-9, R. Schnell co-hosted the 2nd International Conference on Ice Nucleation Bacteria held in Flagstaff, AZ. Two papers presented at this conference bear his authorship.

9. PUBLICATIONS AND PRESENTATIONS BY GMCC STAFF, 1984

Baker-Blocker, A., J. J. DeLuisi, and E. Dutton. Received ultraviolet radiation at the South Pole. Solar Energy 32(5):659-662.

Bodhaine, B. A. The GMCC aerosol program. Paper presented at The Scientific Application of Baseline Observations of Atmospheric Composition, 7-9 November 1984, Aspendale, Australia.

Bodhaine, B. A., E. G. Dutton, and J. J. DeLuisi. Surface aerosol measurements at Barrow during AGASP. Geophys. Res. Lett. 11(5)377-380.

Bodhaine, B. A., E. G. Dutton, and J. J. DeLuisi. Surface aerosol measurements at Barrow. Paper presented at Third Symposium on Arctic Air Chemistry, 7-9 May, Downsview, Ontario, Canada.

Cowherd, C., G. E. Muleski, P. Englehart, and D. Gillette. Rapid assessment of exposure to particulate emissions from surface contamination sites. MRI Draft Report, Midwest Research Institute, Kansas City, MO.

Dayan, U., J. M. Miller, D. W. Nelson. The acidity of Samoan rain - trends and evaluation of the first decade. NOAA Tech. Memo. ERL ARL-132, NOAA Environmental Research Laboratories, Boulder, Colo., 22 pp.

DeLuisi, J. J., T. DeFoor, K. Coulson, F. Fernald, and K. Thorn. Lidar observations of stratospheric aerosol over Mauna Loa Observatory: 1974-1981. NOAA Data Report, ERL ARL-4, NOAA Environmental Research Laboratories, Boulder, CO, 107 pp.

DeLuisi, J. J., C. L. Mateer, and P. K. Bhartia. On the correspondence between standard Umkehr, short Umkehr and SBUV vertical ozone profiles. Proc. Quad. Ozone Symp., Halkidiki, Greece, 3-7 September 1984.

DeLuisi, J. J., C. L. Mateer, and W. D. Komhyr. Effects of El Chichon stratospheric aerosol cloud on Umkehr measurements at Mauna Loa, Hawaii. Proc. Quad. Ozone Symp., Halkidiki, Greece, 3-7 September 1984.

Dutton, E. G., J. J. DeLuisi, and B. A. Bodhaine. Features of aerosol optical depth observed at Barrow, March 10-20, 1983. Geophys. Res. Lett. 11(5):385-388.

Dutton, E. G., and J. J. DeLuisi. Interpretation of Apparent Atmospheric transmission using solar photometer precipitable water measurement. Extended abstracts of CSIRO conference on The Scientific Application of Baseline Observations of Atmospheric Composition, 7-9 November 1984, Aspendale, Australia.

Fall, R. R., and R. C. Schnell. Association of an ice-nucleating Pseudomonad with cultures of the marine dinoflagellate, Heterocapsa niei. J. Marine Res. 43:257-265.Fall, R. R., and R. C. Schnell. Bacterial ice nuclei of marine origin: some recent observations. Preprints, 11 Int. Conf. on Atmos. Aerosols, Condensation, and Ice Nuclei, Budapest, Hungary, 3-8 September 1984.

Fall, R. R., and R. C. Schnell. Isolation of ice-nucleation active bacteria from marine sources. Preprints, 2nd American Conference on Ice Nucleating Bacteria, Flagstaff, AZ, 6-9 June 1984.

Fraser, P. J., M. A. K. Khalil, R. A. Rasmussen, and L. P. Steele. Tropospheric methane in the mid-latitudes of the Southern Hemisphere. J. Atmos. Chem.. 1:125-135.

Gammon, R.H. The response of the global carbon cycle to climatic change. Presentation at EPA Symposium Rising CO_2 and Changing Climate: Forest Risks and Opportunities, Boulder, Colo, June 1984.

Gammon, R. H. Atmospheric methane and climatic change. Presentation at Ocean Industry Sumposium, Woods Hole Oceanographic Institution, Woods Hole, Mass., September 1984.

Gammon, R. H. Carbon cycle trace gas distributions: results from the joint U.S./U.S.S.R. Pacific expedition SAGA of the RV KOROLEV, Fall 1983. Presentation at the U.S./Soviet Symposium on Trace Gases and Climatic Change, Vilnius, Lithuania, September 1984.

Gammon, R. H., W. D. Komhyr, L. S. Waterman, T. J. Conway, and K. W. Thoning. Estimating the natural variation in atmospheric CO_2 since 1860 from interannual changes in tropospheric temperature and the history of major El Niño events. Paper presented at the Chapman Conference on Natural Variations in Carbon Dioxide and the Carbon Cycle, Tarpon Springs, FL, 9-13 January 1984.

Gammon, R. H., W. D. Komhyr, L. S. Waterman, T. J. Conway, K. W. Thoning, and D. Gillette. The 1982/83 ENSO event: The response of the global atmospheric CO_2 distribution. Paper presented at the Conference on the Scientific Application of Baseline Observations of Atmospheric Composition, Aspendale, Australia, 7-9 November 1984.

Grass, R. D., and W. D. Komhyr. Traveling standard lamp calibration checks on Dobson ozone spectrophotometers during 1981-83. Proc. Quad. Ozone Symp., Halkadiki, Greece, September 3-7, 1984.

Harris, J. M. Trajectories during AGASP. Geophys. Res. Lett. 11(5):453-456.

Harris, J. M. and E. C. Nickerson (eds). Geophysical Monitoring for Climatic Change, No. 12: Summary Report 1983. NOAA Environmental Research Laboratories, Boulder, CO, 184 pp.

Hilsenrath, E., J. Ainsworth, A. Holland, J. Mentall, A. Torres, W. Attmanspacher, A. Boss, W. Evans, W. Komhyr, A. J. Miller, M. Proffitt, D. Robbins, S. Taylor, and E. Weinstock. Results from the balloon ozone intercomparison campaign (BOIC). Proc. Quad. Ozone Symp., Halkadiki, Greece, September 3-7, 1984.

Komhyr, W. D., R. D. Grass, R. D. Evans, R. K. Leonard, and G. M. Semeniuk. Umkehr observations with automated Dobson spectrophotometers. Proc. Quad. Ozone Symp., Halkadiki, Greece, September 3-7, 1984.

Komhyr, W. D., S. J. Oltmans, A. N. Chopra, R. K. Leonard, T. E. Garcia, and C. McFee. Results of Umkehr, ozonesonde, total ozone, and sulfur dioxide observations in Hawaii following the eruption of El Chichon volcano in 1982. Proc. Quad. Ozone Symp., Halkadiki, Greece, September 3-7, 1984.

Komhyr, W. D, S. J. Oltmans, A. N. Chopra, and P. R. Franchois. Performance characteristics of high-altitude ECC ozonesondes. Proc. Quad. Ozone Symp., Halkadiki, Greece, September 3-7, 1984.

Mateer, C. L., and J. J. DeLuisi. A comparison of ozone profiles derived from standard Umkehr and short Umkehr measurements from 15 stations. Proc. Quad. Ozone Symp., Halkidiki, Greece, 3-7 September 1984.

Mendonca, B. G., J. J. DeLuisi, and E. G. Dutton. Atmospheric transmission decreases and stratospheric warming at Mauna Loa during the 2 years after the El Chichon volcanic eruption. Extended abstracts of CSIRO conference on The Scientific Application of Baseline Observations of Atmospheric Composition, 7-9 November 1984, Aspendale, Australia.

Nickerson, E. C. On the role of mesoscale meteorological models in assessing the climatological impacts of urbanization in tropical areas. Paper presented at the WMO Technical Conference on Urban Climatology and its Applications with Special Regard to Tropical Areas. Mexico City, 26-30 November 1984.

Nickerson, E. C., D. Medal, E. Richard, and R. Rosset. Mesoscale numerical modeling of heavy precipitation events over mountainous terrain. Paper presented at the Fall AGU Meeting, San Francisco, CA, 5 December 1984.

Parungo, F., C. Nagamoto, J. Harris, B. Rosenuasser, and L. Ruhnke. Analyses of aerosol and precipitation samples collected during a transatlantic research cruise, NOAA Tech. Memo, ERL ESG-5, NOAA Environmental Sciences Group, Boulder, CO, 63 pp.

Patterson, E., J. J. DeLuisi, B. Mendonca, R. Pueschel, R. Castillo, and T. Ackerman. Measurements of the absorption of cold water and unactivated within-cloud aerosols at Whiteface Mt., New York. Proc. International Radiation Symposium, 21-29 August 1984, Perugia, Italy.

Peterson, J. T. Measurements of atmospheric CO_2 at Barrow, Alaska, from the U.S. NOAA/GMCC program. Paper presented at conference on The Scientific Applications of Baseline Observations of Atmsopheric Composition, Aspendale, Australia, November 1984.

Peterson, J. T. Results from AGASP. Paper presented at US-USSR Symposium on Atmospheric Trace Gas Components Affecting Climate, Vilnius, Lithuania, U.S.S.R., August 1984.

Peterson, J. T. The NOAA halocarbon and nitrous oxide measurement program. Paper presented at US-USSR Symposium on Atmospheric Trace Gas Components Affecting Climate, Vilnius, Lithuania, U.S.S.R., August 1984.

Raatz, W. E., and R. C. Schnell. Aerosol distributions and an Arctic aerosol front during AGASP: Norwegian Arctic, Geophys. Res. Lett. 11:369-372.

Reinsel, G. C., G. C. Tiao, J. J. DeLuisi, C. L. Mateer, A. J. Miller, and J. E. Fredrick. Analysis of upper stratospheric Umkehr ozone profile data for trends and effects of stratospheric aerosols. J. Geophys. Res. 89:4833-4840.

Schnell, R. C. Aerosol measurements during the Arctic gas and aerosol sampling program (AGASP): March-April 1983. Preprints, 3rd Arctic Haze Symposium, Toronto, Canada, May 1984.

Schnell, R. C. Arctic Haze: Editorial, Geophys. Res. Lett. 11:359.

Schnell, R. C. Bacterial ice nuclei and their role in the atmosphere. Preprints, 2nd American Conference on Ice Nucleating Bacteria, Flagstaff, AZ, 6-9 June 1984.

Schnell, R. C. Condensation nuclei and aerosol size distribution measurements in Arctic haze. Preprints, 11 Int. Conf. on Atmos. Aerosols, Condensation, and Ice Nuclei, Budapest, Hungary, 3-8 September 1984.

Schnell, R. C. and W. E. Raatz. Vertical and horizontal characteristics of Arctic haze during AGASP: Alaskan Arctic, Geophys. Res. Lett. 11:373-376.

Schnell, R. C.. Arctic Haze and the Arctic gas and aerosol sampling program (AGASP), Geophys. Res. Lett. 11:361-364.

Shapiro, M. A., R. C. Schnell, F. P. Parungo, S. J. Oltmans, and B. A. Bodhaine. El Chichon volcanic debris in an Arctic tropopause fold. Geophys. Res. Lett. 11:421-424.

Steele, L. P., P. J. Fraser, R. A. Rasmussen, M. A. K. Khalil, T. J. Conway, A. J. Crawford, R. H. Gammon, K. A. Masarie, and K. W. Thoning. The global distribution of methane in the troposphere. Paper presented at the Scientific Application of Baseline Observations of Atmospheric Composition (SABOAC) Conference held at CSIRO Division of Atmospheric Research, Aspendale, Victoria, Australia, 7-9 November 1984.

Winchester, J. W., S. Li, S. Fan, R. C. Schnell, B. A. Bodhaine, and P. S. Naegele. Coarse particle soil dust in Arctic aerosols, spring 1984. Geophys. Res. Lett. 11:995-998.

10. ACRONYMS AND ABBREVIATIONS

AES	Atmospheric Environment Service, Canada
AGASP	Arctic Gas and Aerosol Sampling Program
AL	Aeronomy Laboratory, Boulder, CO (ERL)
ALE	Atmospheric Lifetime Experiment
ARL	Air Resources Laboratory, Silver Spring, MD (ERL)
ASCS	Alaska Soil Conservation Service
ASR	Aerosols and Solar Radiation
ATV	all terrain vehicle
BOIC	Balloon ozone intercomparison campaign
BRW	Barrow Observatory, Barrow, Alaska (GMCC)
CAF	Clean Air Facility
CAMS	Control and Monitoring System
CDIC	Carbon Dioxide Information Center, Oak Ridge, TN (DOE)
CIRES	Cooperative Institute for Research in Environmental Sciences, University of Colorado, Boulder
CN	condensation nuclei
CNC	condensation nucleus counter
CNL	Crocker Nuclear Laboratory
CO2	Carbon Dioxide, referring to CAMS
CSIRO	Commonwealth Scientific and Industrial Research Organization, Australia
DAS	data acquisition system
DC	direct current
DEW	Distant Early Warning
DOE	Department of Energy
DOY	day of year, Julian
EC	elemental carbon
ECC	Electrochemical concentration cell
EML	Environmental Measurements Laboratory (DOE)
ENSO	El Niño-Southern Oscillation
EPA	Environmental Protection Agency
ERL	Environmental Research Laboratories, Boulder, CO (NOAA)
FTS	Federal Telecommunication System
FSU	Florida State University
GC	gas chromatograph
G.E.	General Electric
GEOSECS	Geochemical Ocean Sections Study
GMCC	Geophysical Monitoring for Climatic Change, Boulder, CO (ARL)
GPCP	Global Precipitation Chemistry Project
GMT	Greenwich mean time
GSA	Government Service Administration
GSFC	Goddard Space Flight Center (NASA)
HASL	Health and Safety Laboratory (EPA)
HP	Hewlett-Packard
ICDAS	Instrumentation Control and Data Acquisition System
IR	infrared
ISWS	Illinois State Water Survey
ITCZ	Intertropical Convergence Zone
JSC	Johnson Space Center (NASA)
LBL	Lawrence Berkeley Laboratory (DOE)
LST	local standard time

MAP/GLOBUS	Middle Atmosphere Program/Global Budget of Stratospheric Trace Constituents
MAP35	MAP Precipitation Chemistry Project
MLO	Mauna Loa Observatory, Hawaii (GMCC)
MO3	Meteorology and Ozone
MSL	mean sea level
NADP	National Atmospheric Deposition Program
NARL	Naval Arctic Research Laboratory, Barrow, AK
NASA	National Aeronautic & Space Administration
NCAR	National Center for Atmospheric Research, Boulder, CO
NCDC	National Climatic Data Center, Asheville, NC
NESDIS	National Environmental Satellite, Data, and Information Service
NDIR	nondispersive infrared
NH	Northern Hemisphere
NIP	normal incidence pyrheliometer
NILU	Norwegian Institute for Air Research
NMC	National Meteorological Center, Suitland, MD
NOAA	National Oceanic and Atmospheric Administration
NRL	Naval Research Laboratory, Washington, D.C.
NWR	Niwot Ridge, CO
NWS	National Weather Service
NWT	Northwest Territories (Canada)
OGC	Oregon Graduate Center, Beaverton, OR
PMEL	Pacific Marine Environmental Laboratory, Seattle, WA
PMOD	Physikalisch-Meteorologisches Observatorium Davos
PRC	Peoples Republic of China
PV	photovoltaic
QBO	Quasi-biennial oscillation
SABOAC	Scientific Application of Baseline Observations of Atmospheric Composition, CSIRO Conference, Australia
SAGA	Soviet-American Aerosol and Gas Experiment
SBUV	Solar backscattered ultraviolet
SEASPAN	SEAREX South Pacific Aerosol Network
SEAREX	Sea-Air Exchange Program
SH	Southern Hemisphere
SIO	Scripps Institution of Oceanography, La Jolla, CA
SMO	Samoa Observatory, American Samoa (GMCC)
SUNYA	State University of New York at Albany
SPO	South Pole Observatory, Antarctica (GMCC)
SRL	Smithsonian Radiation Laboratory
SRBL	Smithsonian Radiation and Biological Laboratory
SST	sea surface temperature
TTO	Transient Tracers in the Ocean
UIC	Ukpiagvik Inupiat Corporation
URI	University of Rhode Island, Kingston, RI
USGS	United States Geological Survey
UV	ultraviolet
WMO	World Meteorological Organization, Geneva, Switzerland
WPL	Wave Propagation Laboratory, Boulder, CO

*U.S. GOVERNMENT PRINTING OFFICE: 1987-0-773-002/60514